AD-A229 017

SECURITY CLASSIFICATION OF THIS PAGE

REPORT DOCUMENTATION PAGE

DTIC ELECTE NOV 16 1990 S B D

DTIC FILE COPY

Form Approved OMB No. 0704-0188

1a. REPORT SECURITY CLASSIFICATION: UNCLASSIFIED	1b. RESTRICTIVE MARKINGS
2a. SECURITY CLASSIFICATION AUTHORITY	3. DISTRIBUTION/AVAILABILITY OF REPORT: unlimited
2b. DECLASSIFICATION/DOWNGRADING SCHEDULE	
4. PERFORMING ORGANIZATION REPORT NUMBER(S)	5. MONITORING ORGANIZATION REPORT NUMBER(S): AFOSR-TR- 90 1079
6a. NAME OF PERFORMING ORGANIZATION: UNIVERSITY OF MARYLAND	6b. OFFICE SYMBOL (If applicable)
6c. ADDRESS (City, State, and ZIP Code): DEPT. OF MATERIALS AND NUCLEAR ENGINEERING, COLLEGE PARK, MD 20742-2115	7a. NAME OF MONITORING ORGANIZATION: AFOSR/NE
	7b. ADDRESS (City, State, and ZIP Code): BLDG. 410, BOLLING AIR FORCE BASE, WASHINGTON, DC 20332
8a. NAME OF FUNDING/SPONSORING ORGANIZATION: AFOSR/NE	8b. OFFICE SYMBOL (If applicable)
8c. ADDRESS (City, State, and ZIP Code): Bldg 410, Bolling AFB DC 20332	9. PROCUREMENT INSTRUMENT IDENTIFICATION NUMBER: AFOSR-85-0367A
	10. SOURCE OF FUNDING NUMBERS: PROGRAM ELEMENT NO. 61102F; PROJECT NO. 2306; TASK NO. A1; WORK UNIT ACCESSION NO.

11. TITLE (Include Security Classification)
FUNDAMENTAL STUDIES ON HIGH TEMPERATURE DEFORMATION, RECRYSTALLIZATION AND GRAIN GROWTH BEHAVIOR OF TWO-PHASE MATERIALS

12. PERSONAL AUTHOR(S)
S. ANKEM, G. GREWAL AND M.N. VIJAYSHANKAR

13a. TYPE OF REPORT	13b. TIME COVERED	14. DATE OF REPORT (Year, Month, Day)	15. PAGE COUNT
FINAL	FROM 9/1/85 TO 11/30/89	SEPTEMBER 26, 1990	86

16. SUPPLEMENTARY NOTATION

17. COSATI CODES			18. SUBJECT TERMS (Continue on reverse if necessary and identify by block number)
FIELD	GROUP	SUB-GROUP	TITANIUM ALLOYS, TWO-PHASE MATERIALS, FEM, GRAIN GROWTH, PARTICLE COARSENING, HIGH TEMPERATURE DEFORMATION, STRAIN RATE.

19. ABSTRACT (Continue on reverse if necessary and identify by block number)

Two - phase Materials are technologically important because optimum properties can be obtained by proper combinations of phases. Among these materials, two-phase Titanium Alloys are of particular interest for high temperature aerospace applications. To design new alloys or to optimize the properties of existing Titanium alloys, it is essential to understand the deformation behavior and microstructure evolution of alpha, alpha-beta and beta Titanium alloys which is the subject of this investigation. Another aspect of this investigation is to determine the effect of strength difference between phases on deformation behavior of two-phase materials by the Finite Element Method.

It was found that the flow stress drops followed by steady state behavior observed in beta titanium alloys strongly depend on pre-strain, prior heat treatments, and amount and nature of alloying elements. The flow stress drops were attributed to the multiplication of mobile dislocations and the steady state behavior was attributed to the dynamic recovery leading to the formation of subgrains. In regard to the

20. DISTRIBUTION/AVAILABILITY OF ABSTRACT: ☒ UNCLASSIFIED/UNLIMITED ☐ SAME AS RPT. ☐ DTIC USERS	21. ABSTRACT SECURITY CLASSIFICATION: Unclassified
22a. NAME OF RESPONSIBLE INDIVIDUAL: B Boernstein	22b. TELEPHONE (Include Area Code): (202) 767-4933 / 22c. OFFICE SYMBOL: NE

DD Form 1473, JUN 86 — Previous editions are obsolete. SECURITY CLASSIFICATION OF THIS PAGE

DISTRIBUTION STATEMENT A
Approved for public release;
Distribution Unlimited

19. Abstract (continued)

alpha-beta titanium alloys, the flow stresses of alloys with nearly equal volume percent of phases were found to be much smaller than expected. This was attributed to interphase interface sliding.

Based on bulk diffusion considerations and condensing the growth of alpha and beta phases as a two way diffusion process of solute and solvent, the particle coarsening behavior was modeled. Based on these models and particle coarsening exponents, it is suggested that the rate controlling mechanisms changes as the temperature is increased and the mechanisms depend on the diffusivities of the alloying elements. For the first time the matrix grain growth behavior in the presence of growing second phase particles was modeled and the grain sizes predicted by these models were found to be close to those experimentally obtained.

A two dimensional FEM method has been employed to determine the stress strain relationships and stress and strain distributions in two-phase materials where the strength ratio between the stronger phase to the softer phase is varied from 2 to 5.

Department of
Chemical and Nuclear Engineering

Engineering Materials Program

College of Engineering
University of Maryland
College Park

FINAL TECHNICAL REPORT
SUBMITTED TO

Dr. ALAN H. ROSENSTEIN
AIR FORCE OFFICE OF
SCIENTIFIC RESEARCH, ELECTRONIC AND
SOLID STATE SCIENCES

BOLLING AIR FORCE BASE
WASHINGTON DC 20332

FOR THE PERIOD
SEPTEMBER 1, 1985 - NOVEMBER 30, 1989

FUNDAMENTAL STUDIES ON HIGH TEMPERATURE DEFORMATION RECRYSTALLIZATION, AND GRAIN GROWTH OF TWO - PHASE MATERIALS

BY

S. ANKEM, G. GREWAL, AND M. N. VIJAYSHANKAR

AFOSR - 85 - 0367

SEPTEMBER 1990

TABLE OF CONTENTS

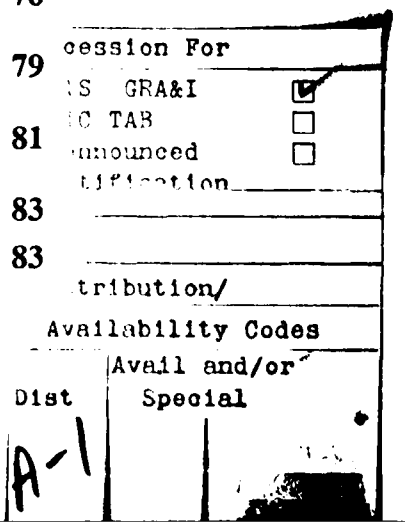

1. INTRODUCTION

Two - phase materials are technologically important because optimum properties can be obtained by a proper combination of the two phases. Among these materials, two - phase Titanium alloys are of particular interest for high temperature aerospace applications. However, there is a lack of understanding in the areas of high temperature deformation, recrystallization and grain growth behavior of two - phase alloys in terms of the properties of the component phases. Such an understanding is essential to develop new titanium alloys with greater high temperature strength and stability for high temperature applications.

The lack of understanding is due to the complex deformation behavior of these two - phase materials. Whenever a material comprising two or more phases is subjected to stress, the component phases deform differently and this results in inhomogeneous strai and stress distributions. In addition," interaction stresses" develop as a result of interactions between the deforming phases. For these reasons, the deformation behavior of two - phase materials cannot be explained by the simple " law of mixture rule ". This is due to the fact that the law of mixture rule always assumes either constant stress or constant strain and as mentioned before, this never happens in reality.

For many single phase materials, isothermal grain growth data can be represented by the empirical equation of the form

$$D = Kt^n$$

where D is the mean grain diameter, t is the time, K is a constant of proportionality and n is the grain growth exponent. It is also known that impurity atoms in solid solution and impurities in the form of inclusions and second phase particles retard grain growth. Furthermore, in two - phase materials, size and and volume fraction of the second phase is also known to effect the grain growth characteristics. However, there is no significant information as to the empirical relationships which can predict grain growth behavior in

two - phase materials. Recently, Ankem and Margolin derived empirical relationships for grain growth of two - phase alloys in terms of the volume fractions of phases. Their derivations are based on the experimental results on $\alpha - \beta$ titanium alloys. They found that under identical conditions $\alpha-$ phase retards grain growth of the $\beta-$ phase much more effectively tnan vice - versa. In addition, no atomistic or any other physical model was suggested for the matrix grain growth and particle coarsening in two - phase materials. Furthermore, it is not known how the diffusivities of the solute and solvent effect the particle coarsening and grain growth in two - phase materials.

The aim of this program is to systematically study the high temperature deformation, recrystallization and grain growth behavior of two - phase materials. While this study will be focussed on two - phase materials where both the phases can deform, it is expected that the information and mechanisms to be developed can be applied to any two - phase material system. It is hoped that the outcome of this study will be useful in improving processing (forging, rolling, superplastic forming, etc.) methods, obtaining optimal microstructures for improved mechanical properties and increasing the high temperature capability of two - phase materials. Such a fundamental knowledge will be of great help in developing new titanium alloys for high temperature applications.

2. OBJECTIVES OF THE PROGRAM

1. Determine the high temperature (923 - 1023 K) deformation behavior of two - phase Ti - Mn and Ti - V alloys. The factors to be varied include volume percent and nature of second phase (strength, diffusivity), temperature and strain rate.

2. Determine the high temperature deformation mechanisms in the two - phase titanium alloys : Slip, interface sliding, etc.

3. Study the particle coarsening and grain growth mechanisms and develop grain growth relationships for two - phase alloys in terms of the volume fraction of phases, diffusivities, temperature, etc.

4. Theoretically predict the stress - strain curves and stress and strain distributions in various two - phase materials.

5. Based on this information, propose models for high temperature deformation, recrystallization and grain growth of two - phase materials.

3. EXPERIMENTAL AND ANALYTICAL PROCEDURES

a. Materials

The materials required for this investigation were obtained from the RMI Company, Niles, Ohio. Six Ti - Mn and six Ti - V alloys were selected for this study. All of the alloys were melted as 13.6 Kg. (30 lbs) ingots. The chemical compositions are listed in Tables 1 and 2 and are also indicated by solid squares in Figures 1 and 2. The ingots were processed to 1.74 cm. (0.685 inch) diameter bars according to the procedure given in Figure 3. It is to be noted that the final processing (rolling) for all of the alloys were done in the a-b phase field. The amount of work given (60 % reduction in area) in this last step was found to be sufficient to recrystallize all of the alloys within 12 hours at 973 K.

b. Heat Treatments

Specimens each having a length of 3.5 inches (8.9 cm) were cut from the as - received bars and were heat treated in a vacuum furnace. Vacuum in the furnace was maintained in the range of 10-5 to 10 -6 mm Hg. A feedback controller was used to control the temperature. The variation in temperature between the front and back walls of the furnace was 7K. Titanium - Manganese alloys (Alloys 1 -6) were heated at 923, 973 and 1023 K for 200 hours whereas the Titanium - Vanadium alloys (Alloys 7 - 12) were heated at 923 and 973 K for 200 hours. On completion of heat treatment, argon gas was let into the chamber to produce a slightly positive pressures before being opened to air. The specimens were then pulled out of the chamber and quenched in water. The entire procedure of water quenching was accomplished within 80 - 90 seconds. These heat treatments resulted in equiaxed type microstructures. It is to be noted that , at a given temperature, though the alloy content varies the chemical compositions of the phases, as determined by the tie line, are expected to remain constant, Figures 1 and 2.

TABLE 1 : ACTUAL INGOT CHEMISTRY OF Ti - Mn ALLOYS					
ALLOY #	COMPOSITION OF THE INGOTS , WT. %				
	Mn	Fe	O*	N	C
1	0.4	0.02	0.071	0.01	0.02
2	3.0	0.01	0.086	0.01	0.02
3	4.8	0.01	0.082	0.006	0.01
4	6.0	0.01	0.083	0.008	0.01
5	9.4	0.02	0.100	0.010	0.02
6	13.0	0.01	0.116	0.012	0.02

* Oxygen content of final product.

Table 2: Aim compositions and the actual ingot chemistry of Ti-V alloys.

Alloy No.	Compositions (weight percent)					
	AIM	ACTUAL COMPOSITIONS OF INGOTS				
	% V	V	Fe	O *	N	C
7	3.9	4.3	0.01	0.078	0.017	0.02
8	6.0	6.2	0.01	0.063	0.015	0.01
9	8.3	8.1	0.01	0.082	0.016	0.02
10	10.5	10.6	0.01	0.075	0.020	0.02
11	12.8	12.6	0.01	0.083	0.019	0.02
12	15.0	14.8	0.01	0.093	0.021	0.02

* Oxygen content of final product.

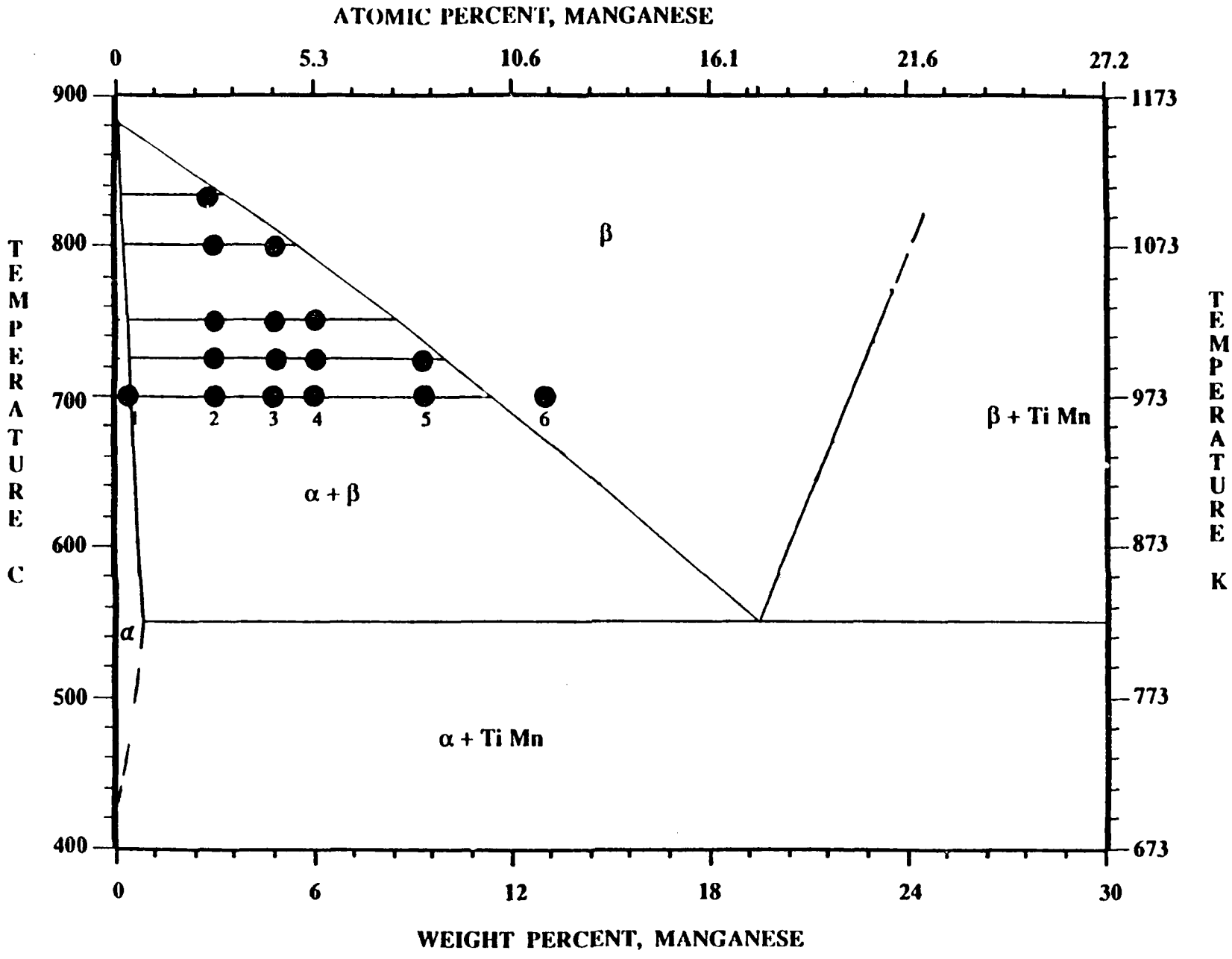

Fig. 1 :PARTIAL Ti END OF THE Ti-Mn PHASE DIAGRAM(10). THE ACTUAL COMPOSITIONS OF ALLOYS 1-6 AND THE TEMPERATURES OF INTEREST ARE INDICATED.

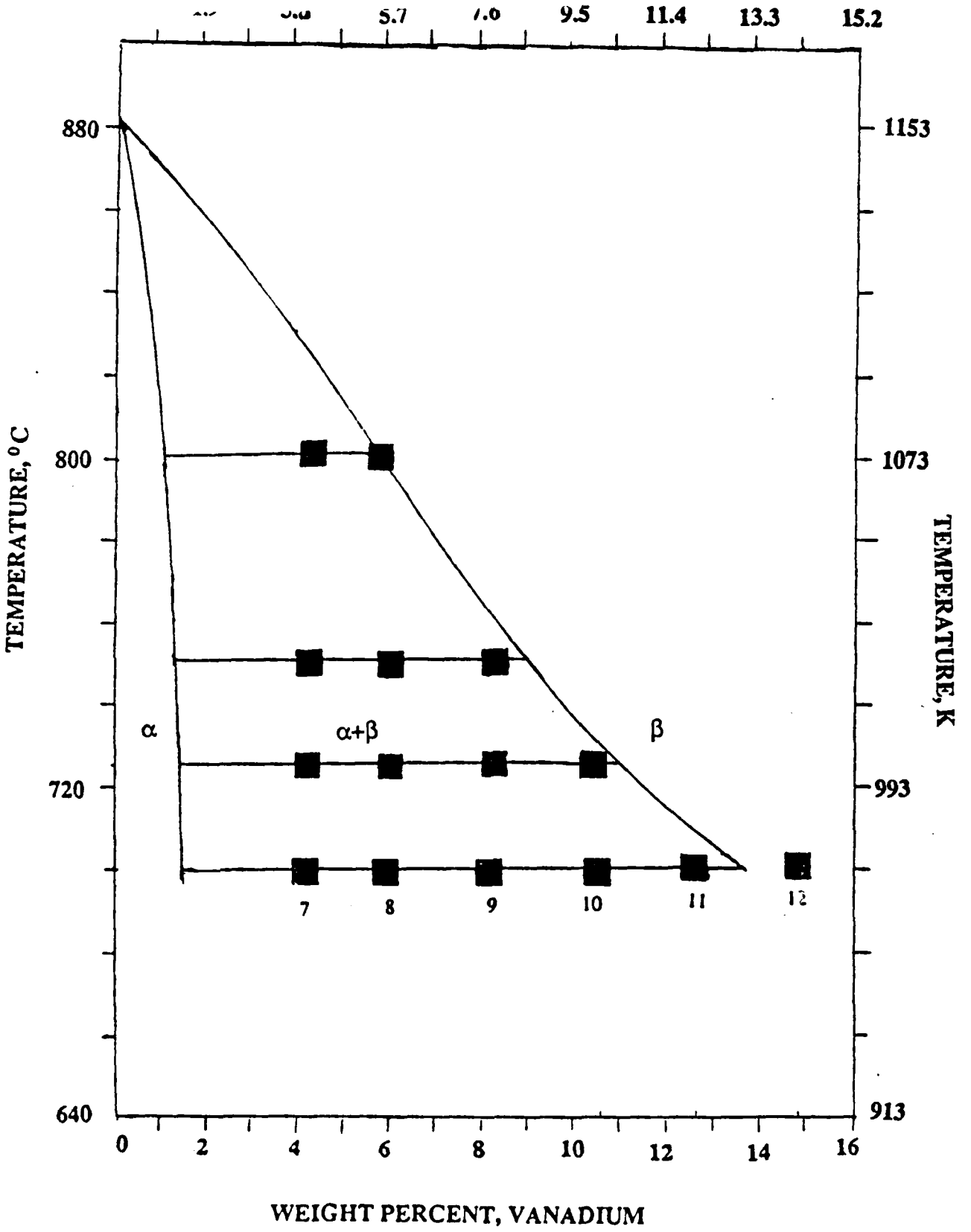

Fig. 2 : PARTIAL Ti OF THE Ti-V PHASE DIAGRAM (11). THE ACTUAL COMPOSITIONS OF ALLOYS 7-12 AND THE TEMPERATURES OF INTEREST ARE INDICATED.

c. Tensile Tests

Special pin type specimens were used for the tensile tests. To ensure that yielding starts at the center section rather than at the pin holes, the remaining transverse area of the specimen head to that of the gage section was maintained at a ratio of 3.08. It is worth mentioning that the grips and the pins were fabricated from special high temperature material, UDIMET 720, which has a 0.2 % yield stress about eight times that of the strongest Titanium alloys, a constant temperature zone of approximately 2 inch (5.08 cm) was used for heating the specimens to the test temperature. Use of the semi - cylindrical furnace facilitated mounting and removal of the specimen. The furnace was surrounded with a ceramic fibre insulation to enhance heating efficiency and to ensure temperature stability. A schematic of the test set - up for conducting the high temperature tensile tests is shown in Figure 3. All the tests were performed in a vacuum chamber, Fig. 3 equipped with a set of mechanical and turbo pumps. Vacuum was maintained in the range of $10^{-4}$to 10^{-5} torr. The temperature of the specimen was controlled and monitored through two sets of chromel - Alumel thermocouples connected to a feedback controller and a digital temperature gauge. The thermocouples were spot welded onto the gage section of the specimen about 1.2 inches apart. Temperature variation was controlled to within 5 ^{o}C. All the tests were conducted at strain rates in the range of 0.00011/s - 0.026/s.

Pin - type specimens provided easy access to mounting and removal of the specimens, especially when the grips were still hot. The specimens were subjected to a cyclic load during the pretesting period. This was done to prevent compression buildup because of the high vacuum and possible misalignment due to the thermal expansions of the specimens at elevated temperatures. The time prior to testing, which was necessary for evacuating the chamber and to bring the specimen to the test temperature, was about 5 hours. After the specimen

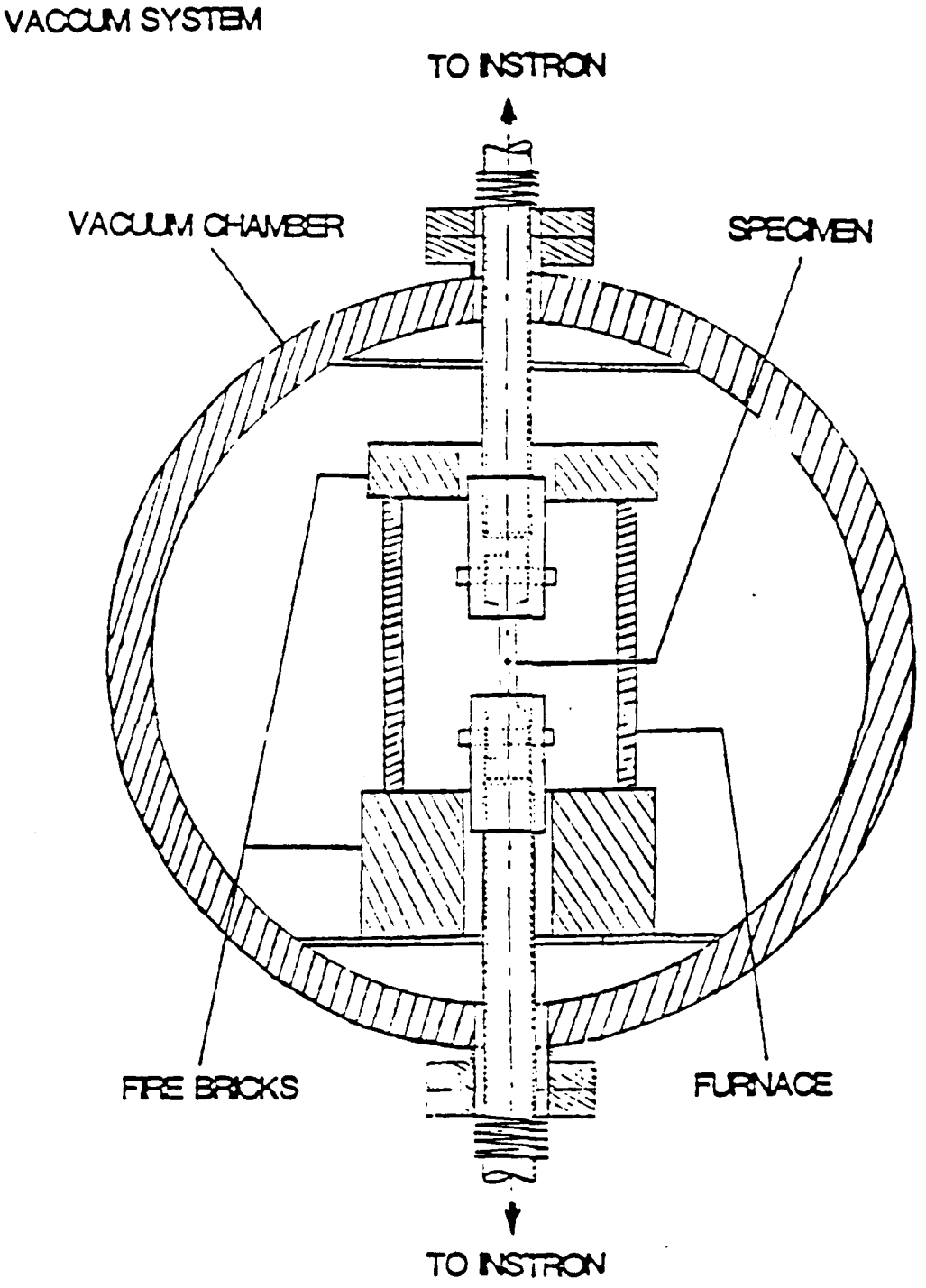

FIG 3: A SCHEMATIC OF THE HIGH TEMPERATURE VACUUM CHAMBER USED FOR THE TENSILE TEST.

had attained the test temperature, it was stabilized for a period of 20 minutes during which time a temperature stability test was conducted. The small preload selected during cycling was such that the creep contribution throughput heat - up and stabilization was insignificant.

d. Determination of Strain Rate Sensitivity Index

The relationship between the flow stress (s) and strain rate (e) at constant temperature and strain (e) can be expressed by the following relationship [1]

$$s = Cem$$

where C is a constant and m is the strain rate sensitivity.

The logarithm of the strain rate (log e) was plotted against the logarithm of the flow stress (log s) for a very low offset strain of 0.001. The slope of the plot gave the strain rate sensitivity (m) . The correlation coefficient obtained for determining the strain rate sensitivity was greater than 0.97 which suggests that the method employed is reasonably good.

e. Optical Metallography and SEM

Specimens for Optical and SEM studies were sectioned from annealed bars as well as from the deformed specimens. The sections were wet ground with 240, 320, 400, 600 mesh abrasive paper. Subsequently, these samples were electropolished using a solution with the following composition:

569 ml. Methanol

30 ml. Sulphuric acid

15 ml. Hydrofluoric acid

Polishing was carried out at a temperature of - 50^{o}C to -60 ^{o}C (233 to 213 K) and the volt-

age was about 20 V. After polishing , the specimens were washed in acetone to remove all traces or the electrolyte.

The alpha alloys were etched with Kroll etch for 10 seconds whereas a two step etching procedure, etching for 10 seconds with A - etch followed by etching with R - etch for 10 seconds, was used for the alpha -beta alloys. The compositions of A, R and Kroll etch are given below:

A - etch

25 ml. Hydrofluoric acid (50 %)

25 ml. Nitric Acid Conc.

50 ml. Glycerine

R -etch

17 ml. Benzalkonium Chloride

35 ml. Ethanol

Kroll - etch

2 ml. Hydrofluoric Acid (50 %)

4 ml. Nitric Acid Conc.

100 ml. Distilled water

For the determination of the volume percents of the α and β phases from Optical or SEM micrographs, a Summagraphics digitizer was used. Volume fractions were determined by the linear intercept method. A computer program was developed to analyse the digitized data

and to determine the volume fraction of the phases.

f. Transmission Electron Microscopy

For TEM studies, 400 - 500 μm thick samples were cut from the annealed and deformed specimens with a diamond saw. From these specimens, 3mm disks were prepared using a spark cutting machine. The disks were then mechanically ground to a thickness of 250 μm followed by electropolishing at -30 ^{o}C (243 K) using the following solution:

10 ml. Perchloric Acid

300 ml. Methanol

100 ml. N - Butanol

The final step consisted of electrothinning with a twin jet electropolishing unit at 25 - 30 ^{o}C (298 - 303 K) until a hole was formed at the center of the disc with the following solution:

10 gms. Zinc Chloride

5 gms. Aluminum Chloride

300 ml. Methanol

50 ml. N - Butanol

A JEOL 100 KV electron microscope was used for all of the TEM studies.

g. FEM Analysis

The NASTRAN computer program [2 -4], Rigid Format No. 6 called "Piecewise Linear Analysis" was used to model the stress -strain behavior of an $\alpha - \beta$ alloy (Alloy 3) comprising 63 % α and 37 % β. A typical FEM mesh is shown in Figure 4. Volume percent of the second phase (shaded) beta is 36.7 %. The unshaded region represents the matrix alpha phase. Each triangle in the mesh, Figure 4, is a two dimensional (plane stress) plate element. The nodes on edge AC are constrained from moving in the x - direction and the nodes

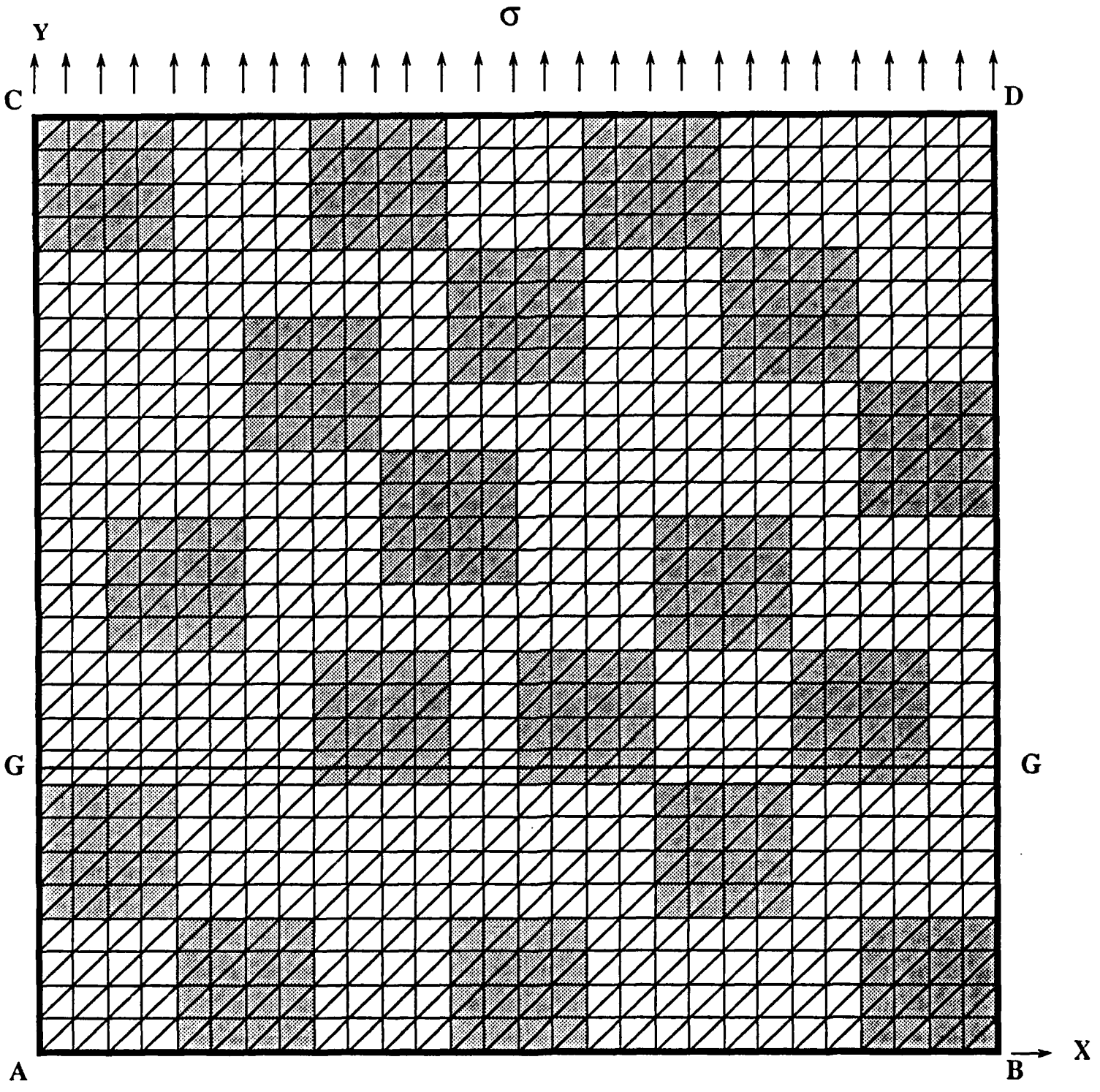

Fig. 4 : Mesh with β particles (36.7 %), shaded, in α matrix, unshaded .

on edge AB are constrained from moving in the y - direction. All the other nodes are free to move both in the x and y - direction. Multipoint constraints were imposed on all nodes on the edge CD so that the displacements are the same for a given stress level. With these constraints, the mesh represents one quarter of a tensile specimen in two dimensions.

The load was applied in the y- direction as shown in Figure 4. This load is increased in predetermined increments and the first few increments are such that all the stresses developed are in the elastic region. The method used to calculate the stress and strain distributions is similar to that used by Ankem and Margolin [4] . The local stresses and strains were calculated for a given section, for example section G-G of Figure 4. The strains in the elements along section G -G are obtained from the relative displacements of the nodes just above and below the section. Since each small square consists of two adjacent triangular slements of the same phase, to obtain the stress at a point (marked as solid circles in figure 8) the stresses in the respective elements are averaged over these elements.

4. RESULTS AND DISCUSSION

This section is divided into three parts. The first part deals with the high temperature deformation behavior of a, a-b and b Titanium alloys. In the second part , the results of the studies on microstructure evolution in two - phase Titanium alloys is given. Finally, predictions of the stress - strain behavior and stress and strain distribution of various two phase materials are given in the third part. It is to be noted that most of the work already published , see publication 1 - 8, and hence only salient features are presented here. With regard to the first part, the work is still in progress and hence the results and the conclusions thereof prescribed here should be considered as prelimnary.

A. HIGH TEMPERATURE DEFORMATION BEHAVIOR OF ALPHA, ALPHA-BETA, BETA ALLOYS.

The heat treatments described earlier resulted in equiaxed type microstructures. The microstructures of Ti- Mn alloys corresponding to the 923, 973, and 1023 K are shown in Figures 5 - 7. Similarly, the microstructures of the Ti - V alloys corresponding to the temperatures 923 and 973 are shown in Figures 8 and 9.

a. Alpha Alloys

True stress true stress-true strain curves of alloy 1 corresponding to 650, and 700^{o}C are shown in Fig. 10 and 11, respectively. Similar curves were obtained for 750 ^{o}C but they are not shown here. These figures show that as increase in strain rate for a given temperature results in increased strain hardening, as expected. In addition, for a given strain rate, the flow stress decreases with an increase in temperature as expected. An extensive analysis of the data and TEM analysis of the deformed specimen is underway. Preliminary results indicate that the activation energy for deformation is close to the self bulk diffusion of titanium indicating that the process is diffusion controlled. Similar observations could not be made for the alpha- phase Ti-V system because, according to the currently available phase diagram in the handbooks for Ti-V, the alloy No. 7 should have been all alpha but to our surprise it has more than 20 % beta at 700 ^{o}C. This point will be discussed in detail in the next section dealing with microstructure evolution.

b. Beta Alloys

An extensive evaluation of the results pertaining to this part of the investigation is pre-

ALLOY 1 (~ 100 % α)

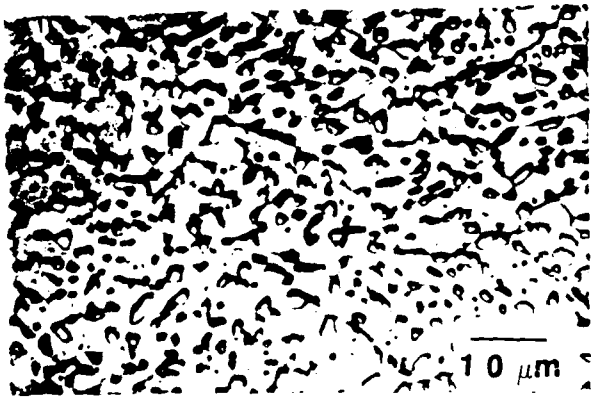

ALLOY 2 (84 % α – 16 % β)

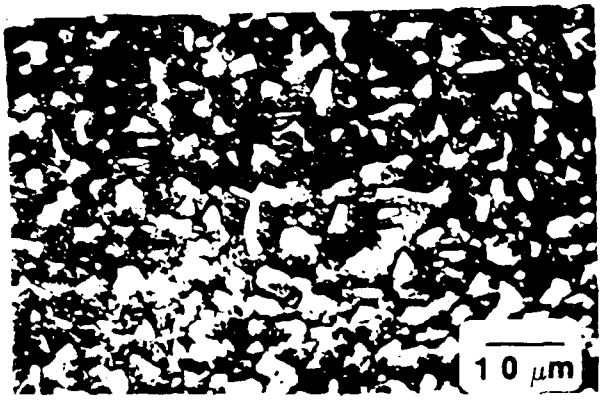

ALLOY 3 (67 % α – 33 % β)

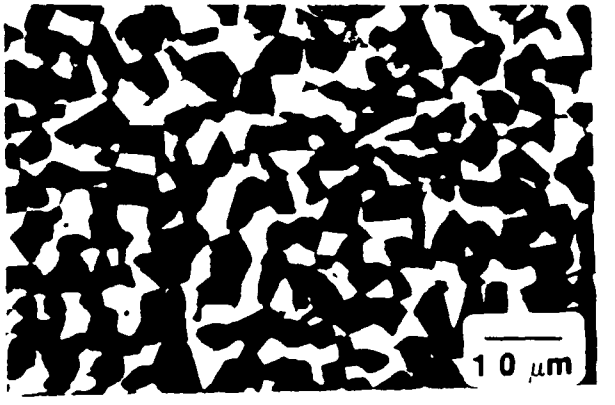

ALLOY 4 (60 % α – 40 % β)

ALLOY 5 (37 % α – 63 % β)

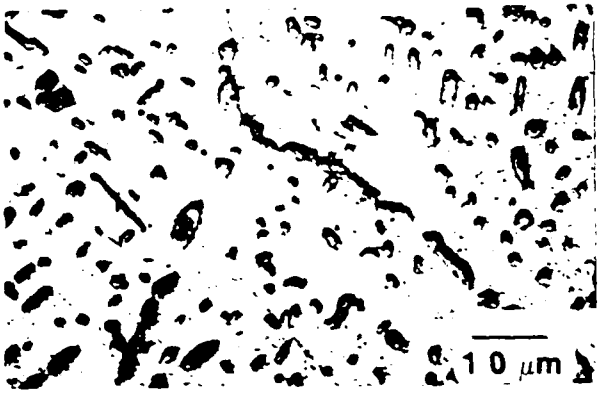

ALLOY 6 (12 % α – 88 % β)

FIG. 5 : MICROSTRUCTURES OF VARIOUS α, α–β AND β Ti- Mn ALLOYS ANNEALED FOR 200 HRS. AT 923 K W.Q.

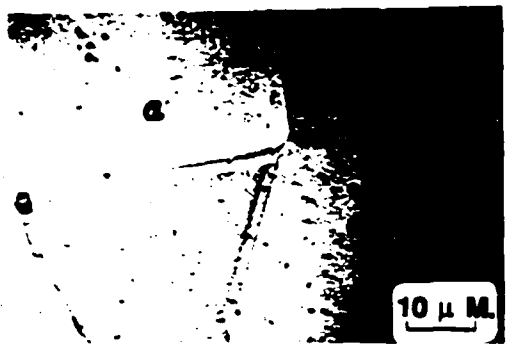

Alloy 1 (~ 100 % α)

Alloy 2 (79 % α + 21 % β)

Alloy 3 (63 % α + 37 % β)

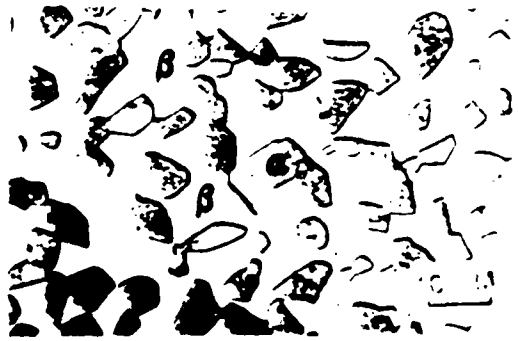

Alloy 4 (45 % α + 55 % β)

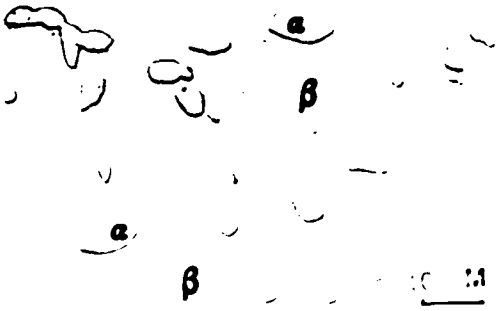

Alloy 5 (10 % α + 90 % β)

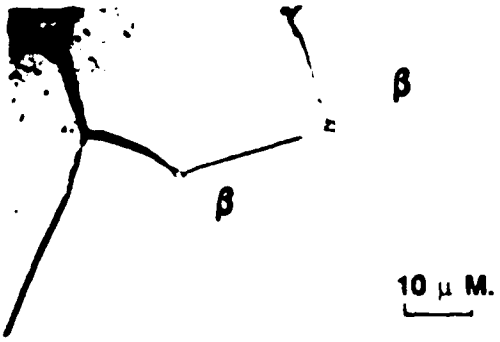

Alloy 6 (~ 100 % β)

FIG. 6 : MICROSTRUCTURES OF VARIOUS α, α–β AND β Ti- Mn ALLOYS ANNEALED FOR 200 HRS. AT 973 K W.Q.

ALLOY 1 (~ 100 % α)

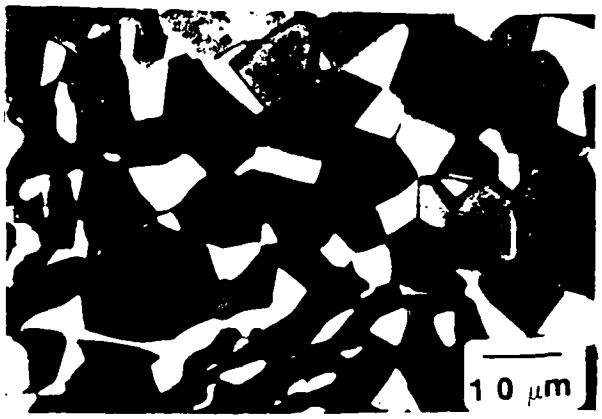

ALLOY 2 (74 % α - 26 % β)

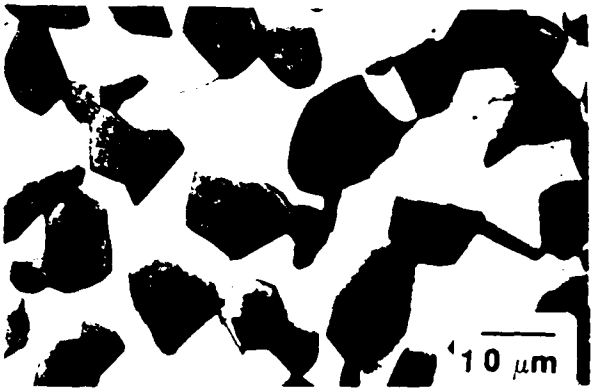

ALLOY 3 (49 % α - 51 % β)

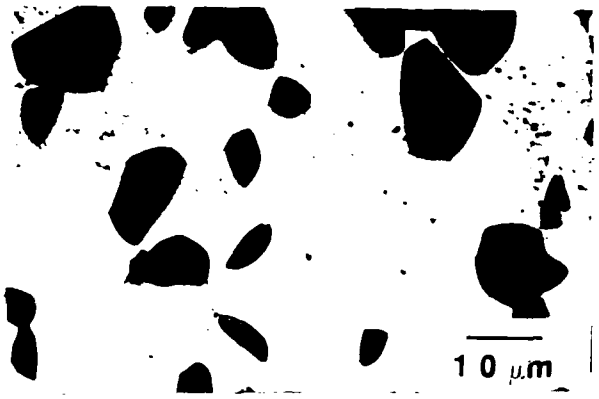

ALLOY 4 (18 % α - 82 % β)

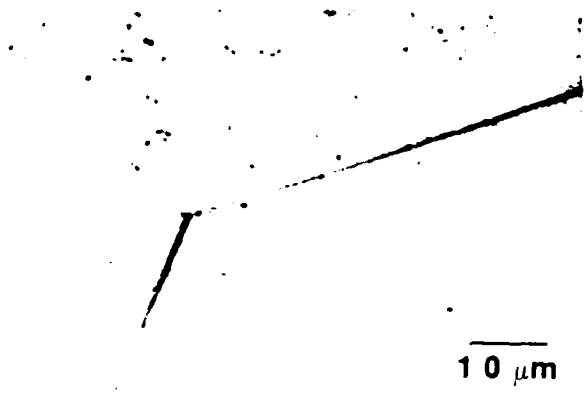

ALLOY 5 (~ 100 % β)

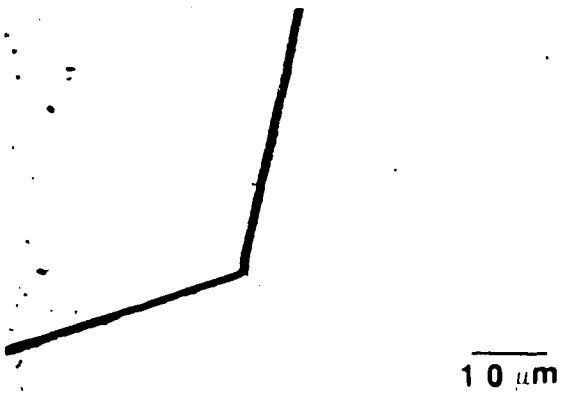

ALLOY 6 (100 % β)

FIG. 7 : MICROSTRUCTURES OF VARIOUS α, α–β AND β Ti- Mn ALLOYS ANNEALED FOR 200 HRS. AT 1023 K W.Q.

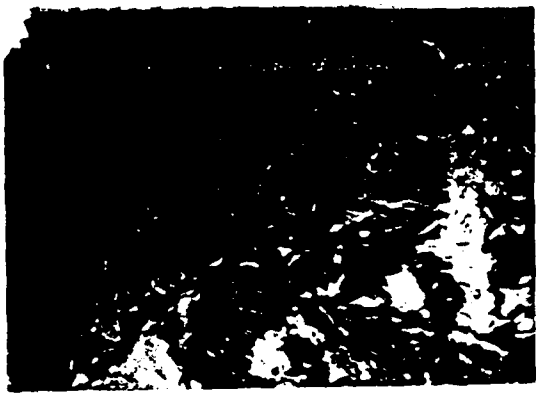

ALLOY 7 (83% α–17% β)

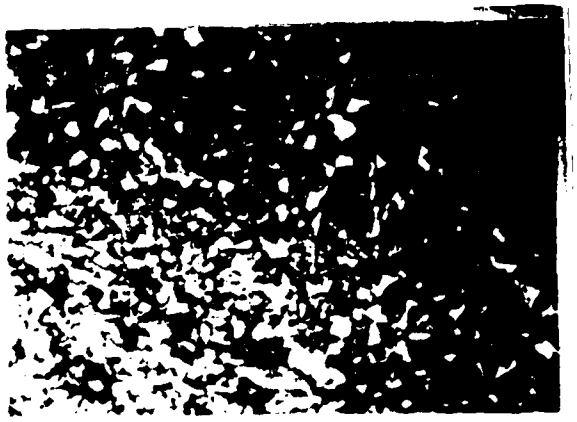

ALLOY 8 (71% α–29% β)

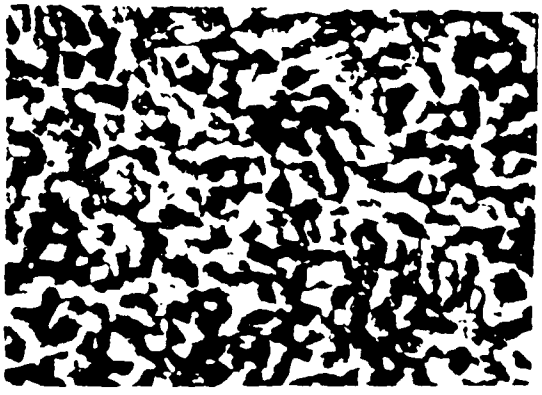

ALLOY 9 (59% α–41% β)

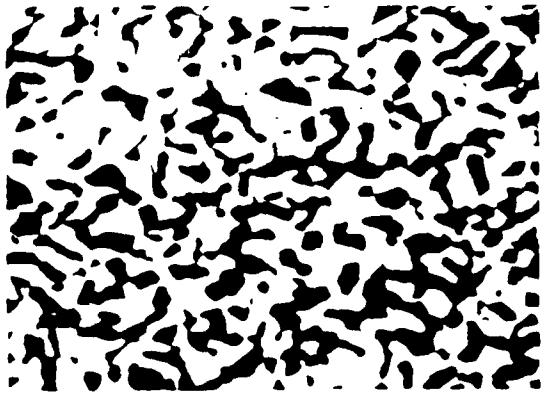

ALLOY 10 (43% α–57% β)

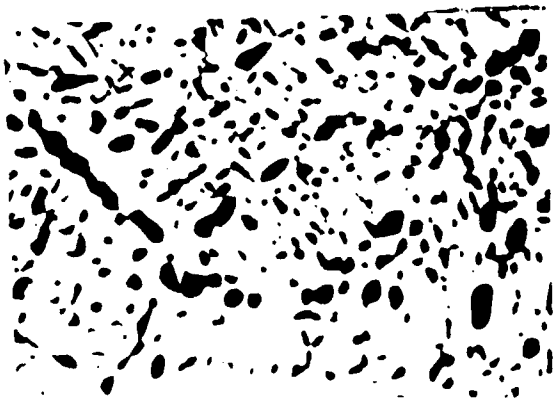

ALLOY 11 (32% α– 68% β)

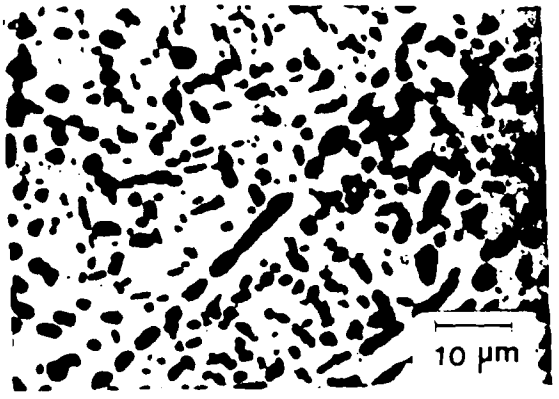

ALLOY 12 (16% α–84% β)

FIG. 8 : MICROSTRUCTURES OF VARIOUS α, α–β AND β Ti -V ALLOYS ANNEALED FOR 200 HRS. AT 923 K

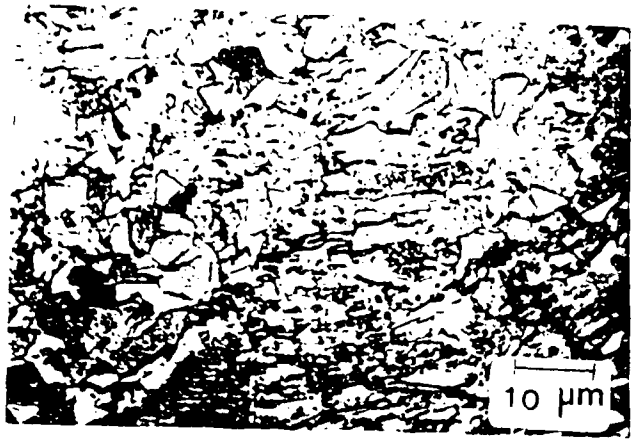

ALLOY 7 (70 % α – 30 % β)

ALLOY 8 (56 % α – 44 % β)

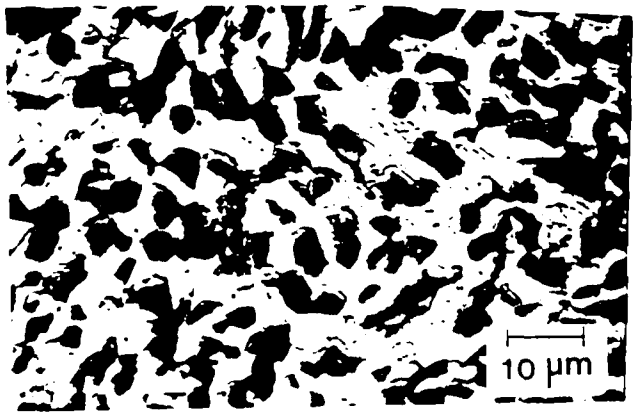

ALLOY 9 (44 % α – 56 % β)

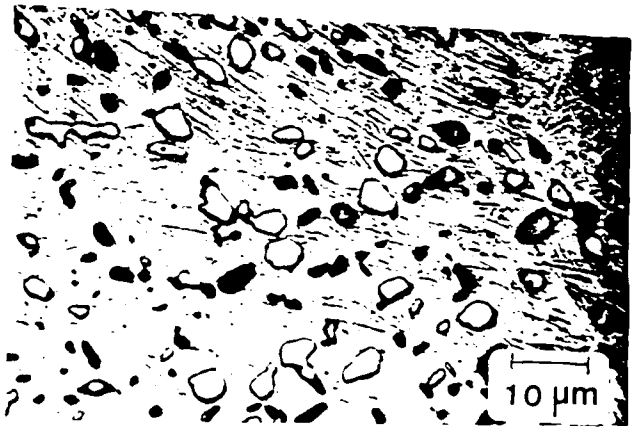

ALLOY 10 (29 % α – 71 % β)

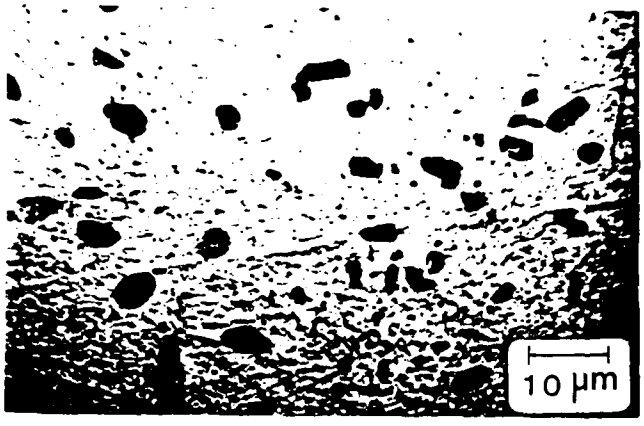

ALLOY 11 (8 % α – 92 % β)

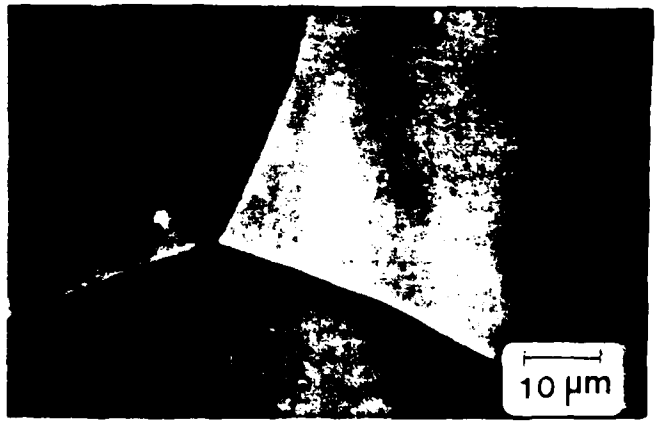

ALLOY 12 (~ 100 % β)

FIG. 9 : MICROSTRUCTURES OF VARIOUS α, α–β AND β Ti- V ALLOYS ANNEALED FOR 200 HRS. AT 973 K W.Q.

FIG10 : TRUE STRESS - TRUE STRAIN CURVES OF ALLOY 1 (100 % α, Ti-Mn ALLOY) TESTED IN VACUUM AT 923 ^{O} C AT DIFFERENT STRAIN RATES.

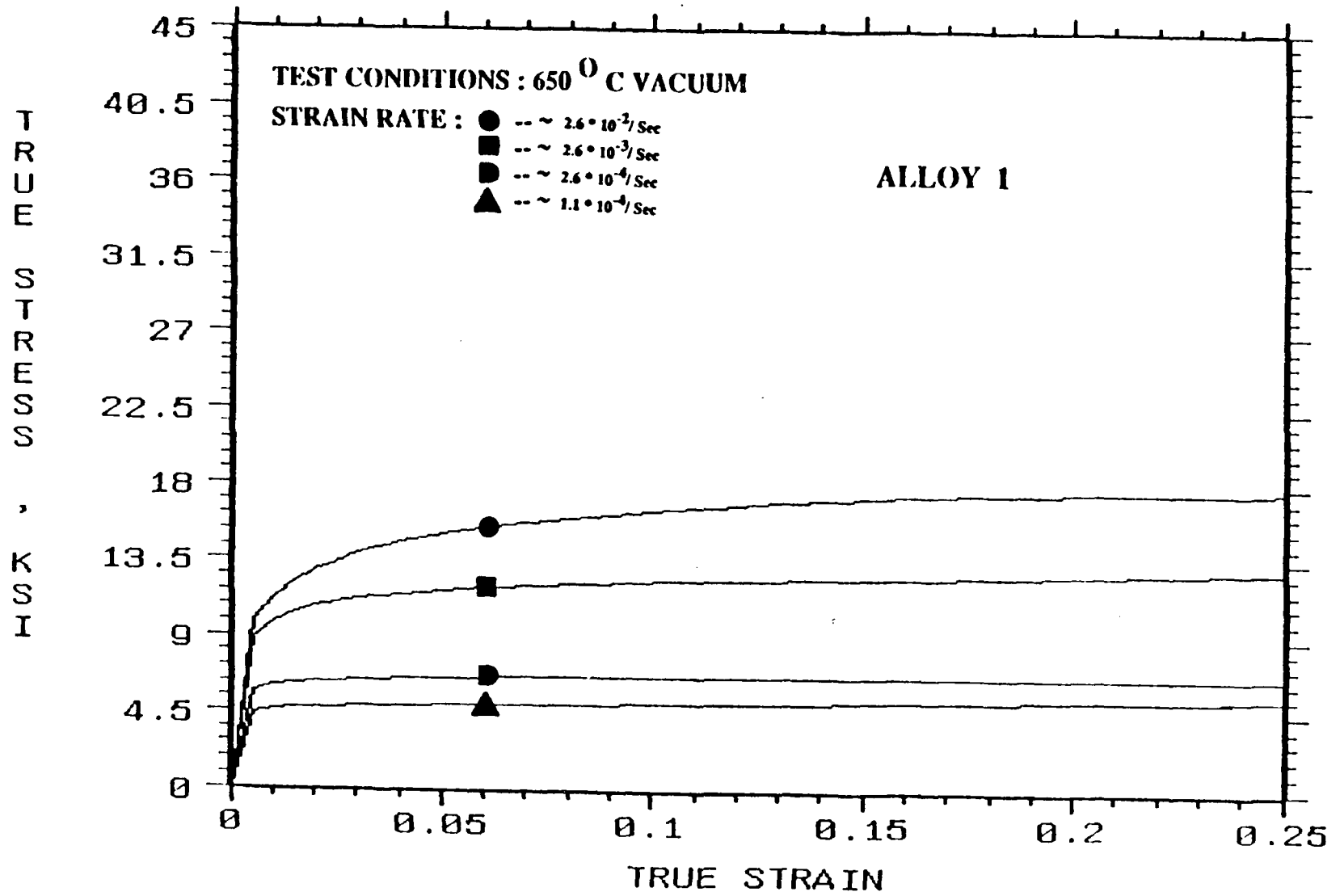

Fig.11: TRUE STRESS - TRUE STRAIN CURVES OF ALLOY 1(100 %α , Ti-Mn ALLOY) TESTED IN VACUUM AT 973 ^{O}K AT DIFFERENT STRAIN RATES.

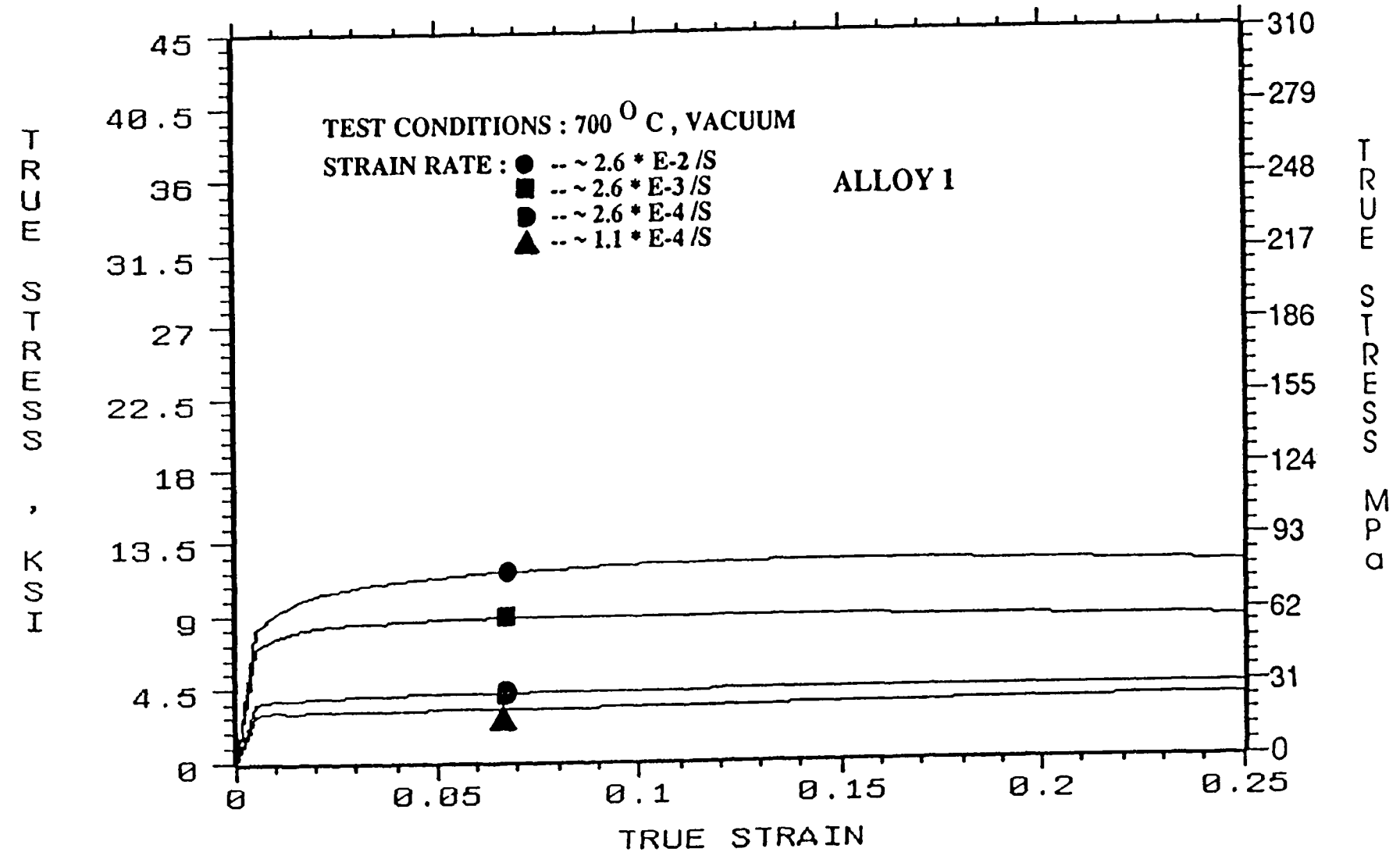

sented in References 6, 10 and 13. Some important features are presented here.

The β -phase alloys exhibited sharp flow stress drops followed by steady state behavior, for example see curve A in figure 12. It was found that the amount of flow stress drop depended on the strain rate, amount of solute content, nature of the alloying elements and prior heat treatments and prestrain. The effect of prestrain can be seen in Fig.12. A small prestrain significantly decreases the flow stresses. This is a very important result because it suggests that the magnitude of flow stress and hence loads to deform the material can be decreased by prestraining.

In the past, both the flow stress drop and the steady state behavior were attributed to the formation of subgrains such as those shown in Fig.13. However, based on various special tests (6,10,12) including that shown in the Fig.12, we have suggested that the initial drop is due to the multiplication of mobile dislocations and the subsequent steady state behaviour is due to dynamic recovery leading to the formation of subgrains.

c. Alpha-Beta Alloys

Some of the results of this part of the investigation have been presented in ref.6. The reader is referred to this refrence fand earlier reports for details. At higher strain rates α–β alloys also exhibited flow stress drops. The extent of drop increased with an increase in β content. For illustration, the stress-strain curves of Alloy3, which is a Ti-Mn alloy consisting of 63% α and 37% β, is shown in Fig.14. Since the alpha-phase has no flow stress drop, it was thought that the stresses in the stronger beta-phase must be higher than the average applied stresses so that the beta-phase plastically deform causing flow stress drop in the α–β alloys. To prove this FEM bar has been enclosed, see Fig.4, where the stress-strian curves of α and β phases corresponding to a load of 71 MPa along the section G-G of Fig.4 are shown in Fig15 and Fig.16 respectively. The stresses are higher and strains lower in the harder β phase.

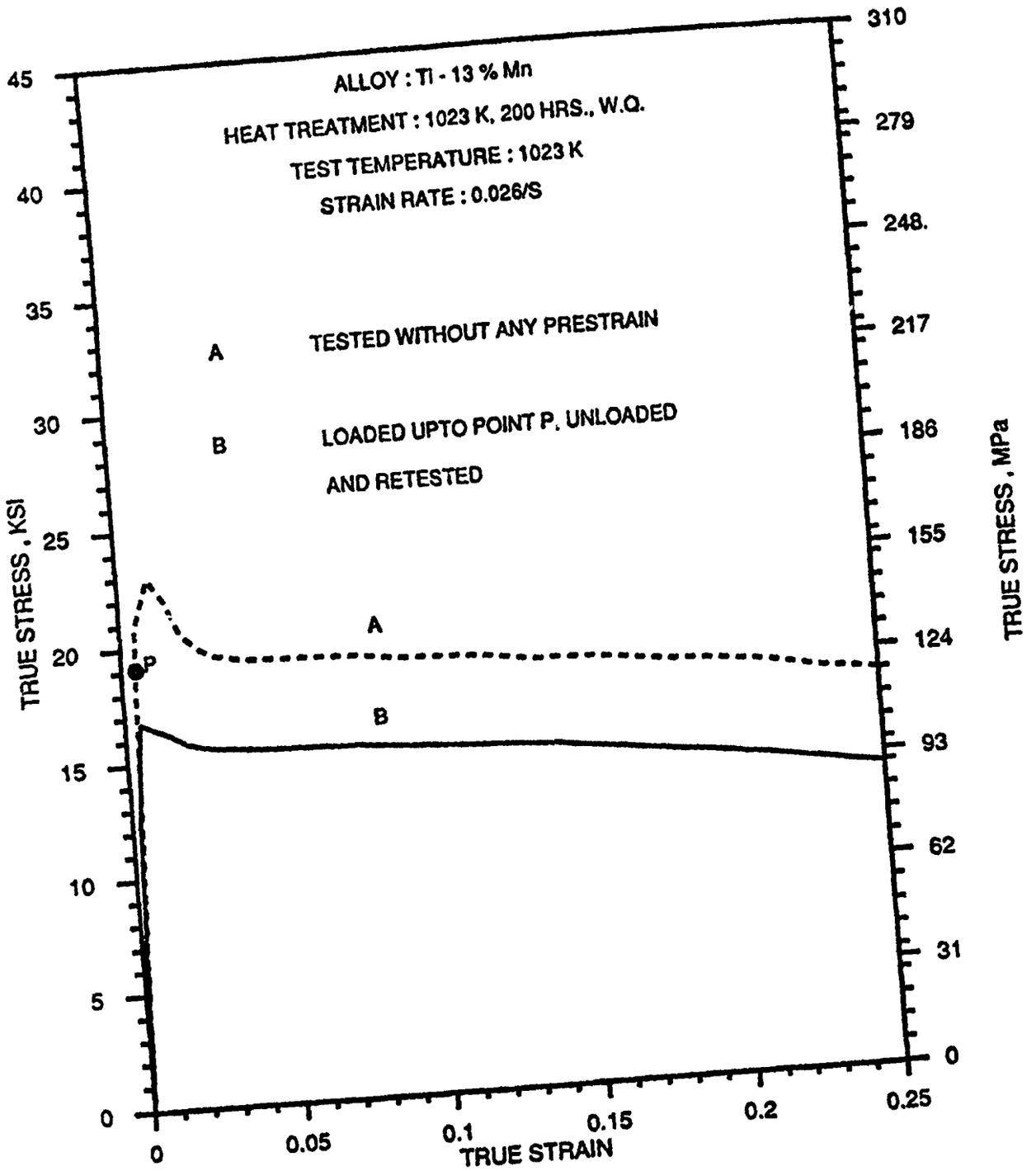

Fig12 : Effect of prestrain on the stress - strain behavior of a beta Ti - Mn alloy.

(a)

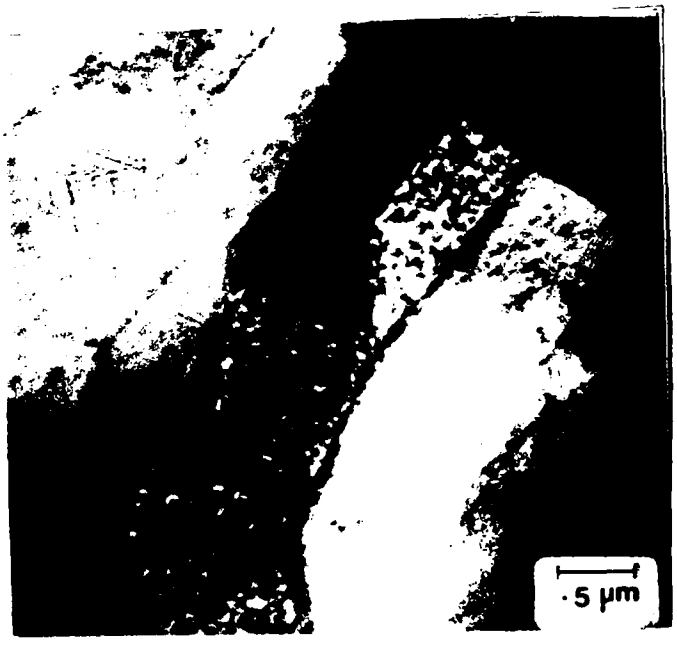

(b)

Fig.13: Transmission electron micrographs of Ti alloys after deformation. Test conditions :973 K, 0.026 s^{-1}, 25 % strain (a) Alloy 6 showing dislocation structure inside subgrains. (b) Alloy 12 showing subgrain formation.

Fig.14: TRUE STRESS-TRUE STRAIN CURVES OF ALLOY 3 (63 % α - 37 % β, Ti - Mn ALLOY) TESTED IN VACUUM AT 973°K AT DIFFERENT STRAIN RATES.

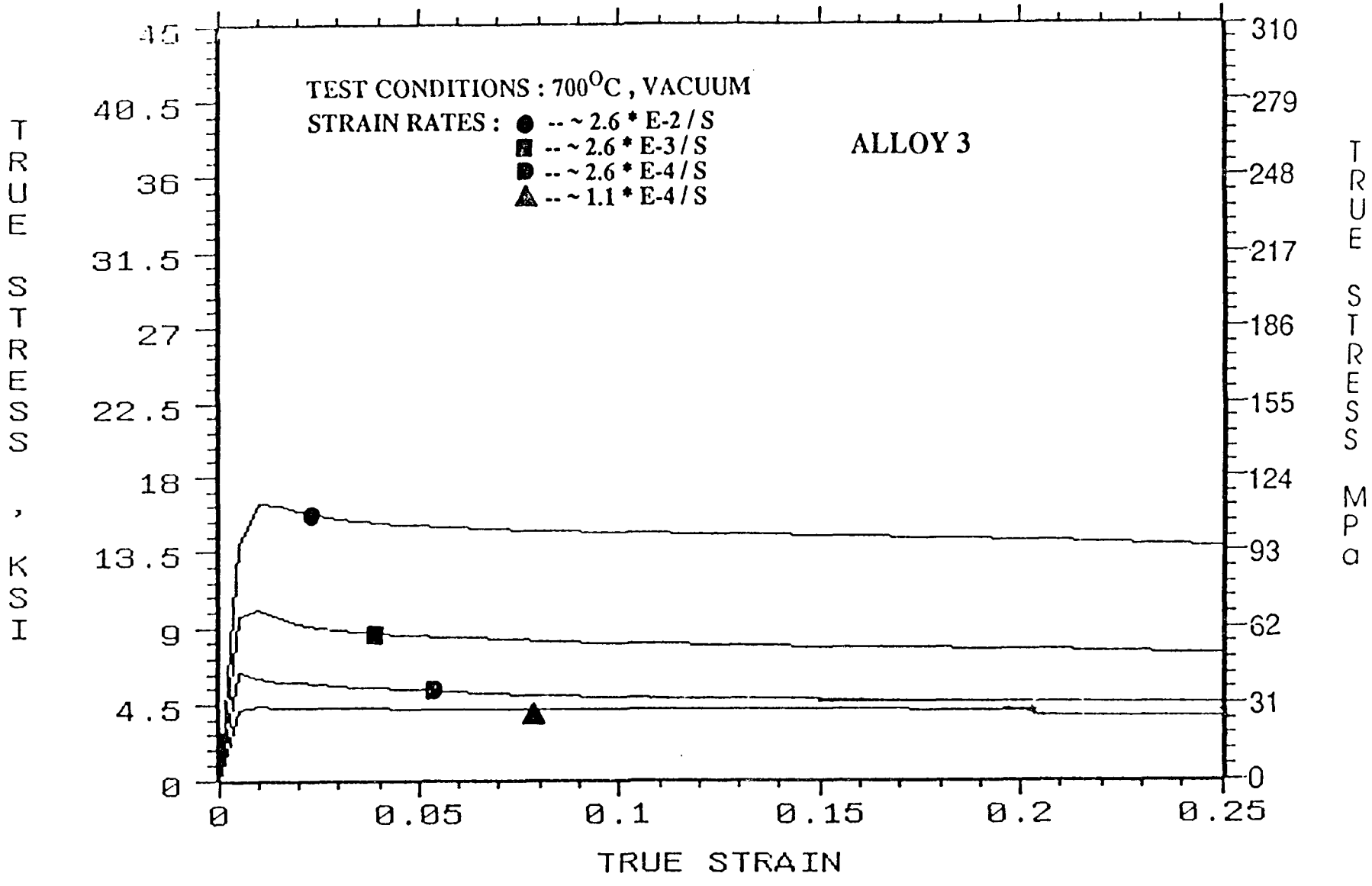

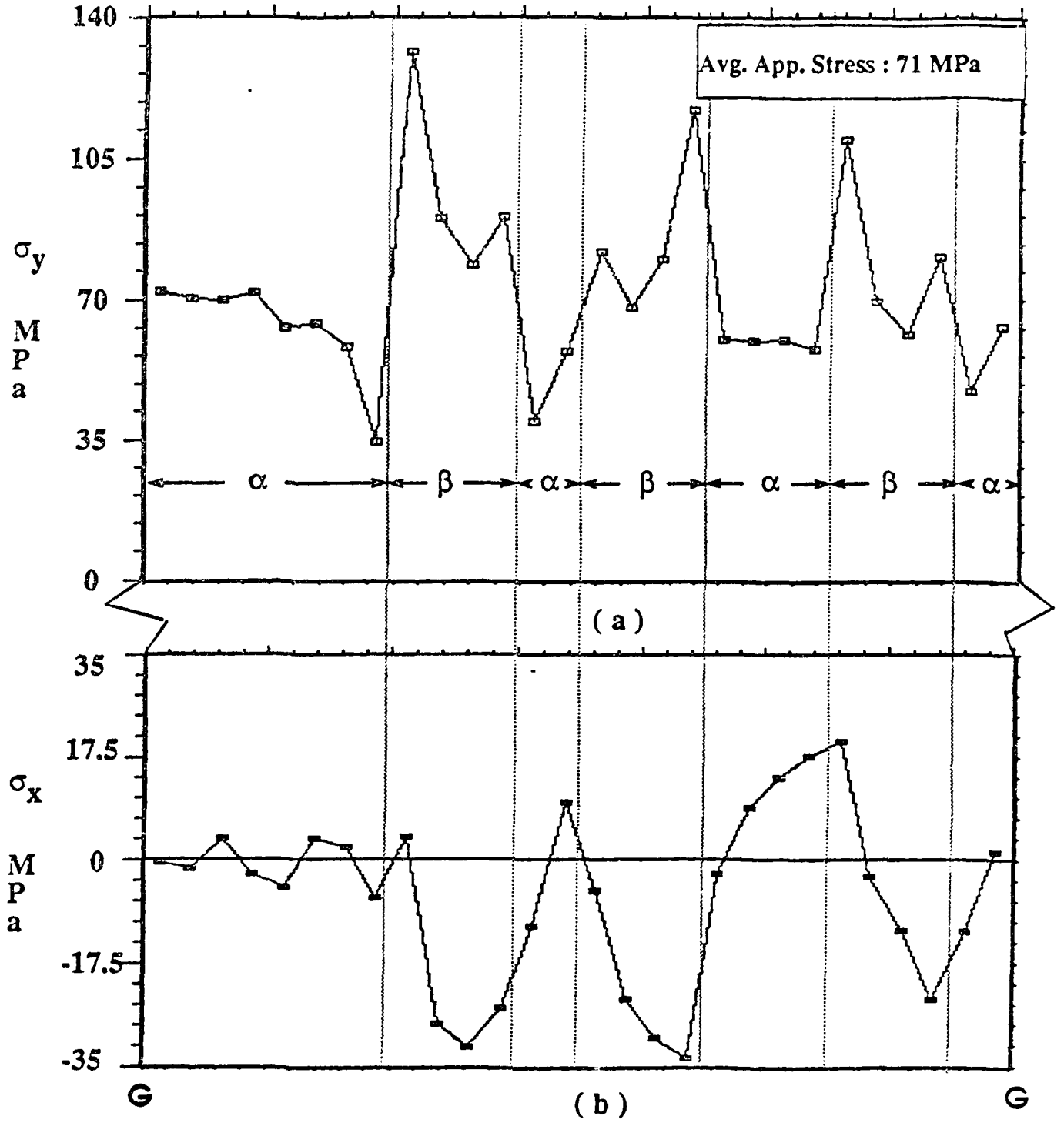

Fig. 15: Longitudinal and transverse stress distribution along section G - G of Fig. 4 : (a) Longitudinal stress distribution. (b) Transverse stress distribuiton.

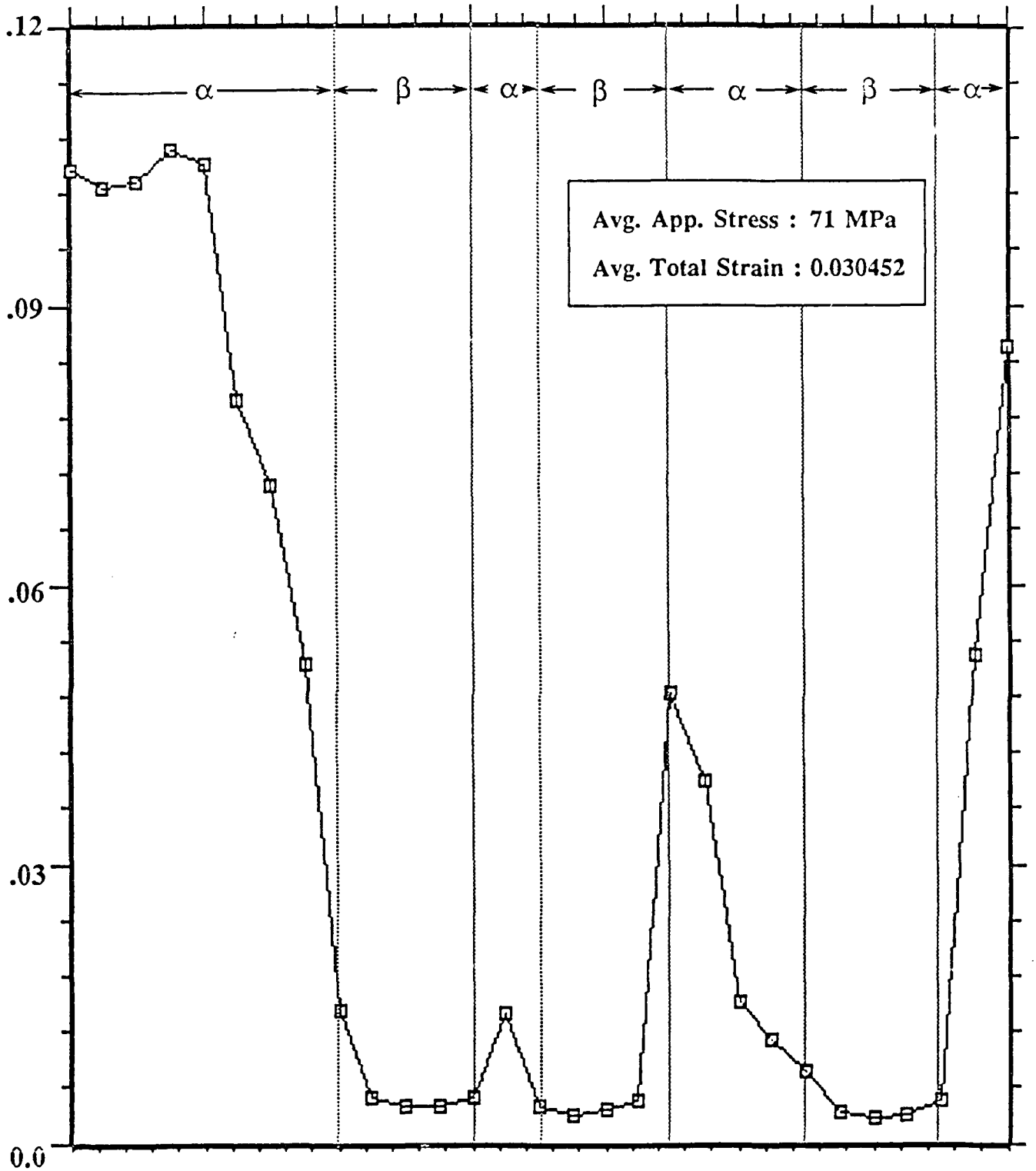

Fig.16- Longitudinal strain distribution along section G - G of Fig.4

With respect to the flow stresses of $\alpha-\beta$ alloys at low strain rates, very interesting results were obtained.. The flow stress of alloys with nearly equal volume percent of phases are much lower than expected- figure 17 and 18. In fact, there is no significant difference in the flow stresses corresponding to 650 and 700 ^{o}C for alloys with near equal volume percents of phases. The strain rate sensitivity were also found to be higher (6) for those alloys. Based on those results, we have suggested that interface sliding is a major deformation mechanism at the temperature and strain rate employed. We are currently in an extensive analysis of the stress-strain data including estimation of activation energies and TEM examination of $\alpha-\beta$ Ti-Mn and Ti-V alloys. Preliminary results indicate that the lower flow stresses of $\alpha-\beta$ titanium alloys with near equal volume percent of phases is due to interface sliding.

B. MICROSTRUCTURE EVOLUTION IN TWO PHASE ALLOYS

a. Solubility of Vanadium in Alpha, and Beta Titanium

During the initial stages of the investigation on microstructural coarsening behavior of two phase titanium alloys it was found that the Ti-V phase diagram available to date is incorrect with respect to the solubility of vanadium in alpha phase. The diagram predicted 0.04 vol. fraction of the beta phase, while the experimentally obtained volume fraction of the beta phase was about 0.24. The main objectives of this investigation was to revise the Ti-V phase diagram and to accurately determine correct solubility of vanadium in alpha and beta phases in the temperature range 973-1098 K. For this investigation five two phase Ti-V alloys were used. The alloys were heat treated in vacuum at 973 K, 1023 K, 1073 K and 1098 K for 400 hours followed by water quencing. To determine the two phase boundaries of the phase diagram a two fold approach comprising of microprobe analysis of the individual phases and metallographic determination of volume fraction of individual phases was used. The new phase diagram obtained is compared with the existing diagram in Fig. 19. Details

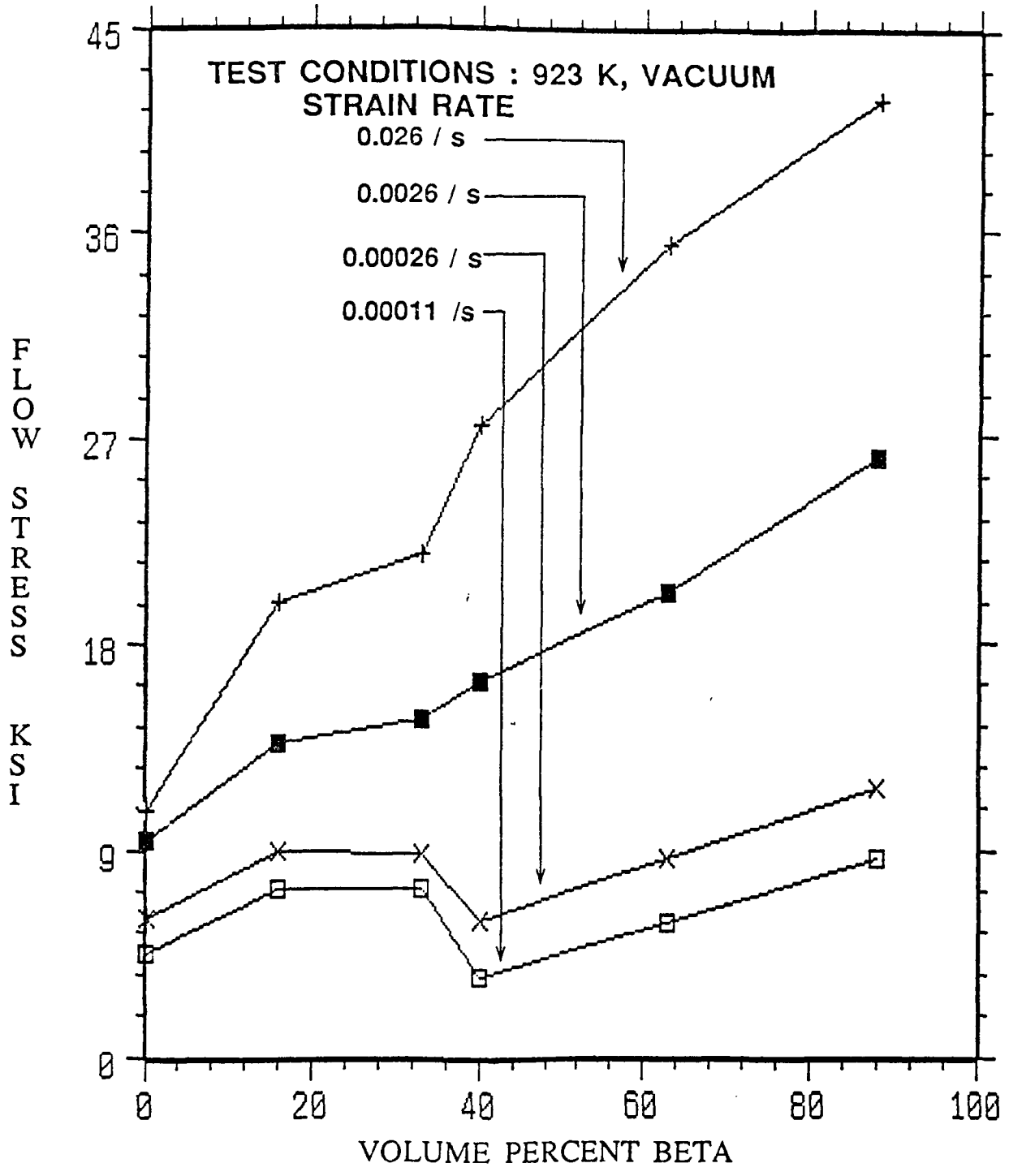

Fig 17: FLOW STRESS Vs β VOL. % FOR DIFFERENT α – β Ti - Mn ALLOYS. FLOW STRESS CORRESPONDS TO 0.2 % PLASTIC STRAIN.

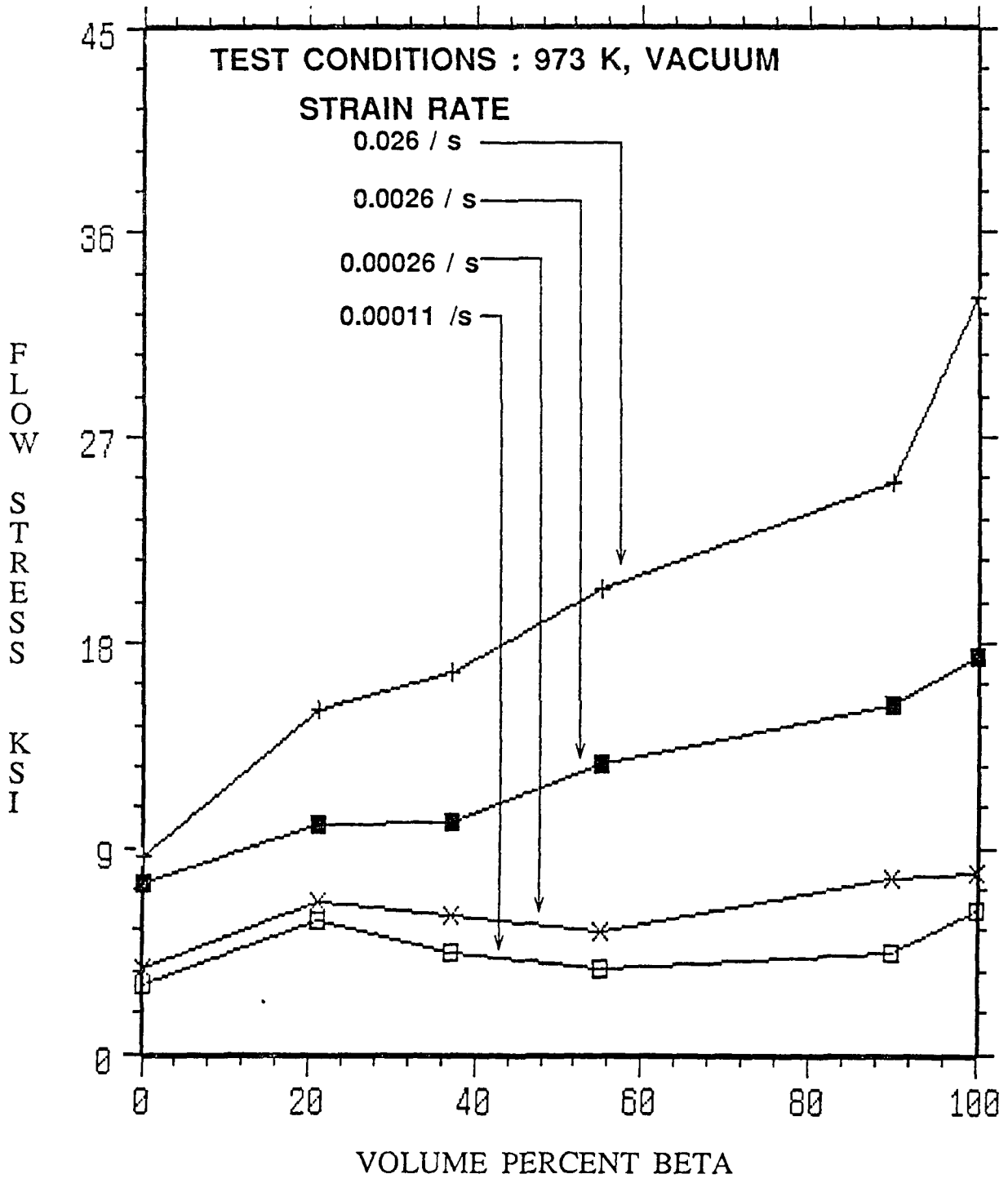

Fig18 : FLOW STRESS Vs β VOL. % FOR DIFFERENT α – β Ti - Mn ALLOYS. FLOW STRESS CORRESPONDS TO 0.2 % PLASTIC STRAIN.

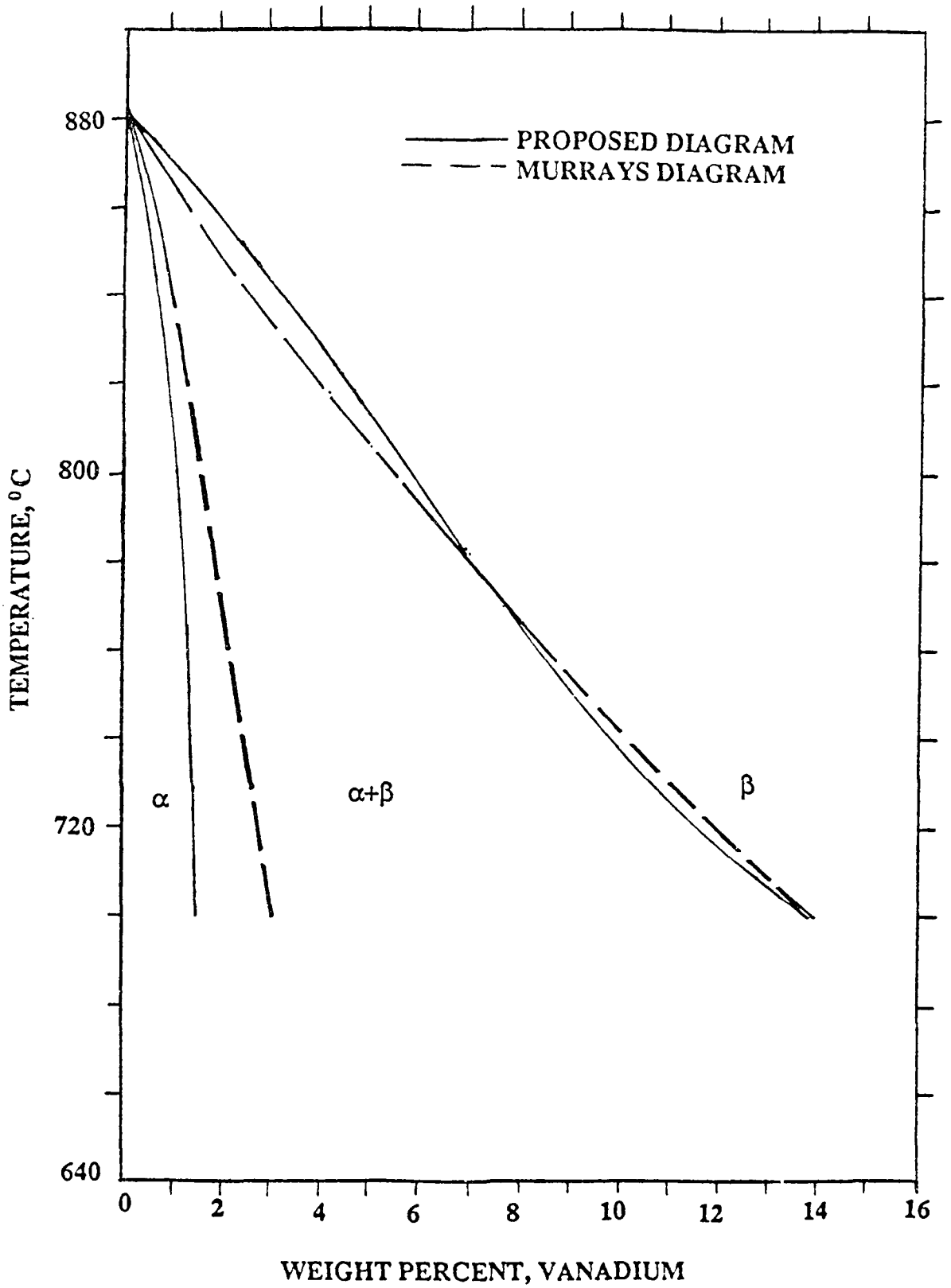

Fig. 19: A COMPARISON OF THE PROPOSED Ti RICH END OF THE Ti-V PHASE DIAGRAM WITH THAT OF MURRAYS (41).

are given in Ref. 7.

b. Isothermal Particle Growth in two Phase Titanium Alloys

The aim of this study was to systematically study the effect of volume percents of phases, temperature and diffusivity of the alloying elements on the particle growth kinetics of $\alpha - \beta$ titanium alloys. It is hoped that such an understanding will be helpful for optimizing the microstructure of $\alpha - \beta$ titanium alloys through thermo-mechanical treatments and in developing new titanium alloys with increased microstructural stability for high temperature applications.

Isothermal particle growth studies were carried out on six Ti-Mn and six Ti-V alloys. These systems were selected because the intrinsic diffusivities as well as the interdiffusion coefficient in the Ti-Mn system are approximately an order of magnitude higher than the corresponding diffusivities in Ti-V system. These alloys were heat treated for 25, 50, 100, 200 and 400 hours at 973 K followed by water quenching. The heat treatments were carried out in vacuum encapsulated quartz tubes. The specimens were sealed in batches of twelve at a pressure less than or equal to 10^{-5} torr. The technique adopted to determine the volume percents as well as the particle sizes was the linear intercept method It was found that the particle growth kinetics of the α and the β phases could be represented by simple equations in terms of time and volume percents of the phases.

$$d_{\beta}^{\alpha-\beta} = (K_{\beta} / V_{\alpha}^{m_{\alpha}}) . t^{n}$$

$$d_{\alpha}^{\alpha-\beta} = (K_{\alpha} / V_{\beta}^{m_{\beta}}) . t^{n}$$

To rationalize the observed coarsening behavior of two phase alloys an atomistic model was developed. The growth process is modeled as a two-way diffusion process where the solvent and the solute atoms move in opposite directions resulting in conversion of α to β and β to α leading to the growth of the particles. In addition, the Lifshitz - Wagner - Slyozov theory, which considers only solute diffusion for growth of particles, is modified to incorporate the diffusion of both solute and solvent into the growth equation. A schematic showing

this two way interdiffusion process is shown in Fig. 20. Using this two way intediffusion model with bulk diffusion considerations, the ratio of α particle size at 973°*K* in *Ti-Mn* system to that in *Ti-V* system was theoretically predicted. This ratio was found to be significantly larger than that obtained experimentally. This discrepancy was attributed to a mixed, grain boundary plus bulk, diffusion control in these alloys at 973°*K*.

In a similar fashion, considering bulk diffusion, the ratio of the size of α particles in a β matrix to that of β particles in an α matrix was theoretically predicted for the *Ti-Mn* system. This ratio was also found to be significantly larger than that obtained experimentally and this discrepancy was also attributed to a mixed, grain boundary plus bulk, diffusion control at 973°*K*. Details of the investigation and various growth models for α–β Titanium alloys are presented are presented in Ref. 8.

c. Particle Coarsening Behavior of $\alpha - \beta$ Titanium Alloys

The main objectives of this investigation are to develop particle coarsening relationships in terms of time, temperature and volume percents of phases and to determine the rate controlling mechanisms for the coarsening of α-β Ti-Mn and Ti-V alloys. For this study, six Ti-Mn and six Ti-V alloys were used. These systems were selected because the intrinsic diffusivities as well as the interdiffusion coefficient in the Ti-Mn system are approximately an order of magnitude higher than the corresponding diffusivities in Ti-V system. These alloys were heat treated for 12.5, 25, 50, 100, 200 and 400 hours at 973 K, 998 K 1023 K , 1073 K, and 1108 K followed by water quenching. The heat treatments were carried out in vacuum encapsulated quartz tubes. The specimens were sealed in batches of twelve at a pressure less than or equal to 10^{-5} torr. The technique adopted to determine the volume percents as well as the particle sizes was the linear intercept method. It was found that for a given temperature, the particle sizes of α phase can be represented by empirical equations of the form :

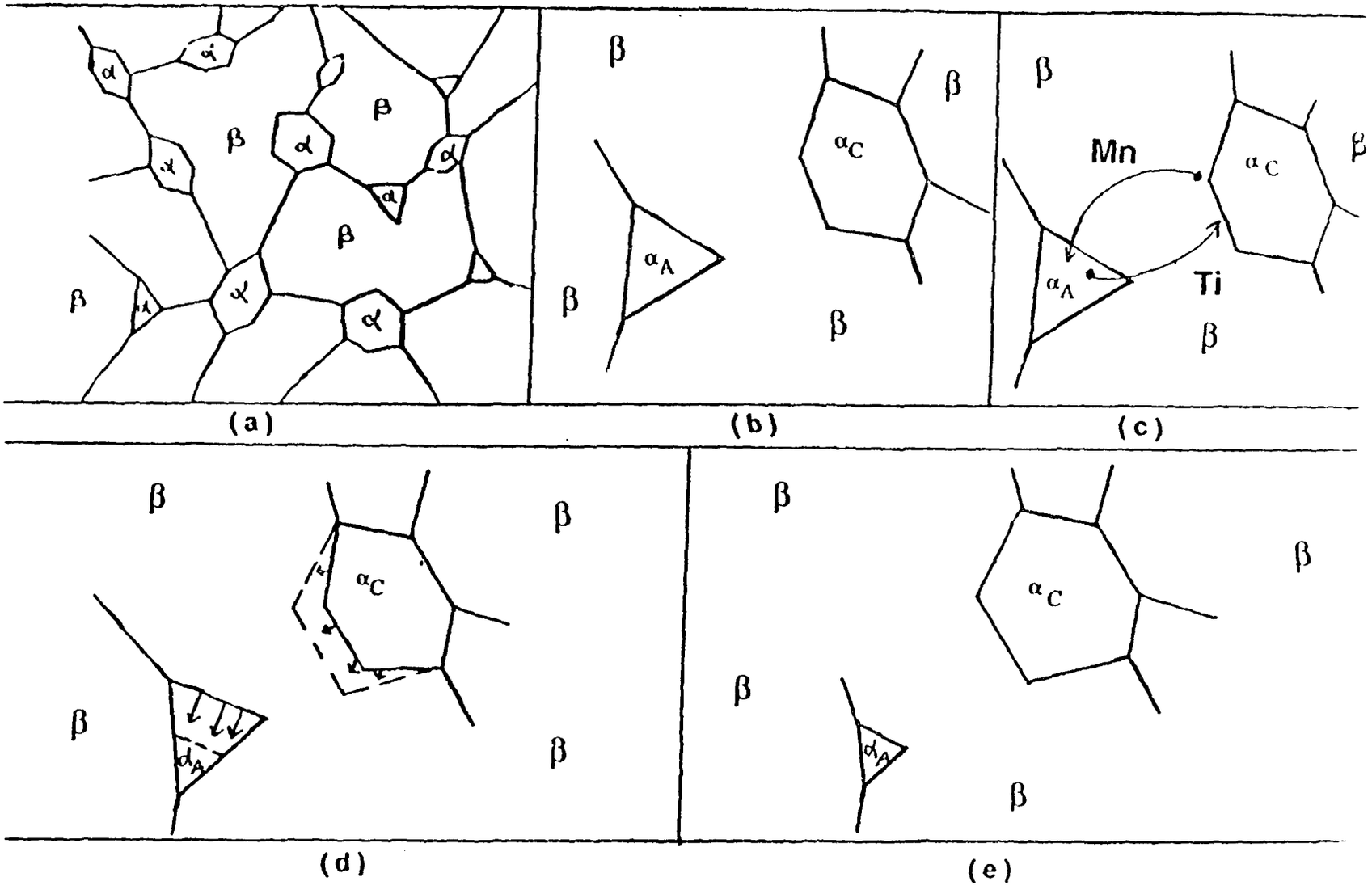

Fig.20 : A SCHEMATIC OF PARTICLE GROWTH IN CLASS 1 (α IN β MATRIX) MICROSTRUCTURES.

$$d_{\alpha}^{\alpha-\beta} = (K_{\alpha} / V_{\beta}^{m_{\beta}}) t^{n}$$

The values of K_{α} , m_{β} as well as n depend on the system and the temperature. A similar expression was obtained for the particle sizes of β phase. It was found that coarsening exponents increased from 0.24 to 0.29 and from 0.28 to 0.32 for Ti-V and Ti-Mn systems, respectively, when the temperature was increased from 973 K to 1073 K. In addition, it was found that the activation energy changes as the temperature is increased from 973 K to 1108 K for the Ti-Mn system. Based on the observation of a systematic increase in n values as well as an increase in activation energy with increase in temperature, it is suggested that the rate controlling mechanism for particle coarsening in the Ti-Mn system changes from mixed (grain boundary + bulk) diffusion control at 973 K towards predominately bulk diffusion control at 1108 K

Similarly, for the Ti-V system, it is suggested that the rate controlling mechanism changes from predominantly grain boundary diffusion control at 973 K towards mixed (grain boundary + bulk) diffusion control at 1073 K. These results clearly indicate that the rate controlling mechanisms for particle coarsening in equiaxed type microstructures of two phase titanium alloys depend on the diffusivities of the alloying elements as well as the temperature. Details of the investigation are presented in Ref. 9.

d. Modelling Matrix Grain Growth in the Presence of Growing Second Phase Particles

In two phase systems such as alpha-beta titanium alloys, second phase particles as well as the matrix grains grow simultaneously. The main objective of this investigation was to understand matrix grain growth behavior in the presence of growing particles of the second phase. The experimental portion of this work consisted of vacuum annealing six alpha, alpha-beta and beta Ti-Mn alloys at 973 K for 25, 50, 100, 200 and 400 hours. The grain boundaries were revealed by a special technique and standard quantitative metallography methods

were used to determine the grain sizes of the alpha and beta phases. It was found that the grain sizes of the alpha and beta phases in alpha-beta Ti-Mn alloys could be expressed by simple empirical equations in terms of volume percents of the respective phases and time.

Computational models of growth of alpha matrix in the presence of growing particles of beta particles were developed using classical expressions for the driving pressure for grain growth and a modified form of Zener retardation to account for the fact that most beta particles are located at triple junctions of the alpha grains. These models resulted in first order non-linear differential equations which were solved by a computer program based on the Runge-Kutta method. In these models, the particle shape effect as well as the grain boundary curvature contributions to the retardation force have been incorporated. The grain sizes predicted by these models were found to be close to those experimentally obtained. Similarly, the growth of beta matrix in the presence of growing alpha particles was also modeled. For this case, the modified Zener retardation is used only when the volume percent of beta particles is more than 20 %. For beta volume percents less than 20 % the particles were found to be uniformly distributed. For both of these cases, the contribution of particle shapes and grain boundary curvature to the retardation force have been incorporated. In this case also, theoretically predicted grain sizes were found to be close to those experimentally observed. Details of the investigation are presented in Ref. 11.

C. FEM MODELLING OF STRESS - STRAIN BEHAVIOR OF TWO PHASE MATERIALS

a. Introduction

Many technologically important materials consist of two or more phases. These materials include two-phase steels, two-phase brasses and α–β Ti alloys and various composite materials. To improve the mechanical properties of the existing two phase materials or to design materials with improved properties, it is necessary to understand the deformation behavior of the two-phase materials in terms of the volume fraction, morphology and strength of the component phases. There is a lack of understanding in this area. This is due to the fact

that whenever a two phase material is subjected to stress, the component phases deform differently resulting in inhomgeneous stress and strain distributions.

A number of investigators studied the stress-strain behavior of two-phase materials [3,4,13-30]. The deformation behavior of dual phase, ferrite-martensite steels, was studied by Davies. He found that the 0.2% Yield Strength varies linearly with volume fraction of martensite and obeys the law of mixture rule. He also found that the tensile strength and ductility of dual phase steels are in agreement with Milieko's [21] and Garmong and Thompson theory[22] which is meant for composites with continuous fibers.

The above models do not consider the effect of morphology of the phases on the stress-strain behavior of the two phase materials. Ankem and Margolin [3,4,31] modelled the stress-strain behavior of two phase materials taking into consideration the shape, size and volume percent of the phases by the Finite Element Method. Their FEM results were in good agreement with experimental results indicating that FEM is a good method for modelling the deformation behavior of two-phase materials.

The inhomogeneous stress and strain distributions mentioned above results in interaction stresses due to compatibility requirements. Non-uniform strains in the constituent phases have been reported by many investigators [34-40]. Unckel [34] studied the shape change of particles embeded in a matrix and from that he inferred that the hard particles deformed less and the soft particles more. Honeycombe and Boas [35] have studied the deformation behavior of α–β brasses. From recrystallization studies, they found that the α phase deforms more than the β phase. Bollenrath et al. [40] measured the internal stresses in a Cu-Fe two phase material before and after plastic deformation. After deformation, compressive stresses were found in Cu and tensile internal stresses were observed in the iron phase. This is because of inhomogeneous deformation of the phases. Ankem and Margolin [4] used the Finite Element Method to obtain the stress-strain distributions in the constituent phases during the deformation of a two-phase material for a strength ratio of 3. Their FEM calculated strain distributions were close to those obtained experimentally. Apart from

these studies, no other significant information is available in regard to the inhomogeneous deformation behavior. For example, it is not known how the stress and strain distributions change for a given two phase material as the strength of the harder phase is increased.

In this investigation, FEM has been employed to to systematically study the stress-strain behavior including stress and strain distributions of various two-phase materials as a function of the volume percent and strength difference between phases by the FEM method.

b. Procedure

The NASTRAN Computer Program [2] in particular, Rigid Format No. 6 called "Picewise Linear Analysis" was used in conjunction with a UNIVAC computer. This Computer Program is based on the FEM principles.

Typical meshes used in this analysis are shown in Figures 21 to 23. Each triangle in the meshes is a two-dimensional (plane stress) plate element. The nodes on edge AC are constrained from moving in the X-direction and the nodes on edge AB are constrained from moving in the Y-direction. All the other nodes are free to move in both the X and Y directions. A multiple point constraint was used for the nodes on edge CD such that they have the same displacement at any given stage of deformation. With these constraints, the mesh represents one quarter of a tensile specimen in two dimensions. In fact, stress-strain curves by the two-dimensional approximation was found to be close to the experimentally obtained stress-strain curves with cylindrical specimens by Ankem and Margolin [3,4] . This appears to be related to the fact that the field equations governing deformation for two and three dimensions are similar in nature [12]. The meshes used here are even more refined than those used by Ankem and Margolin [3]. Each mesh consists of 1568 elements. The elements can be made to represent the α or the β phase by inputing the respective properties. In inputing the stress-strain curves care was taken to closely represent the actual curves by

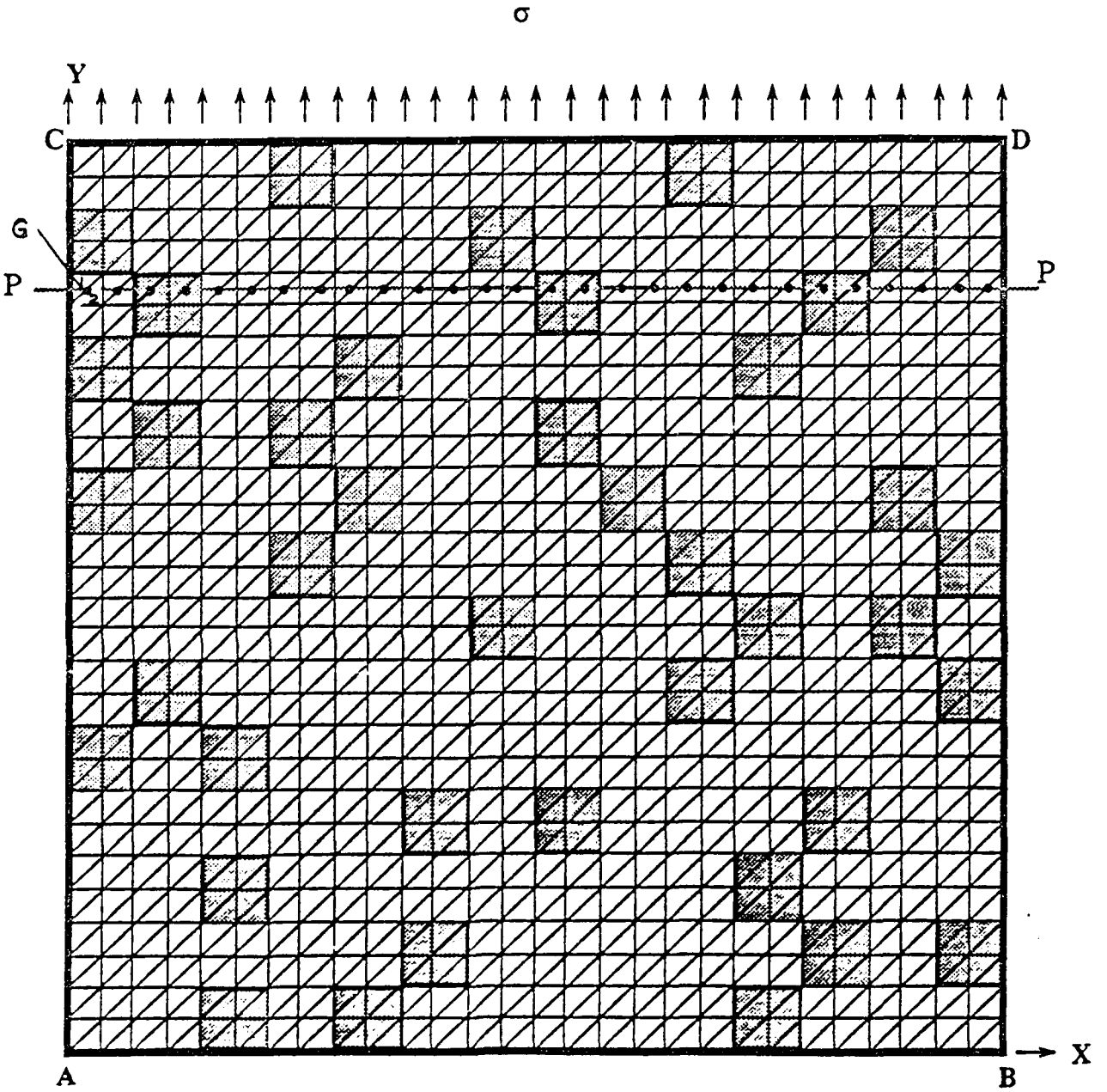

Fig. 21 Finite Element Mesh with 80 vol. %α and 20 vol. %β.
The shaded regions correspond to β particles.

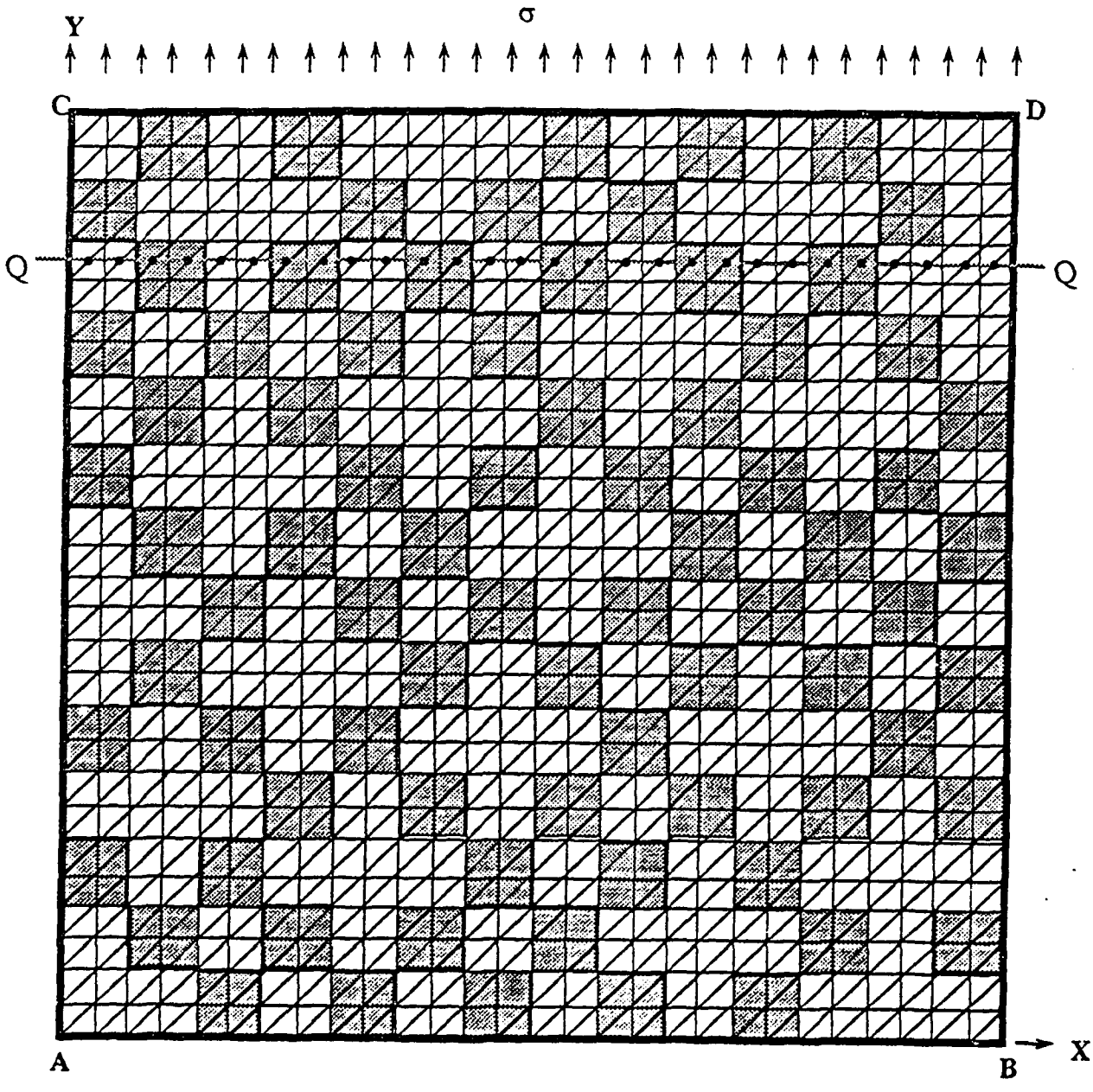

Fig. 22 Finite Element Mesh with 60 vol. %α and 40 vol. %β.
The shaded regions correspond to β particles.

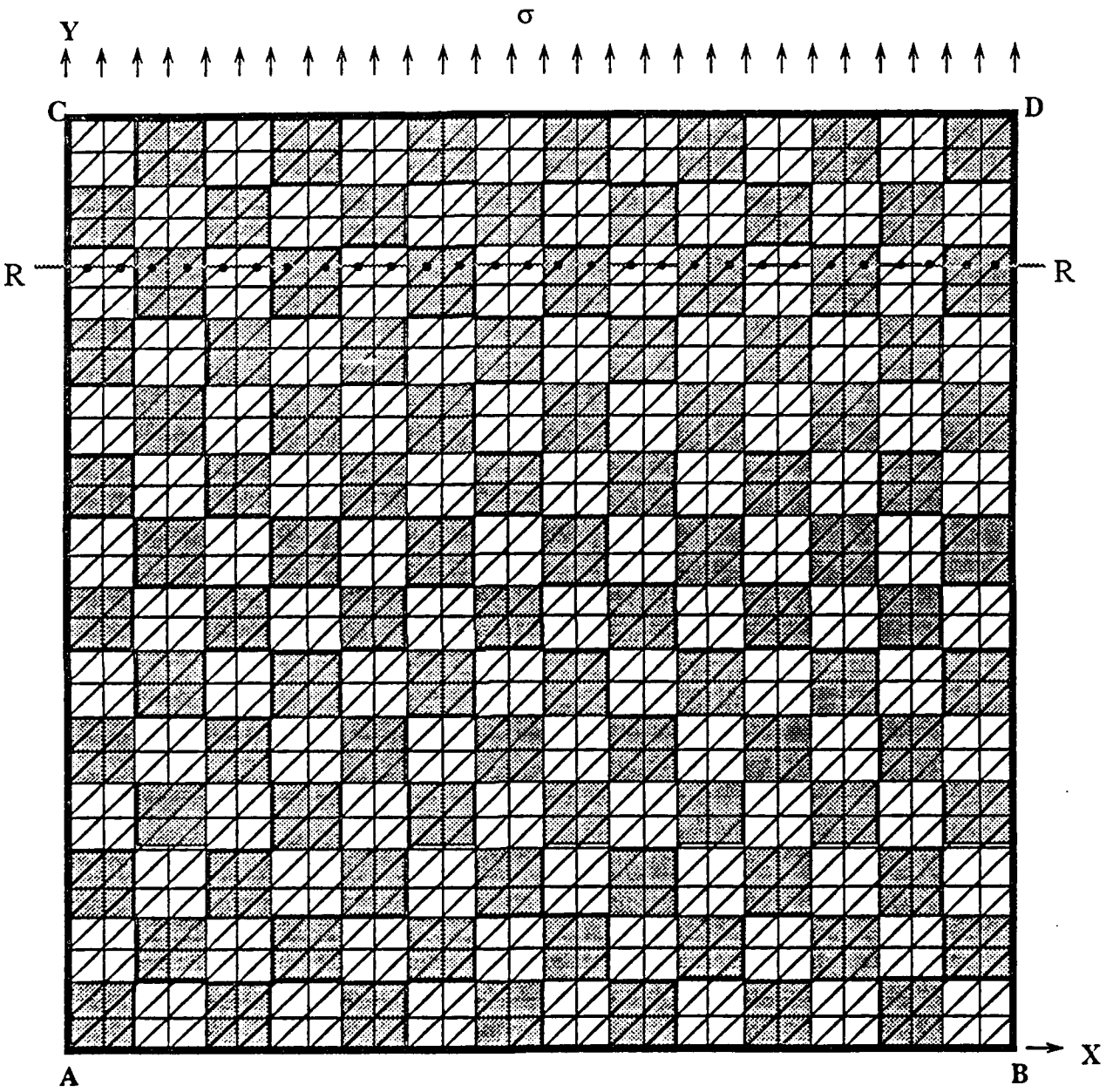

Fig. 23 Finite Element Mesh with 50 vol. %α and 50 vol. %β.
The shaded regions correspond to β phase.

selecting a large number of stress-strain points near the elastic to plastic transition region.

The load was applied in the Y-direction as shown in Figures 21to 23. This load is increased by predetermined increments and the first few increments are such that all the stresses developed are in the elastic region.

To determine the effect of the strength ratio of the phases on the stress-strain behavior, the strength of the α curve was kept constant while the strength of the β curve was varied such that the β to α strength ratio varied approximately from 2 to 5. Input curves of α and β phases are shown in Fig. 24. For a given strength ratio, the volume percent of β was varied from 20 to 80. The meshes shown in Figs. 21to 23 correspond to 80% α + 20% β, 60% α + 40% β, and 50% α + 50% β, respectively. For higher volume percent of β ranging from 60 to 80, the same meshes shown in Figs. 21 and 23 were used except for the fact that the particle phase in these meshes is α.

The method used to calculate the average stresses and strains is similar to that used by Ankem and Margolin [4]. The NASTRAN program calculates the displacements of all the nodes in the X and Y directions and the σ_{xx} and σ_{yy} stresses in each element. The average σ_{yy} stress in the α phase is found by adding the σ_{yy} stresses in all of the α elements and dividing the sum by the total number of α particles. The average σ_{yy} stress in the β phase is obtained in a similar way. The average σ_{xx} stresses were also obtained similarly. To obtain the average strain in a particular phase, the total strain of all the lines in each phase is divided by the number of lines in each phase. If a line is shared by two phases, one-half of the line is assigned to each phase. The overall stress and strain is related to the individual stress and strain by the following equations:

$$\sigma_{\alpha-\beta} = \sigma_\alpha V_\alpha + \sigma_\beta V_\beta$$

$$\varepsilon_{\alpha-\beta} = \varepsilon_\alpha V_\alpha + \varepsilon_\beta V_\beta \text{ , where } \sigma_\alpha, \sigma_\beta \text{ are the average stresses in the } \alpha$$

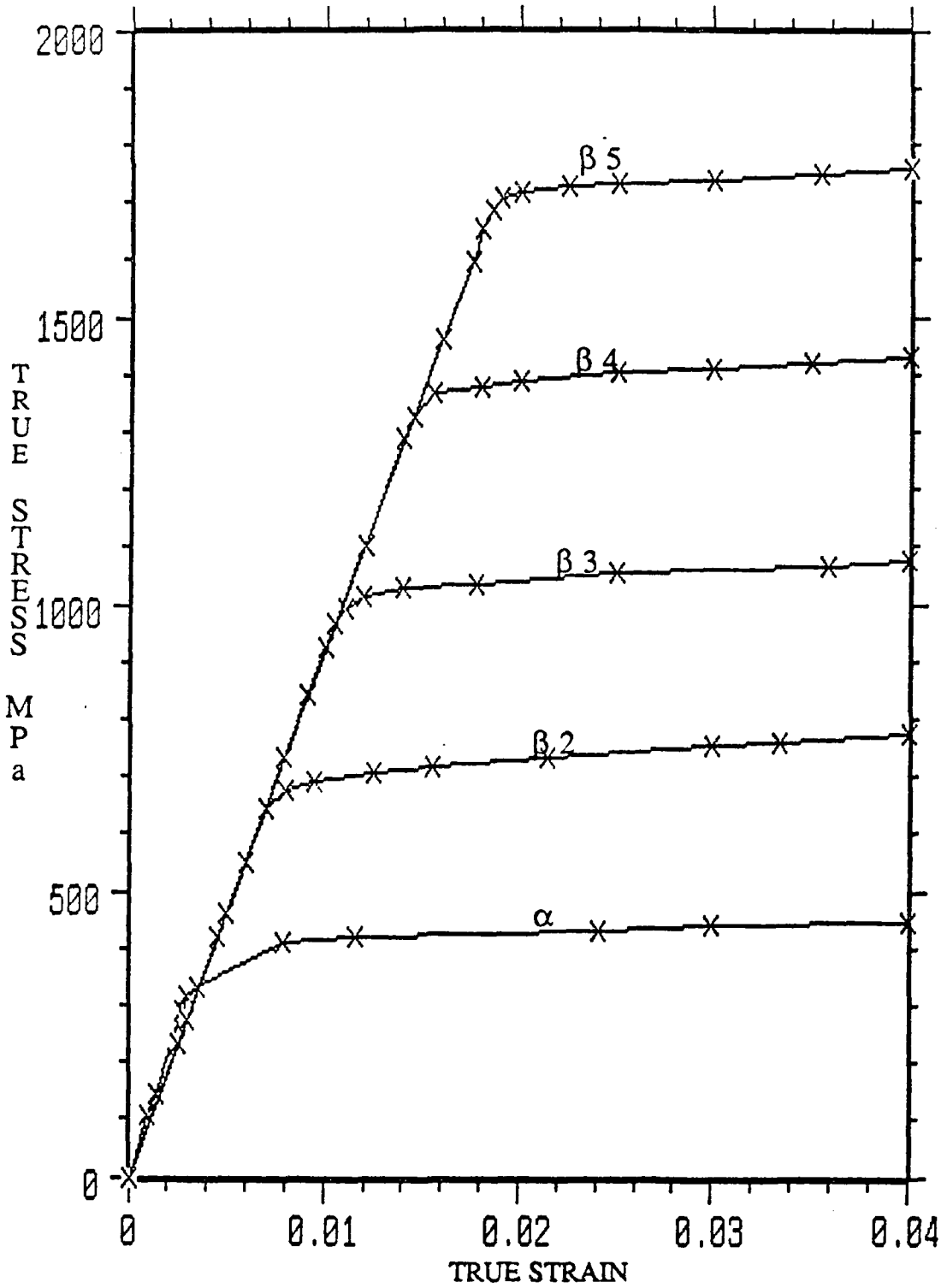

Fig. 24 Stress-Strain Curves of α and β used for FEM calculations. Note that four different β curves are used to determine the effect of strength difference.

and β phases respectively, ε_α, ε_β are the average strains in the α and β phases and $\sigma_{\alpha-\beta}$, $\varepsilon_{\alpha-\beta}$ are the overall stress and strains of the two phase alloy.

The local stresses and strains were calculated for the elements along sections P-P and R-R of Figs. 6 and 8. Similar calculations were made for a 80 % β two-phase material along a section S-S and the mesh is similar to that shown in Fig. 21 except that the particle phase was α. Each of these section passes through 56 triangular elements. The strains in the elements along the section P-P, R-R and S-S are obtained from the relative displacements of the nodes just above and below the section. Since each small square consists of two adjacent triangular elements of the same phase, to obtain the stress at a point (marked as solid circles) along any given section, the stresses in the respective elements are averaged over these two elements. For example, the stress at point G of section P-P of Fig. 21 is obtained by taking the average of the stresses in elements 1 and 2 .

The above calculations were repeated for materials with different volume percents and for different strengths of the β phase. The β to α strength ratios varied approximately from 2 to 5 and the volume percent of β was varied from 20 to 80 percent.

c. Results and discussion

The stress-strain curves obtained by the FEM method for different volume percents and strength ratios of the α and β phases are shown in Figs. 25 to 29. The data points in Figures 15 to 19 correspond to the actual stress-strain points obtained by the FEM method. These stress-strain curves are used to obtain the flow stress plots shown in Figs. 30-33.

1. Effect of Volume Fraction on Yield Strength

Observation of Figs. 25 and 30 shows that the addition of 20 vol % β phase to α phase with a strength ratio of 2 increases the flow stress slightly. For the same volume percent further increasing the strength ratio does not significantly affest the 0.2 % flow stress. This

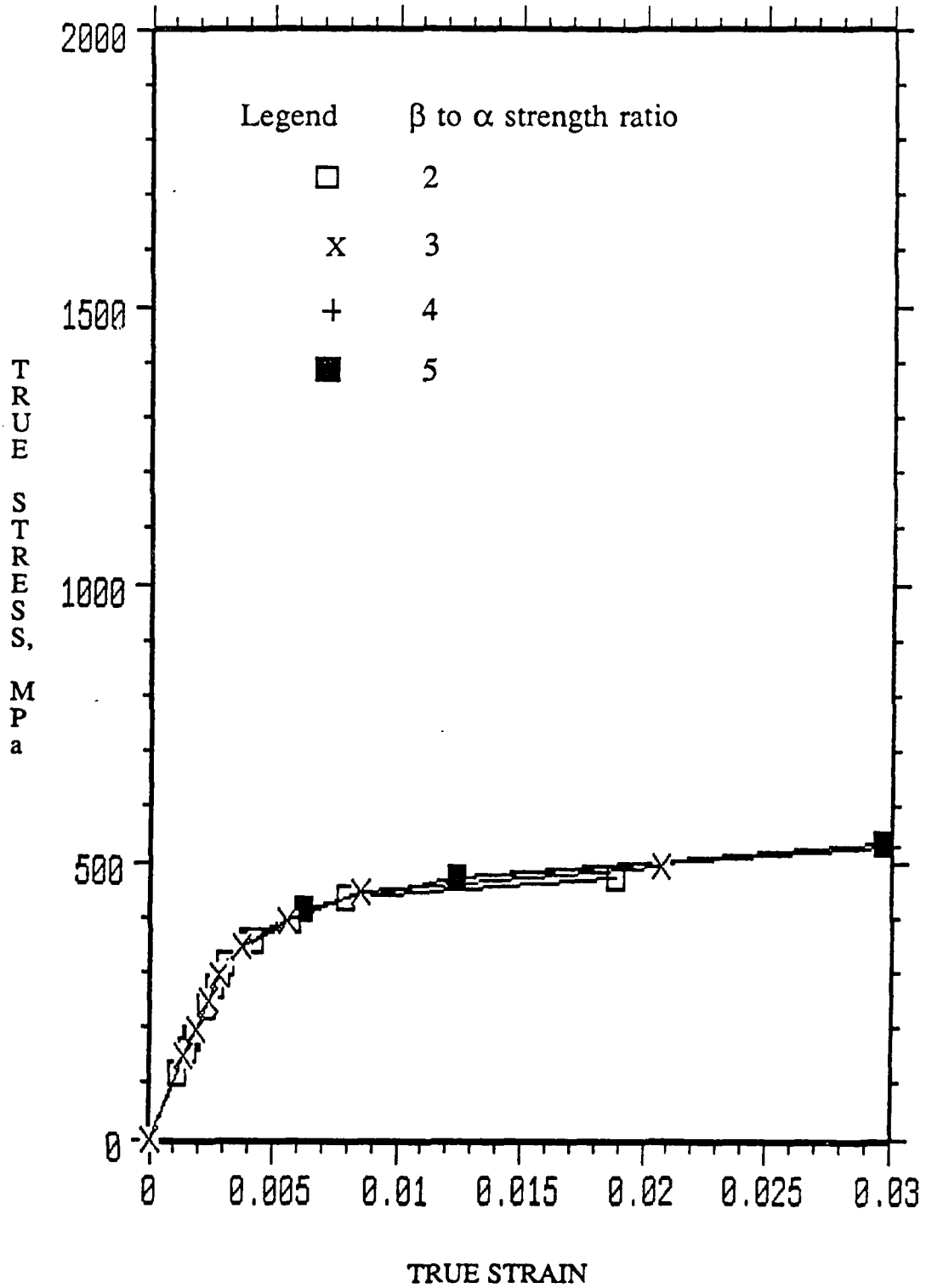

Fig. 25 FEM calculated stress-strain curves for 80 vol. % α + 20 vol. %β material for four different β to α YS ratios.

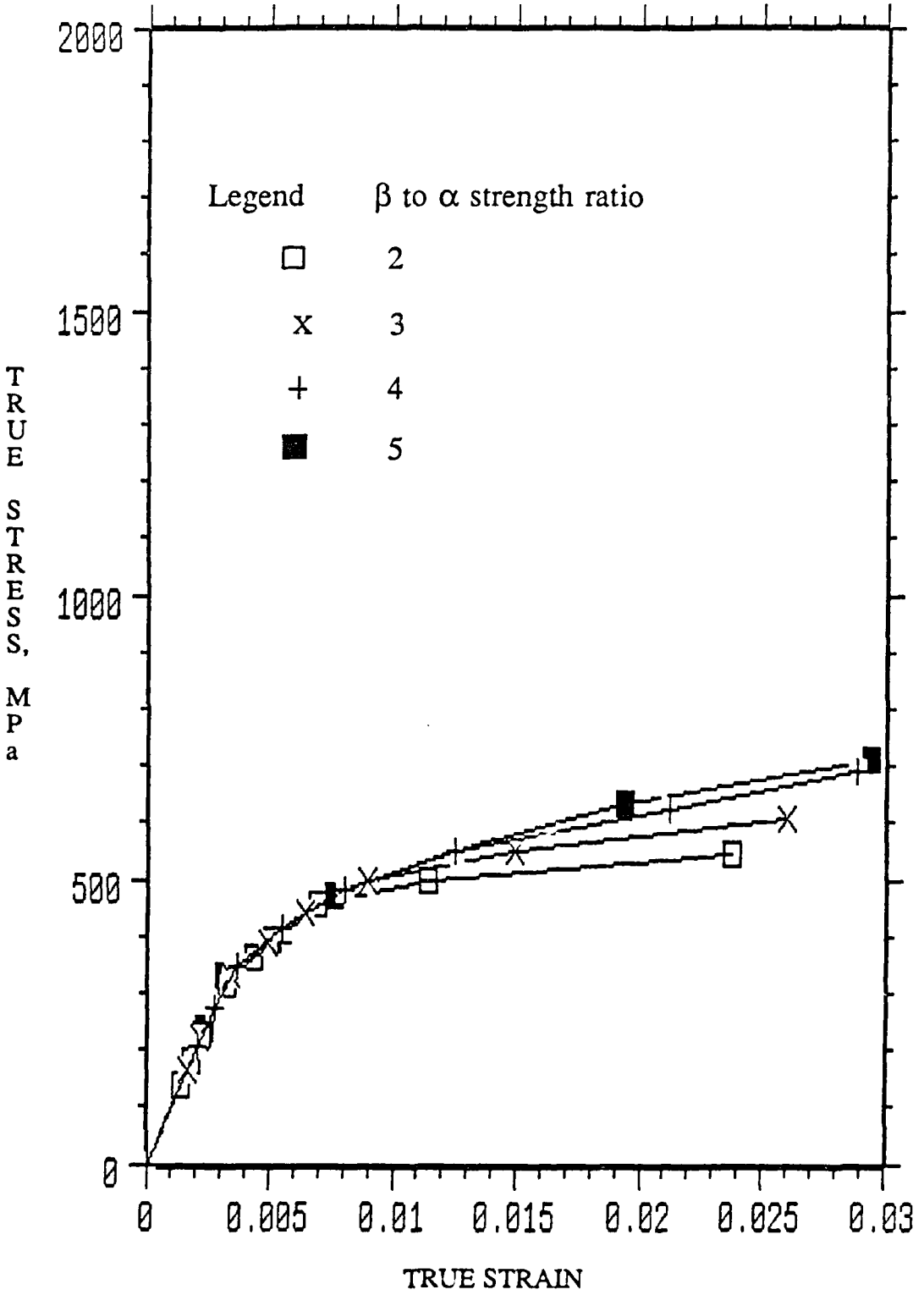

Fig. 26 FEM calculated stress-strain curves for 60 vol. % α + 40 vol. %β material for four different β to α YS ratios.

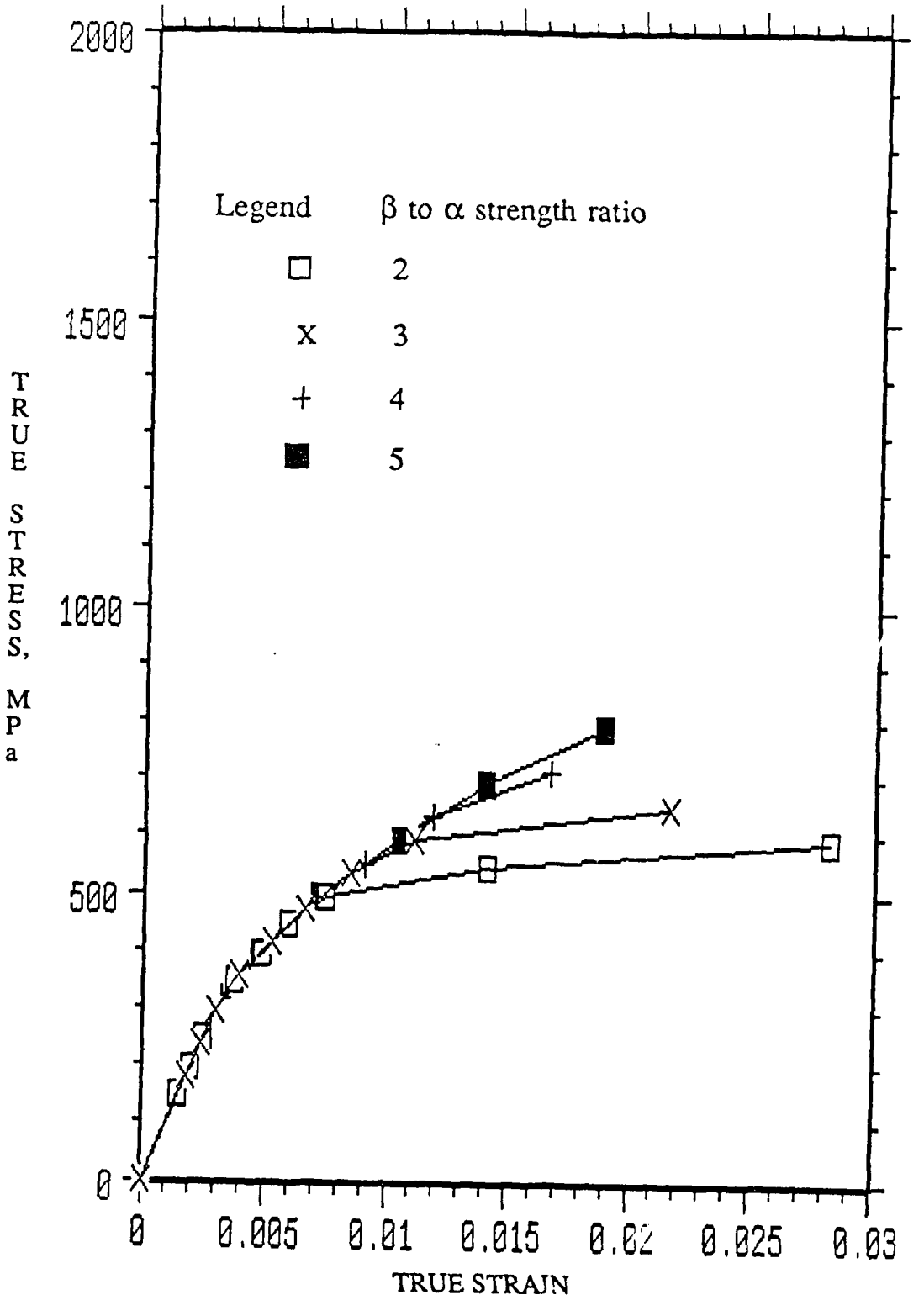

Fig. 27 FEM calculated stress-strain curves for 50 vol. % α + 50 vol. %β material for four different β to α YS ratios.

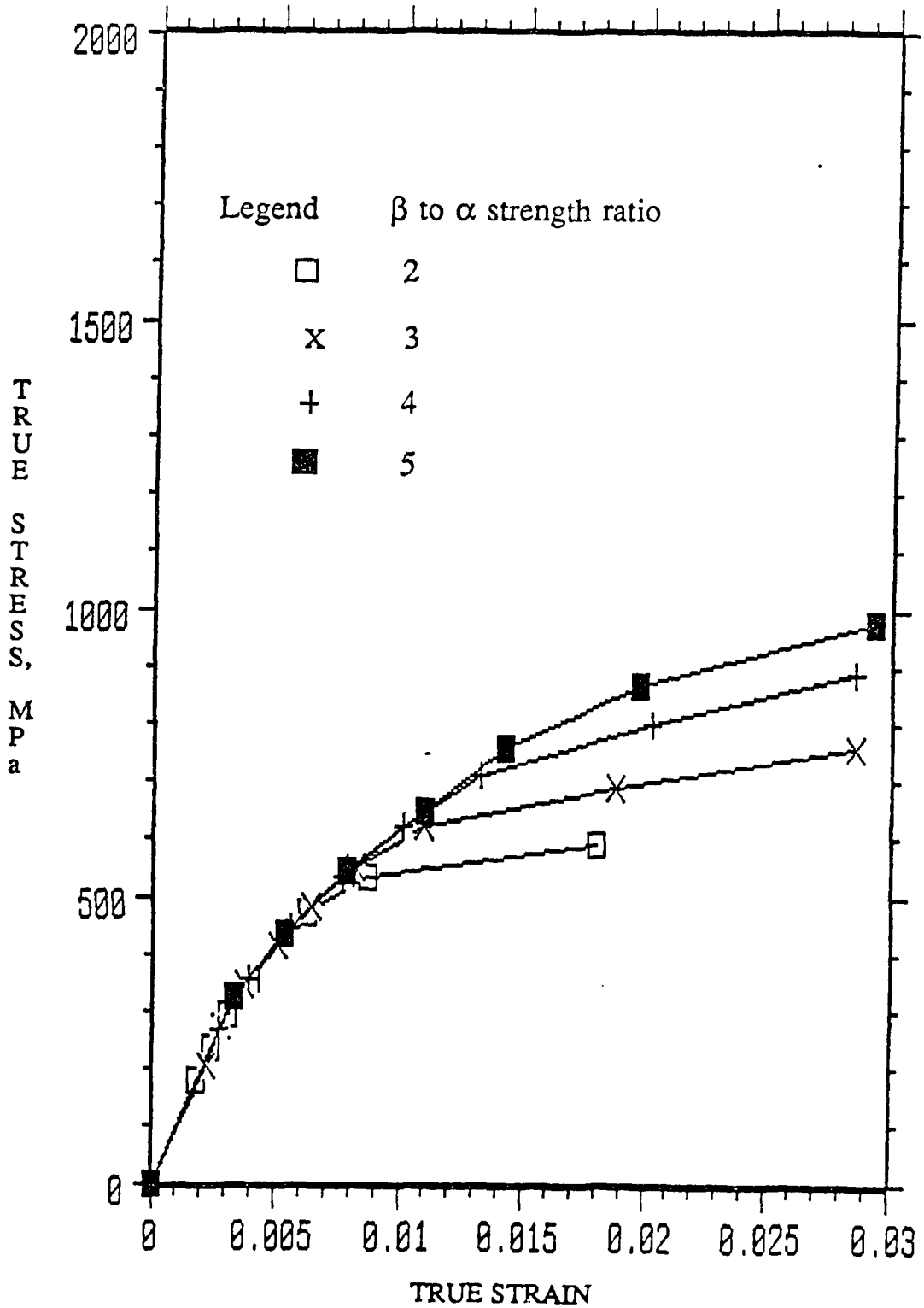

Fig. 28 FEM calculated stress-strain curves for 40 vol. % α + 60 vol. %β material for four different β to α YS ratios.

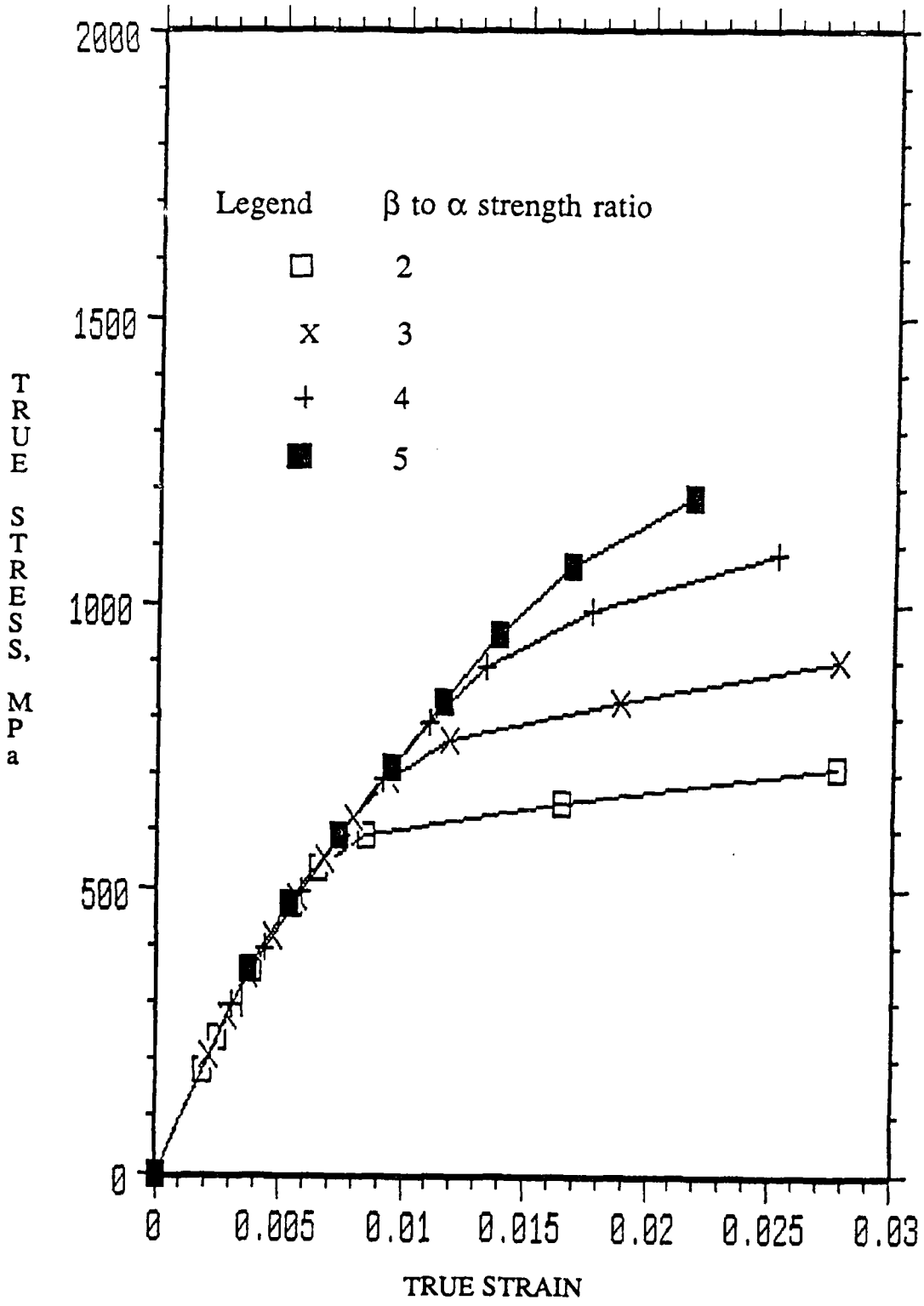

Fig. 29 FEM calculated stress-strain curves for 20 vol. % α + 80 vol. %β material for four different β to α YS ratios.

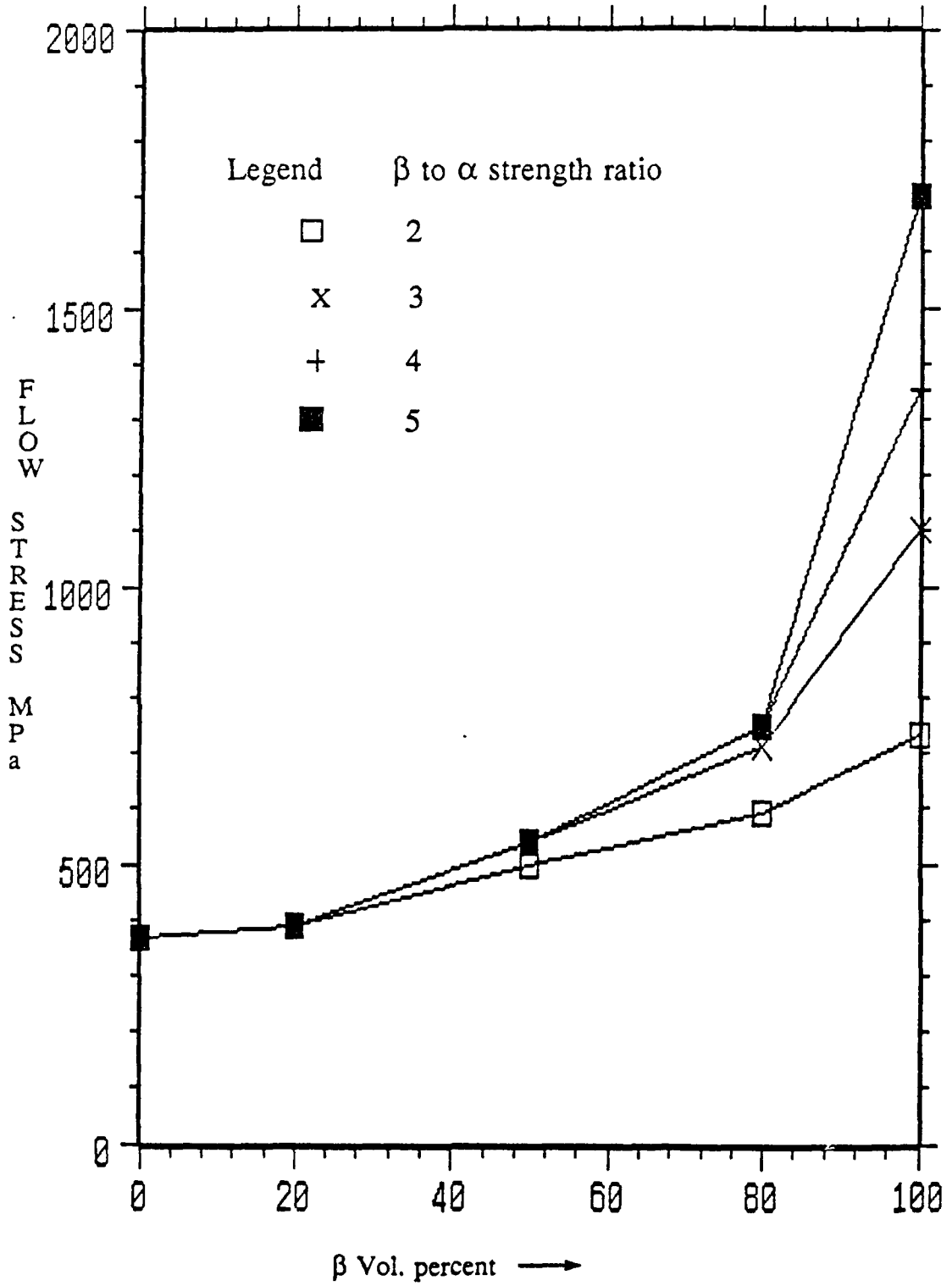

Fig.30 Variation of 0.2 % flow stress of α–β (two-phase) alloy with β volume percent for different β to α strength ratios

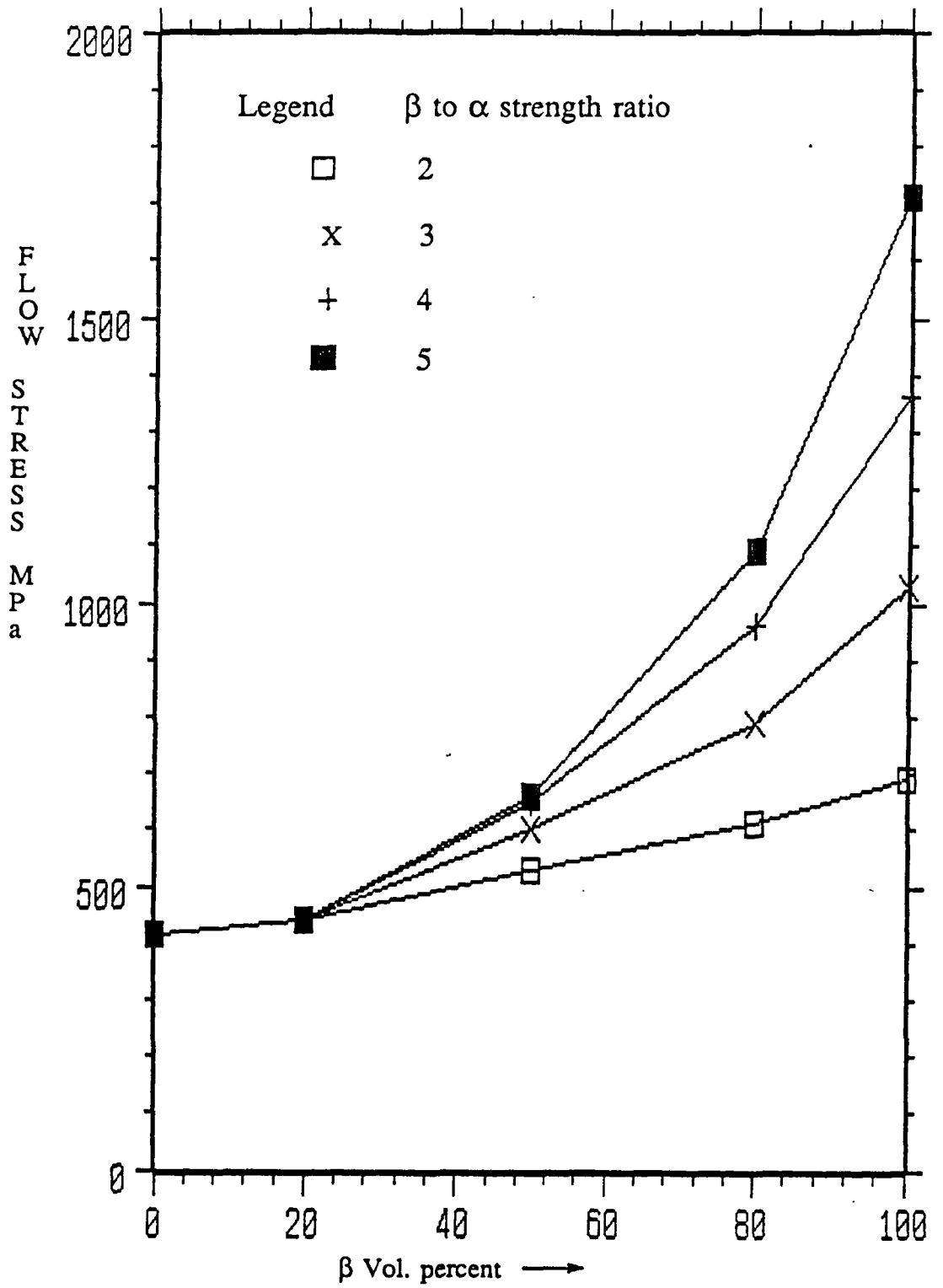

Fig. 31 Variation of 0.5 % flow stress of α–β (two-phase) alloy with β volume percent for different β to α strength ratios

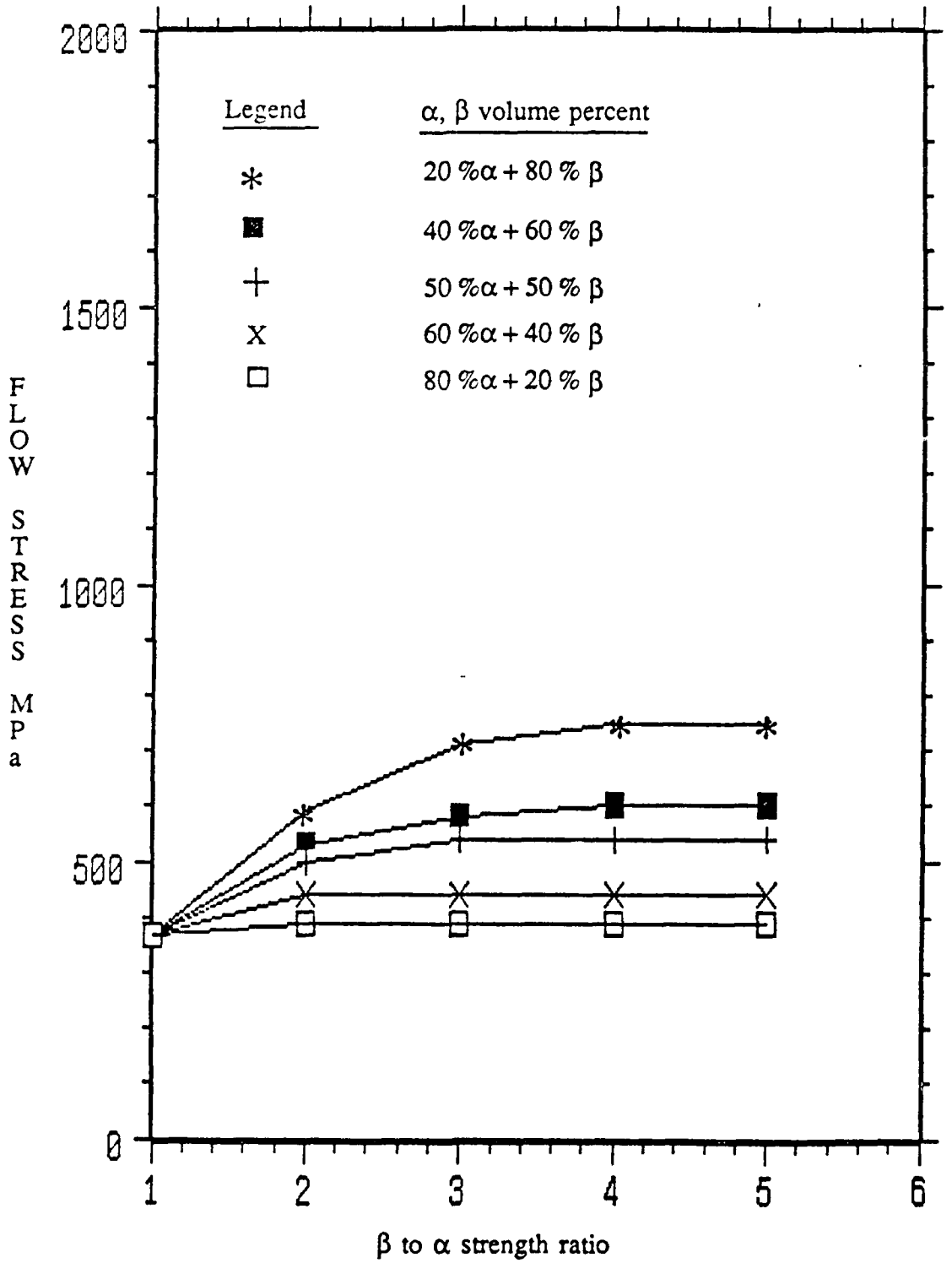

Fig. 32 Variaiton of 0.2 % flow stress with β to α strength ratio for different volume percents of α and β

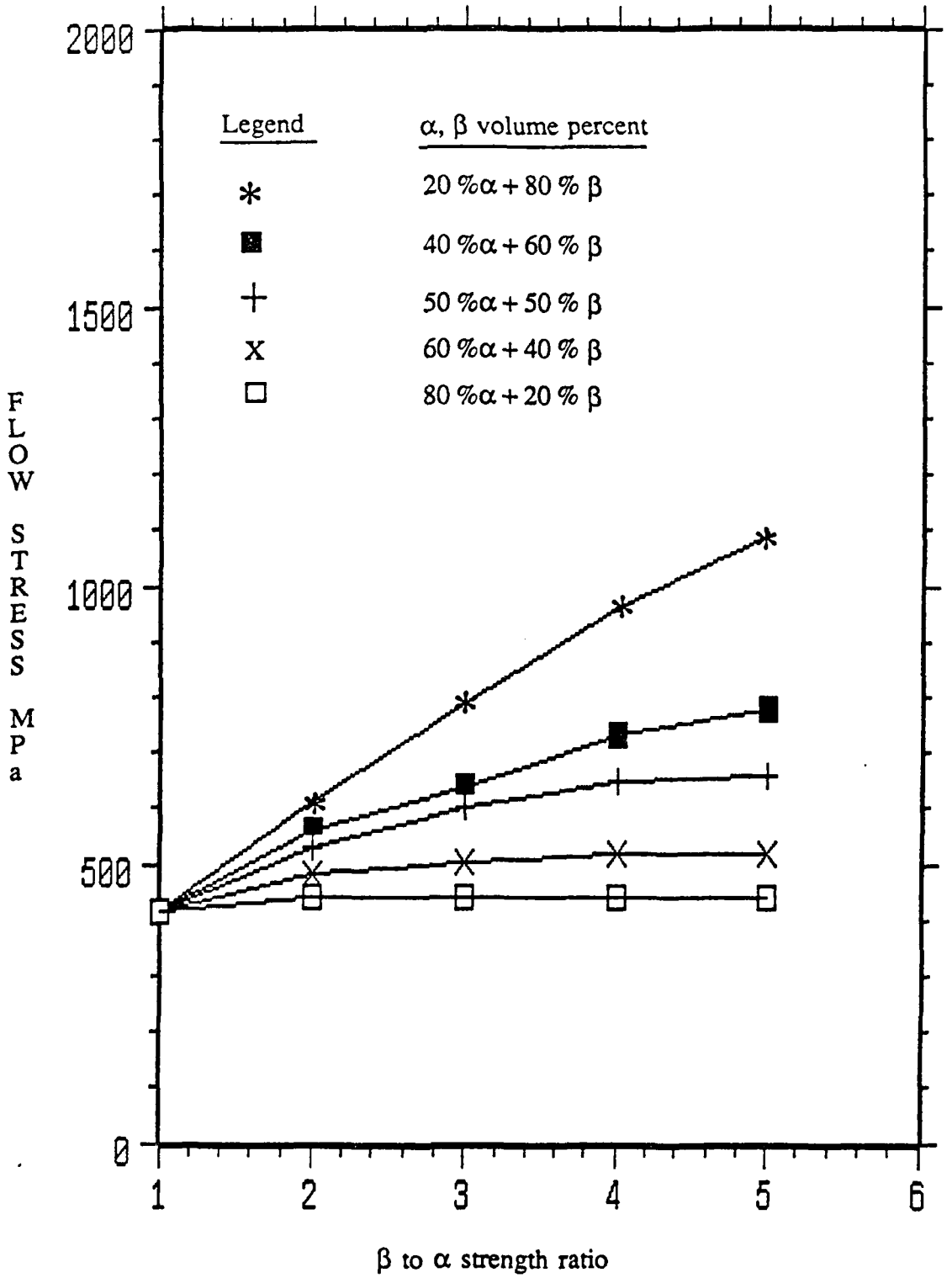

Fig. 33 Variaiton of 0.5 % flow stress with β to α strength ratio for different volume percents of α and β

is related to the fact that at this low strain, β will be deforming in the elastic range and the matrix, α, phase can deform relatively freely. However, as the β volume percent is increased, the amount of α/β interface, where the β phase can apply constraint on the α phase increases, and this results in increased flow stresses.

As the plastic strain increases from 0.2 to 0.5 %. for low volume percents of the β phase, there is no significant increase in the flow stress with β to α strength ratio indicating that the α phase can deform relatively freely as explained before. However, for larger volume percents of β (>20 %) the flow stress significantly increases with volume percent for a given strength ratio and the increase is most significant for highest volume percents of β (>50 %). When the volume percent of β is more than 50 %, the stronger β phase will be the matrix and it is difficult for the α phase to deform significantly without deforming the β phase. For a given volume percent (>50 %), the constraints from the β phase increases with increase in β to α strength ratio.

2. Effect of β to α Strength Ratio on the Yield Strength

To better understand the effect of strength ratio on flow stress, the 0.2 % and 0.5 % flow stresses are plotted as a function of β to α strength ratio for different α- β alloys in Figs. 32 and 33. It is interesting to note in Fig. 32 that for the 20 volume percent and 40 volume percent β alloys, the addition of β phase with a strength ratio of 2 increases the flow stress slightly. However, further increase in the strength ratio from 2 to 5 has no significant effect. This is related to the fact that β with a strength ratio of 2 is in the elastic range and hence further increase in strength of β would not affect the flow stress of the material. However, as the amount of β is increased much beyond 40 %, the amount of α/β interface increases and so do the constraints imposed by β on α. This means that for α to deform plastically, β adjacent to α has to deform plastically which results in higher flow stresses as shown in Fig. 32. Once β is in the plastic range, the flow stress does increase with the strength of the

β phase which is the reason for continued increase of flow stress with β to α strength ratio, as shown for the strength ratios of 2, 3 and 4 of a 60 volume percent β material. When the strength ratio is 4, for this material, the β will be again in the elastic range for a plastic strain of 0.2 %. Therefore, further increase of strength ratio from 4 to 5 does not change the flow stress of 80 volume percent β alloy significantly.

For higher plastic strains i.e 0.5 % the effects of the strength ratios are much more significant as compared to those at 0.2 %. This is related to the fact that as the amount of strain increases in the α phase, the regions of β adjacent to the α phase are forced to deform plastically at higher volume percents of the β phase. This results in increased flow stress with increased strength ratio. For example, for the 60 volume percent alloy, β undergoes plastic deformation and therefore increasing the strength of the β phase increases the flow stress of the material. However, further increase in the strength ratio will make the β to be in the elastic region and hence further increase in the strength ratio i.e. beyond 5 will not significantly change the flow stress. In fact, such observations were made by Davies [19]. He showed that for the dual phase ferrite-martensite steels, for a given volume percent of martensite, the 0.2 and 1 % flow stresses of the dual phase steel did not vary even though the strength ratio of martensite to ferrite varied approximately from 6 to 8. The strength of the martensite was varied by changing the quench temperature which in turn changes the carbon content in the martensite. These results can be explained on the basis of the above discussion that the martensite did not deform plastically due to its high strength and hence any further increase in the strength of martensite would not contribute to the strength of the dual phase steel

3. Average Stress and Strain Distributions

The average stress and strain distributions for two phase materials with different

volume percents and different β to α strength ratios are shown in Figures 34 to 39. Stress-strain points of the two phase materials and the corresponding stresses and strains in α and β phases are connected with straight lines. Similar plots were made for other volume percents and strength ratios but are not shown here. These figures clearly indicate that neither the stresses nor the strains are constant as expected. For two phase materials with a β to α strength ratio of 2 and for a true strain of 0.02, as the volume percent of β is increased from 20 to 80, deformation in β changes from only elastic to plastic as seen in Figures 34, 36 and 38. For a higher strength ratio of 5, β is elastic at 20 volume percent and mostly remains elastic at 80 . This is due to the fact that for a true strain of 0.02, the overall stress-strain curve of the two-phase material with 80 percent β has very little plastic deformation.

To get a better idea about the strain partitioning, the longitudinal strain ratios, $\varepsilon_\alpha/\varepsilon_\beta$, are plotted as a function of volume percent of β in Fig. 40 for a total true strain of 0.018. These ratios are obtained by dividing the strain in α to that in β. The strains used to calculate these ratios are connected with a dashed line in Figs. 34 to 39. For a 20 volume percent β material the strain ratio is approximately 2.7 irrespective of the strength ratio as seen in Fig. 40. As explained before, this is related to the fact that increasing the β to α strength ratio from 2 to 5 has no significant effect on the overall stress-strain behavior because the softer α phase can deform relatively freely thereby carrying most of the strain. As the volume percent of β is increased, the amount of α/β interface increases and so does the extent of the constraints of the β phase on the α phase. This results in increased homogeneous strain distribution resulting in low strain ratios. For a given shape of the particles (rectangular in this case), the highest amount of α/β interface area corresponds to a volume percent of β equal to 50 and for this volume percent the strain ratios will be lowest as shown in Fig. 40. As the amount of β is increased beyond 50 percent the amount of α/β interface starts to decrease and inhomogeneities in the strains increase. This results in increased ratio of the

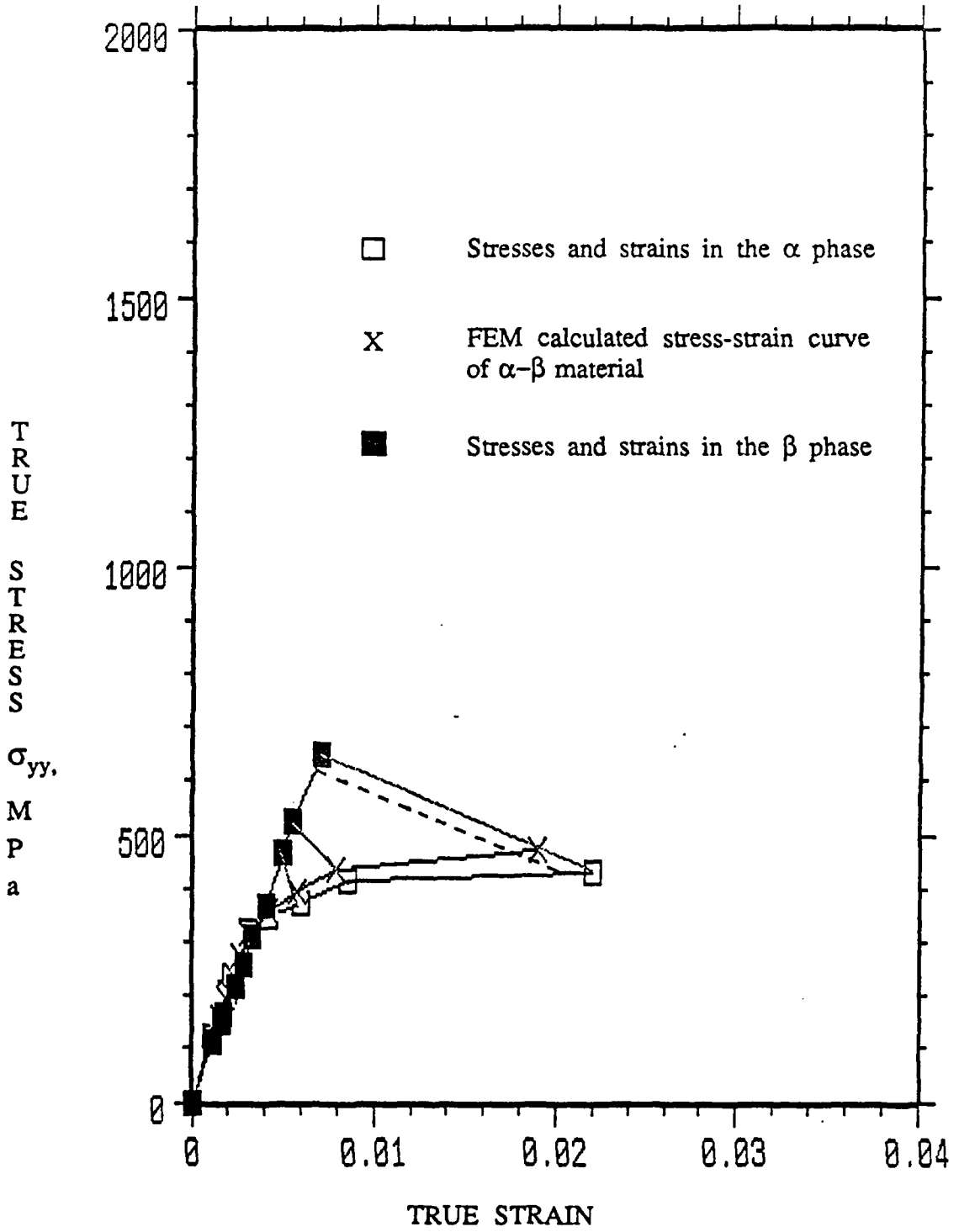

Fig. 34 FEM calculated stress and strain distributions for a 80 vol. % α + 20 vol. % β material with β/α strength ratio of 2. The corresponding average stresses and strains in α and β are connected with dotted lines. It is to benoted that the stresses are higher and strains are lower in the harder β phase..

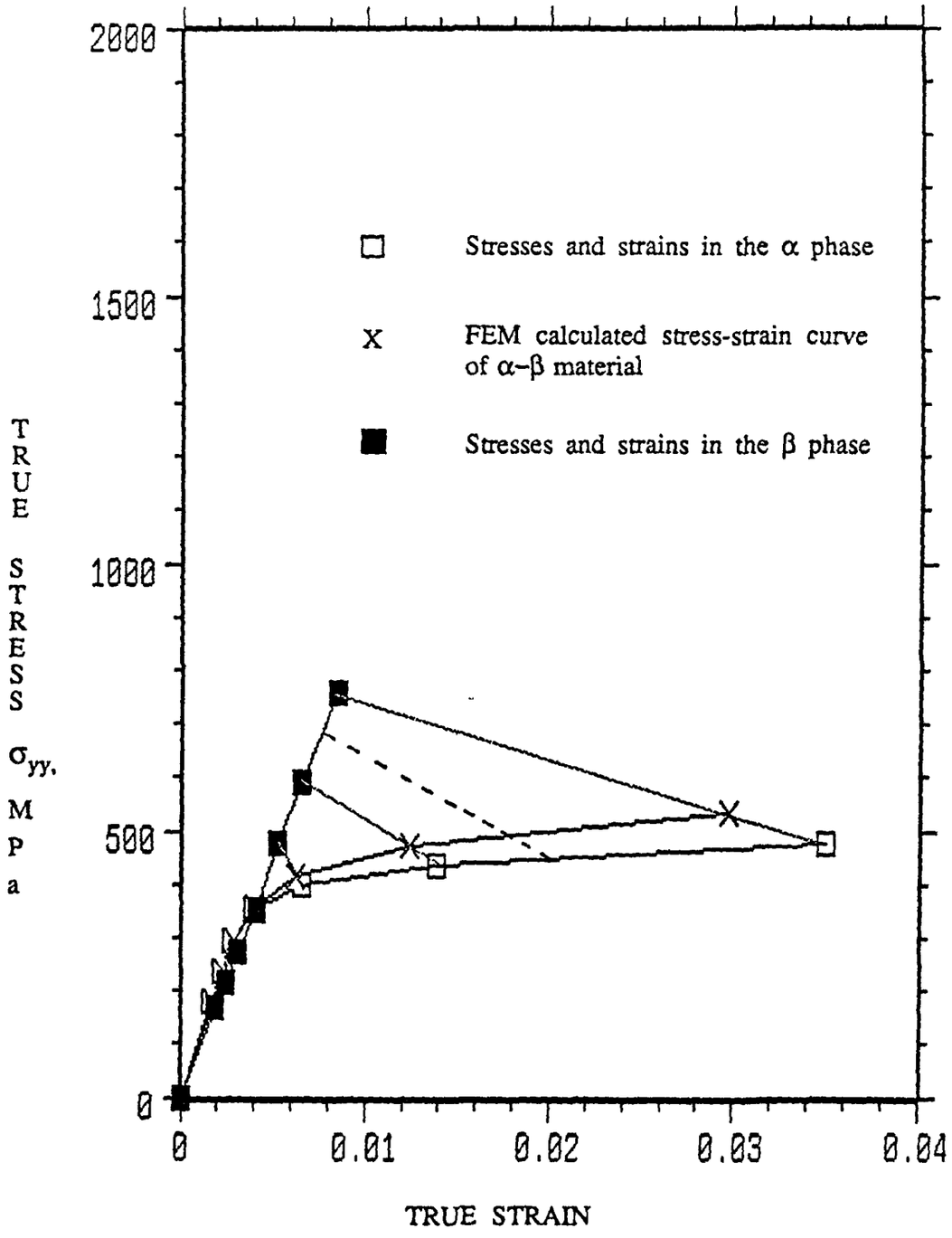

Fig. 35 FEM calculated stress and strain distributions for a 80 vol. % α + 20 vol. % β material with β/α strength ratio of 5. The corresponding average stresses and strains in α and β are connected with dotted lines. It is to benoted that the stresses are higher and strains are lower in the harder β phase..

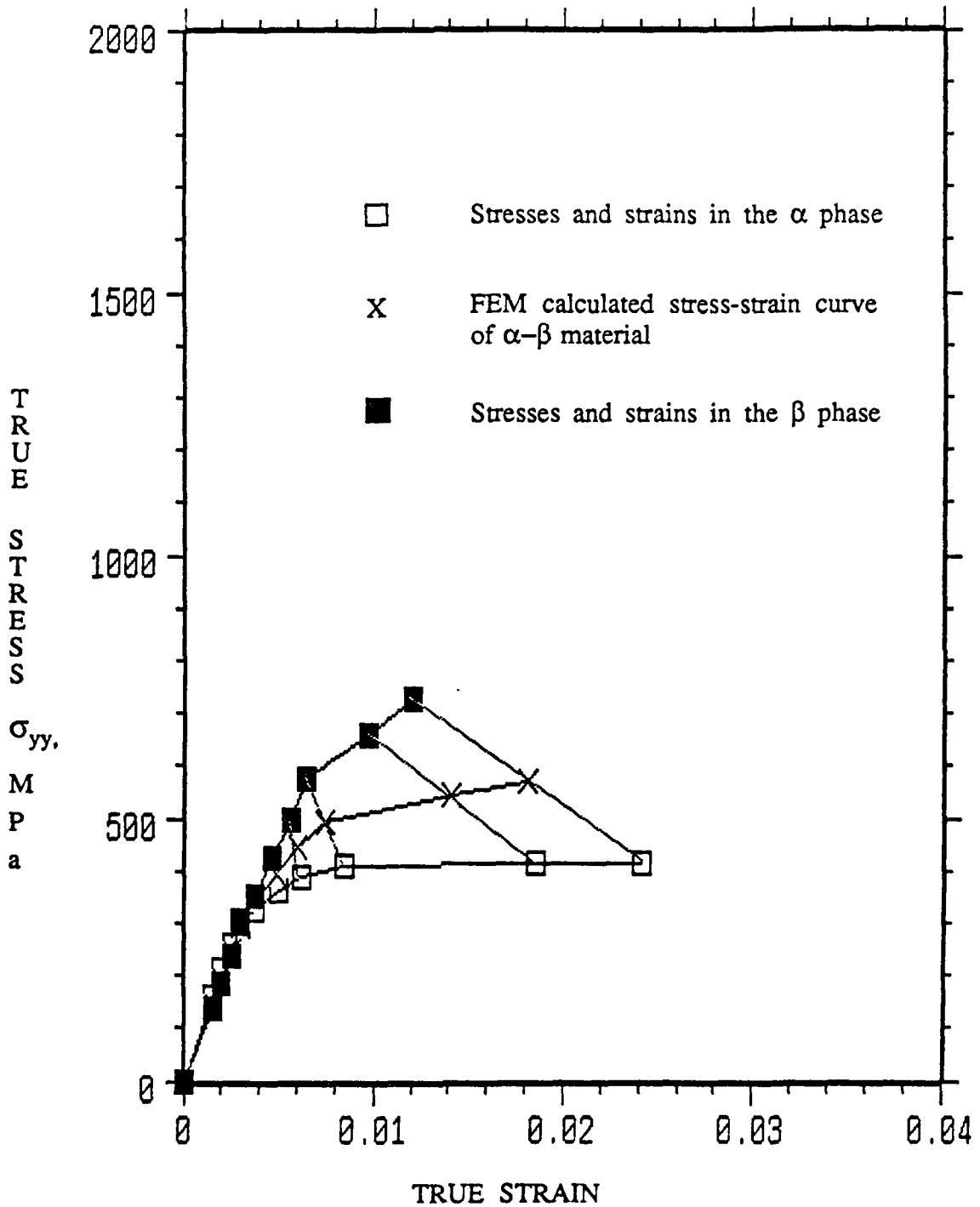

Fig. 3.6 FEM calculated stress and strain distributions for a 50 vol. % α + 50 vol. % β material with β/α strength ratio of 2. The corresponding average stresses and strains in α and β are connected with dotted lines. It is to benoted that the stresses are higher and strains are lower in the harder β phase..

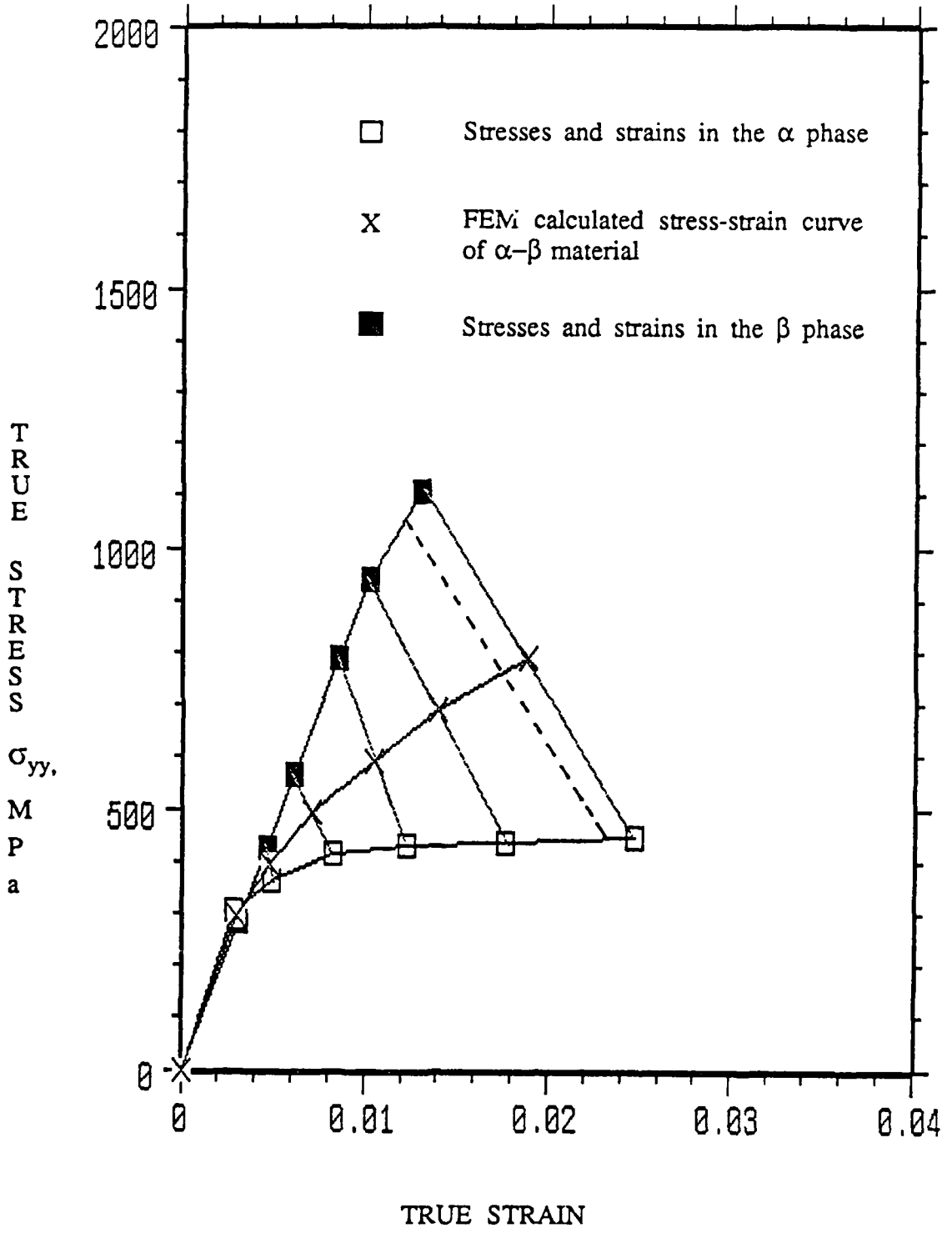

Fig. 37 FEM calculated stress and strain distributions of a 50 vol. % α + 50 vol. β material with β/α strength ratio of 5. The corresponding average stresses and strains in α and β are connected with dotted lines. It is to benoted that the stresses are higher and strains are lower in the harder β phase..

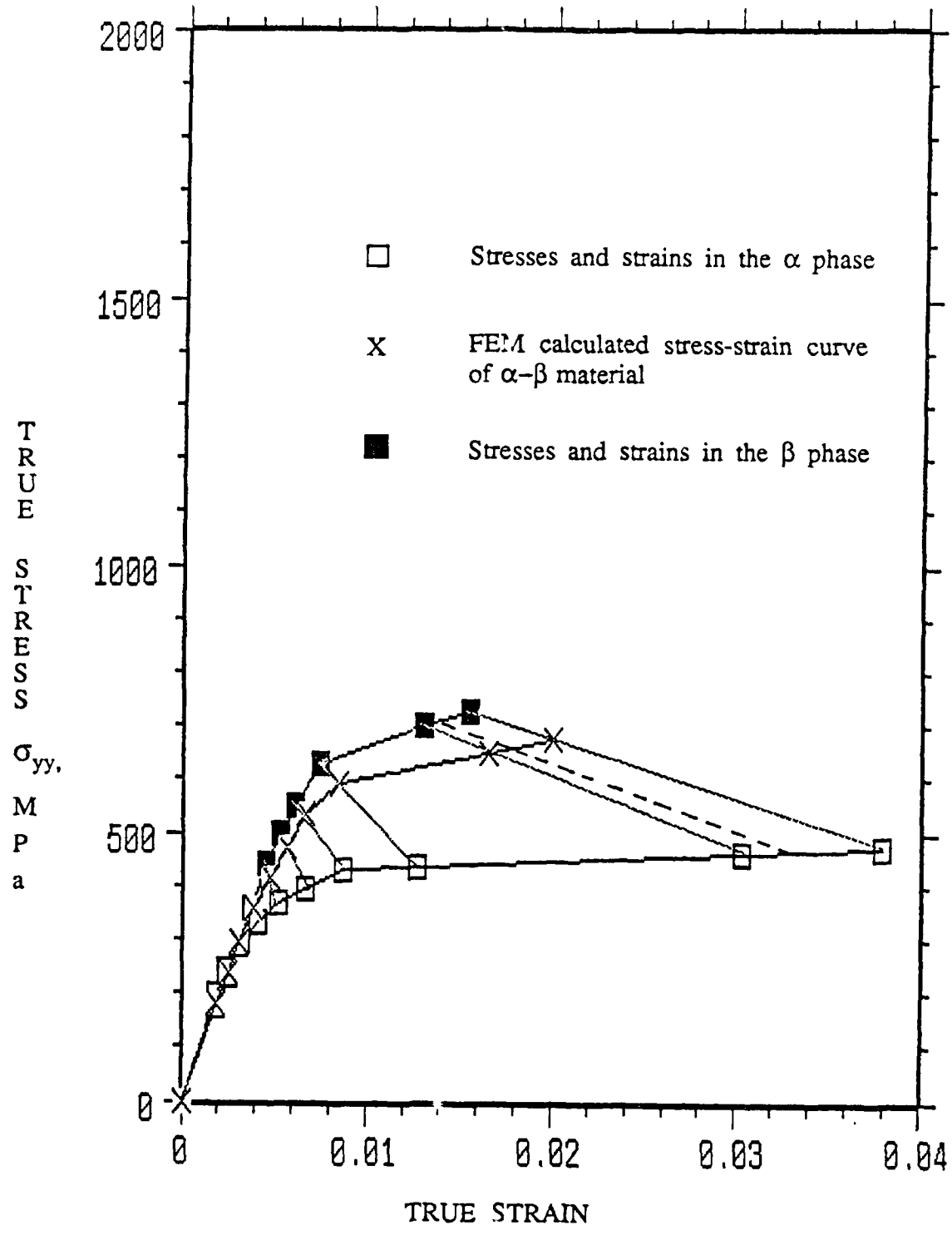

Fig. 38 FEM calculated stress and strain distributions of a 20 vol. % α + 80 vol. β material with β/α strength ratio of 2. The corresponding average stresses and strains in α and β are connected with dotted lines. It is to benoted that the stresses are higher and strains are lower in the harder β phase..

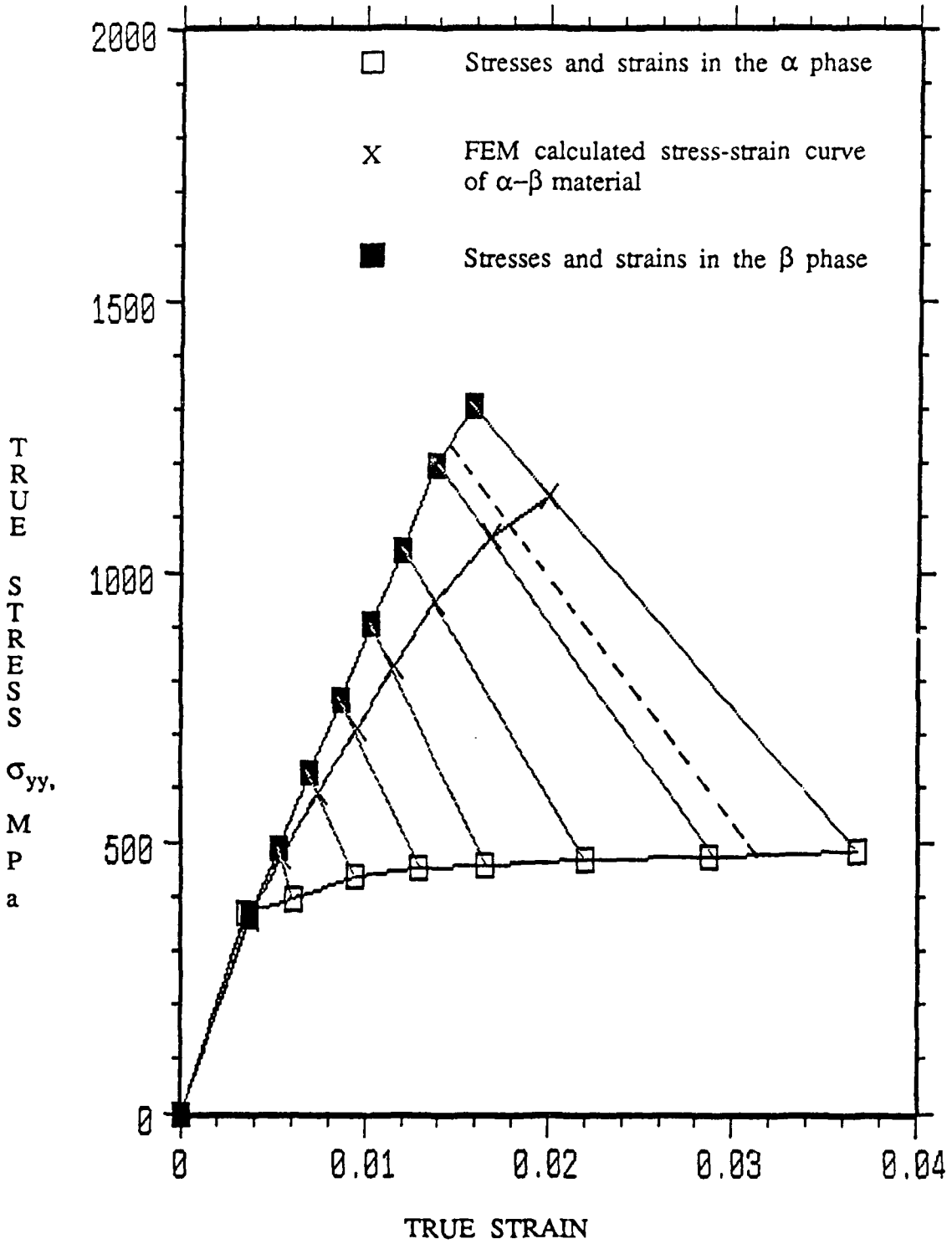

Fig. 39 FEM calculated stress and strain distributions of a 20 vol. % α + 80 vol. β material with β/α strength ratio of 5. The corresponding average stresses and strains in α and β are connected with dotted lines. It is to benoted that the stresses are higher and strains are lower in the harder β phase..

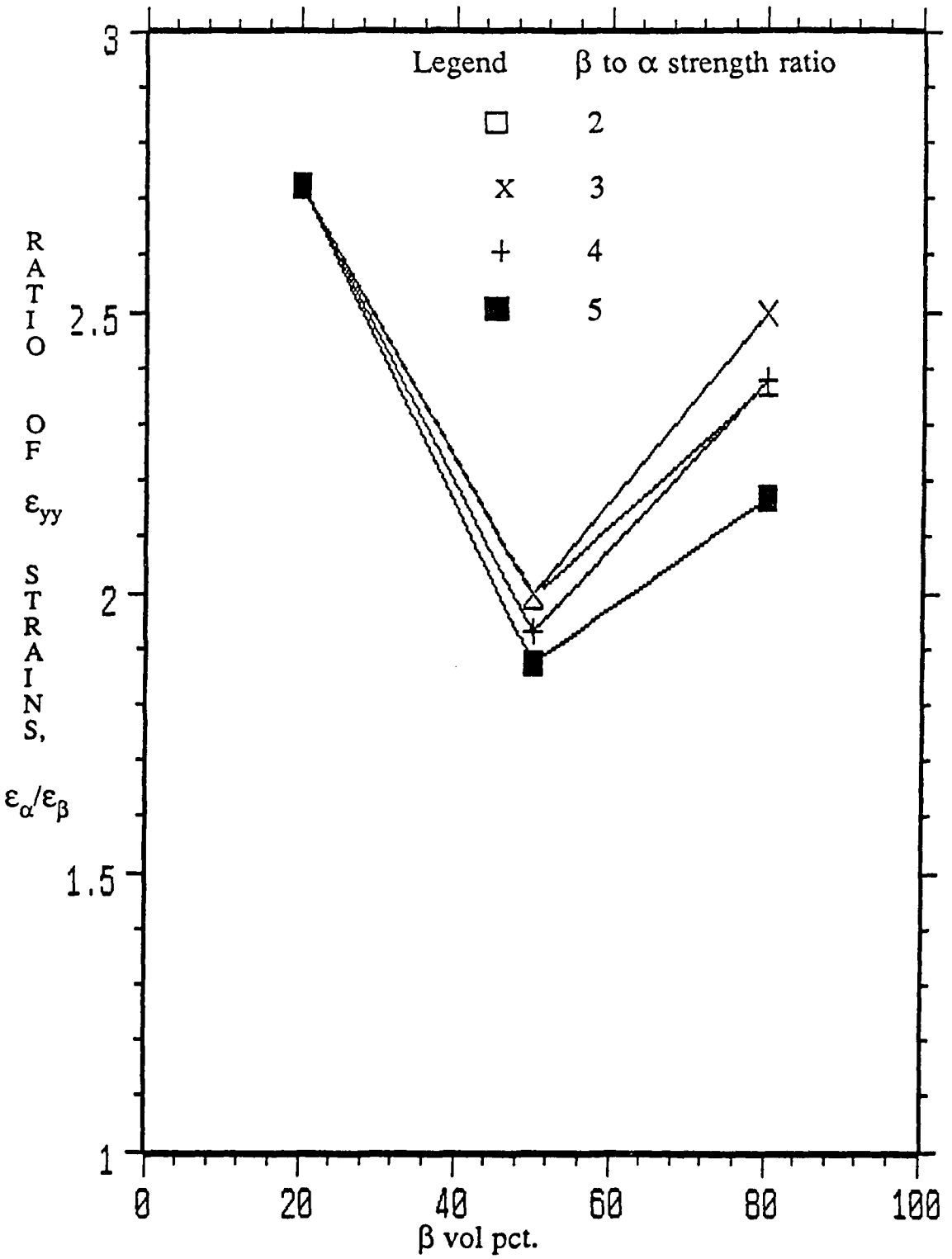

Fig.40 Longitudinal strain ratios, $\varepsilon_\alpha/\varepsilon_\beta$, for various $\alpha-\beta$ materials vs. β volume percent. These strain ratios correspond to a total strain of 0.018.

strains. For a given volume percent of β in α and α in β, for example, the alloys containing 20 volume percent of β-80 volume percent of α, and 80 volume percent of β-20 volume percent of α, the strain ratios of the latter is smaller because the softer α phase is constrained much more effectively by the harder β phase. Comparison of the strain distributions for different strength ratios for the material having 80 volume percent α reveals interesting results. These results can also be seen in Fig. 41. As the strength ratio is increased from 2 to 3, the strain ratio also increases as expected. However, for a further increase in the strength ratio from 3 to 4 and 4 to 5, the strain ratio decreases. This is unexpected because one would expect a higher strain ratio because the strength ratio is higher. In reality what happens is that when the strength of the matrix is increased most of the strain tends to be elastic, see Fig. 39. Therefore, the harder β phase would not allow the softer α phase to deform significantly in the plastic range and this results in lower strain ratios. These trends can also be seen in Fig. 41 where the strain ratios are plotted as a function of β to α strength ratio.

The results shown in Figs. 40 and 41 and discussed above correspond to a total strain of 0.018. For this total strain, as mentioned above, in some instances the strains consist of both elastic and plastic and in some other instances mostly elastic. Therefore, an attempt has been made to obtain the strain ratios for 0.2 % and 0.5 % off-set plastic strains. These ratios are shown in Figs. 42 and 43. It is interesting to note that, in general, the strain ratios shown in Fig. 42 are much smaller than the ratios shown in Figs. 40 and 41. This is related to the fact that for the 0.2 % off-set plastic strain, the corresponding total strains are much smaller than 0.018. Given that the moduli used is similar in both the α and β phases the strain ratios are smaller i.e. corresponds to smaller inhomogeneities. However, for the 0.5 % off-set plastic strain the corresponding total strains are much larger and the strain ratios obtained here are higher than shown in Fig. 42 but lower than shown in Fig. 41. These figures show that the strain partitioning i.e. the strain ratios increase as the amount of strain is increasing. It is to be noted that the nature of the strain distributions are similar

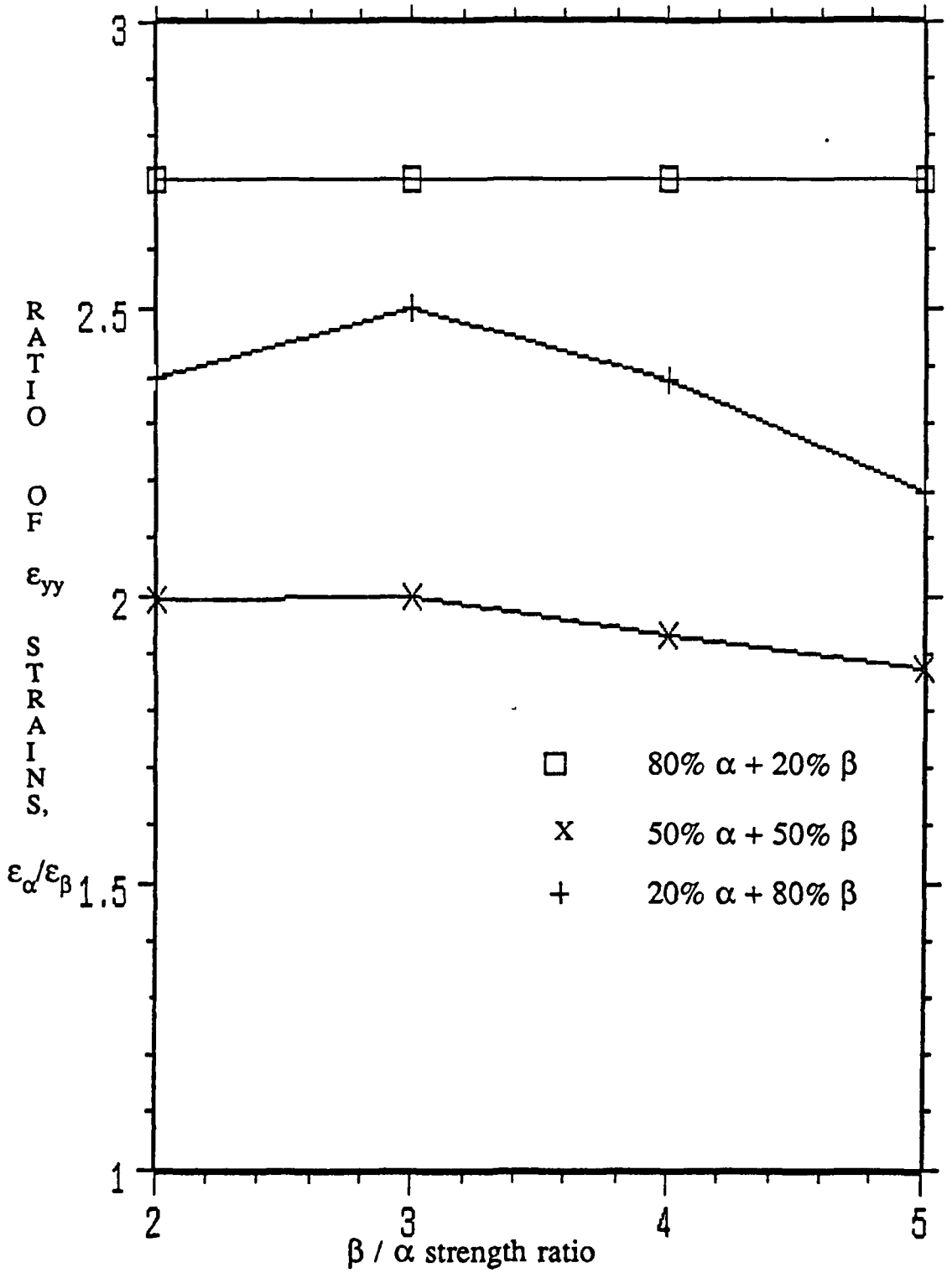

Fig. 41 Longitudinal strain ratios, $\varepsilon_\alpha/\varepsilon_\beta$, for various α–β materials as a function of β / α strength ratio. These strain ratios correspond to a total strain of 0.018.

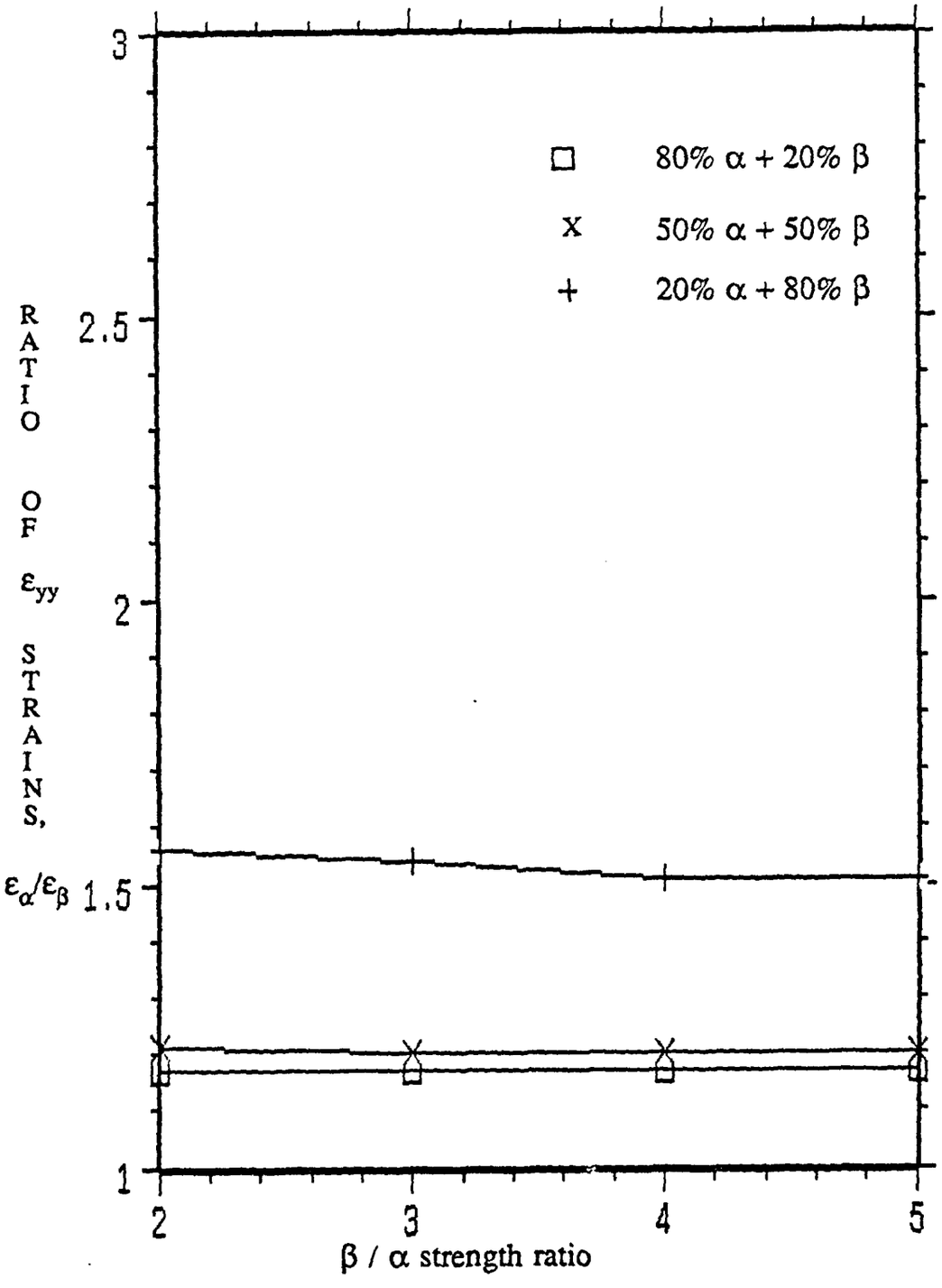

Fig.42 Longitudinal strain ratios, $\varepsilon_\alpha/\varepsilon_\beta$, for various α–β materials as a function of β / α strength ratio. These strain ratios correspond to a 0.2 % off-set plastic strain.

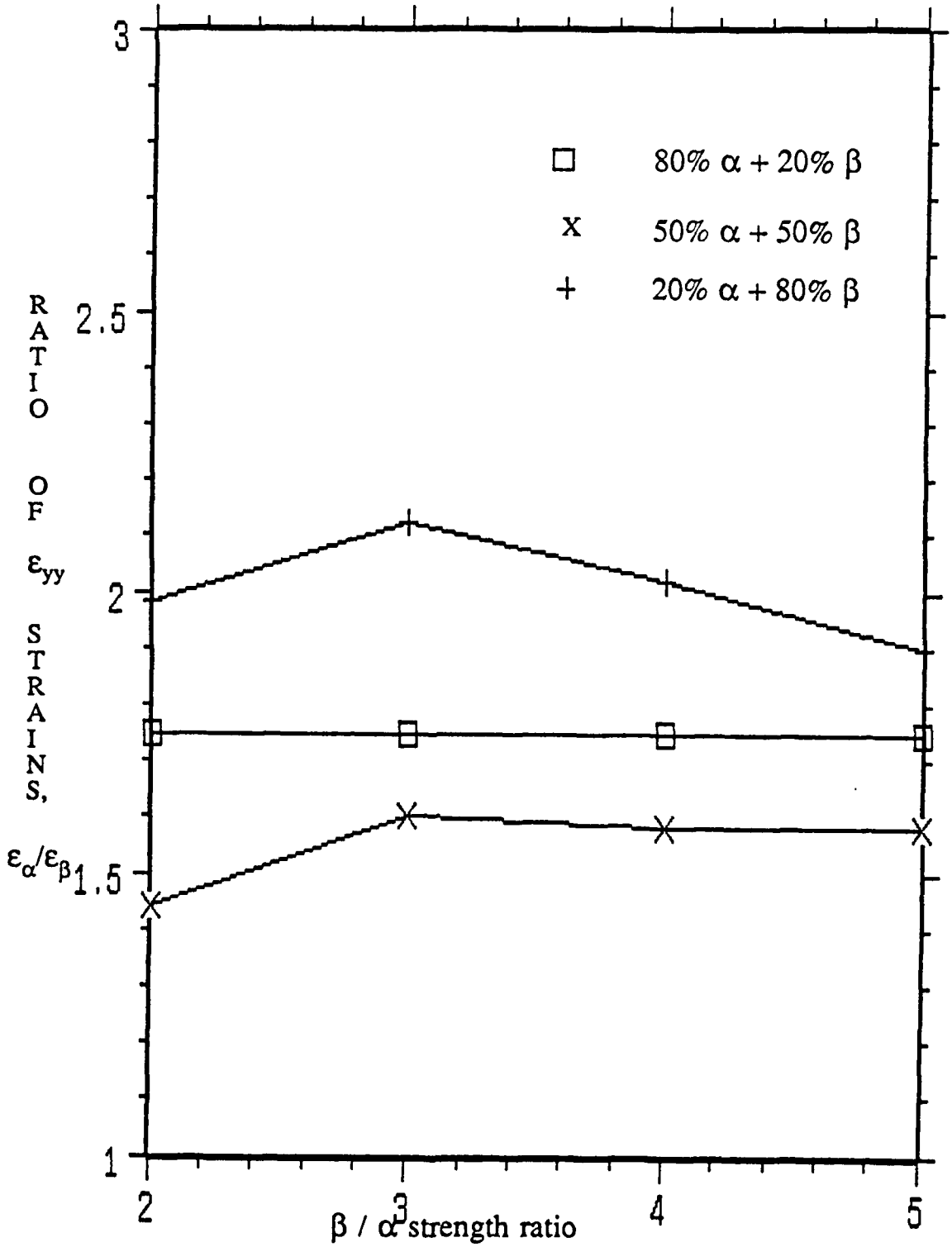

Fig. 43 Longitudinal strain ratios, $\varepsilon_\alpha/\varepsilon_\beta$, for various $\alpha-\beta$ materials as a function of β / α strength ratio. These strain ratios correspond to a 0.5 % off-set plastic strain.

and hence the explainations given in Fig. 41 are expected to hold for these figures also.

4. Local Stress and Strain Distributions

It is important to understand the local stress and strain distributions because many mechanical properties depend on the local stress-strain distributions. Various local stress and strain distributions corresponding to the sections described in the procedure (for eg. P-P in Fig. 21) are plotted and a few of those distributions are shown for illustration in Figs. 44 to 47. In general, these figures show that most of the strain is taken up by the softer phase and the stresses are taken up by the harder phase, and that the transverse stresses, σ_{xx} are developed as a result of the interaction between phases. For the 20 volume percent β material, Fig. 44, in general the transverse stresses are positive in the α phase and negative in the harder β phase and also the magnitude of the transverse stresses are highest in the α phase slightly away from the α/β interface. Since the positive transverse stresses mean biaxial tensile stresses in two-dimensions (i.e. hydrostatic in three-dimensions), it is reasonable to suggest that the most preferred sites for the formation of voids, in general, are regions in the softer α phase slightly away from the two phase interface. However, since the local stress distribution strongly depends on the shape and distribution of the second phase, it is possible that voids can form at other regions within the two phase material.

As the amount of β phase is increased from 20 to 80 percent, the positive transverse stresses are also present at the α/β interfaces and in β phase near the interfaces in addition to regions within the α phase. Therefore, all of the regions can be considered as preferred regions for formation of voids in materials containing predominantly the harder phase. Comparison of the local strain distributions for the 20 volume percent β alloy with different strength ratios indicate no significant differences. This is related to the fact that as the strength of the β phase is increased from 2 to 5, no significant difference was observed in the average stress-strain behavior because the softer α phase could deform relatively easily. However, for the materials containing 80 volume percent β, this is not the case. Here, the increase in

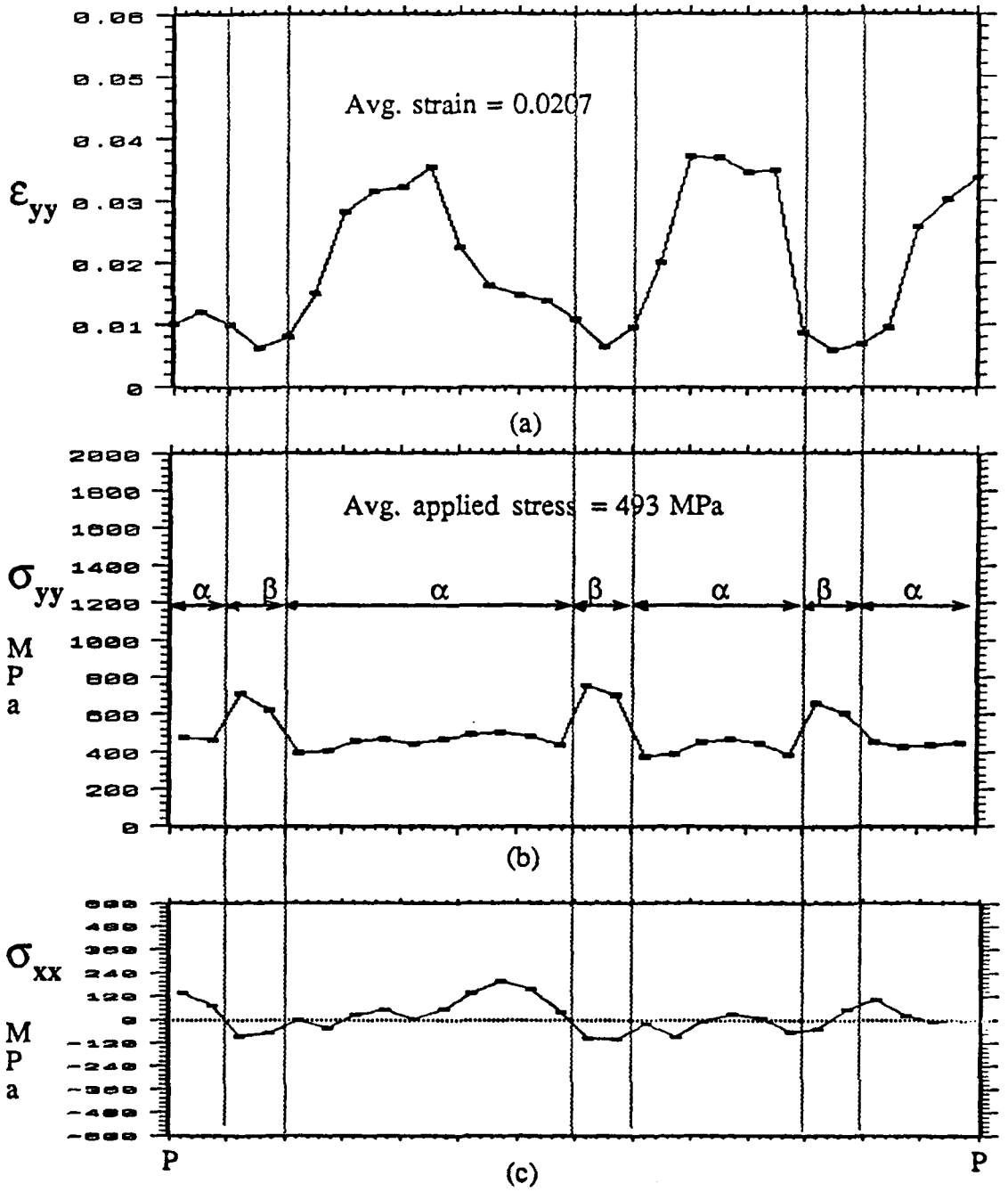

Fig. 44 Stress and strain distributions along section P-P of Fig. 6 with a β/α strength ratio of 3 for a 80 vol. % α–20 vol. % β material:
(a) Longitudinal strain distribution,
(b) Longitudinal stress distribution, and
(c) Transverse stress distribution.

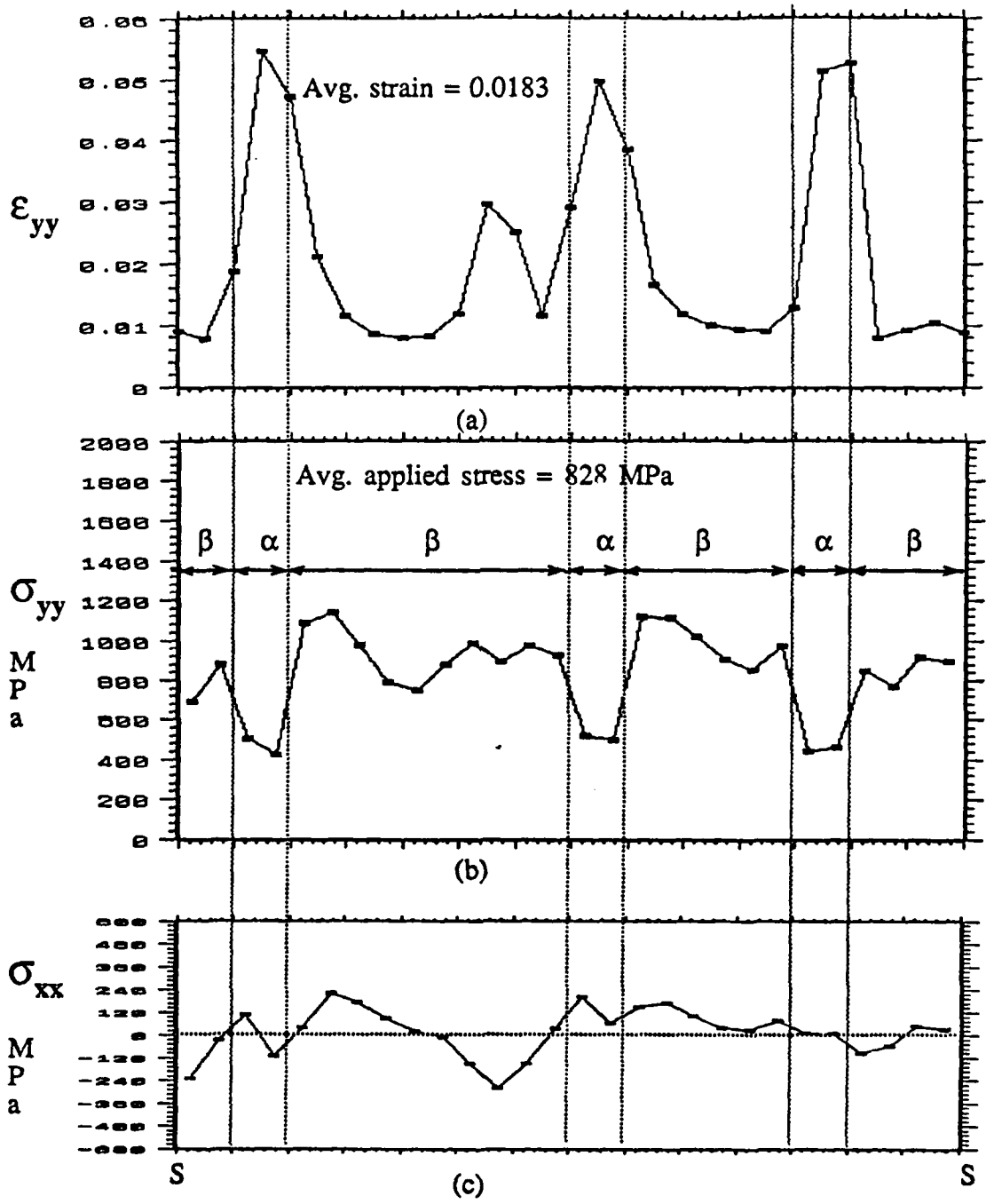

Fig. 45 6 Stress and strain distributions along section S-S of Fig. 6 with a β/α strength ratio of 3 for a 20 vol. % α–80 vol. % β material:
(a) Longitudinal strain distribution,
(b) Longitudinal stress distribution, and
(c) Transverse stress distribution.

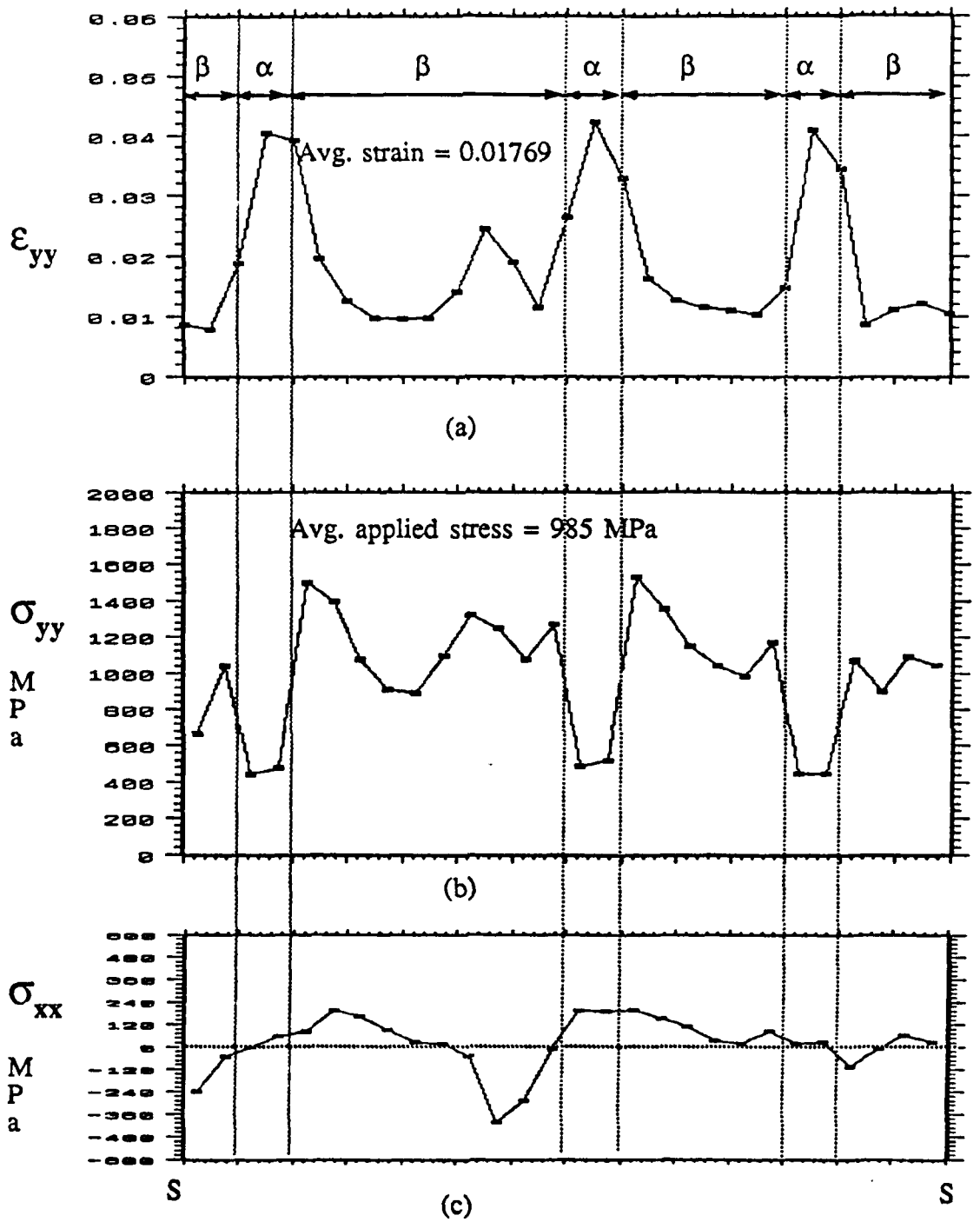

Fig. 46 Stress and strain distributions along section S-S of Fig. 6 with a β/α strength ratio of 4 for a 20 vol. % α–80 vol. % β material:
(a) Longitudinal strain distribution,
(b) Longitudinal stress distribution, and
(c) Transverse stress distribution.

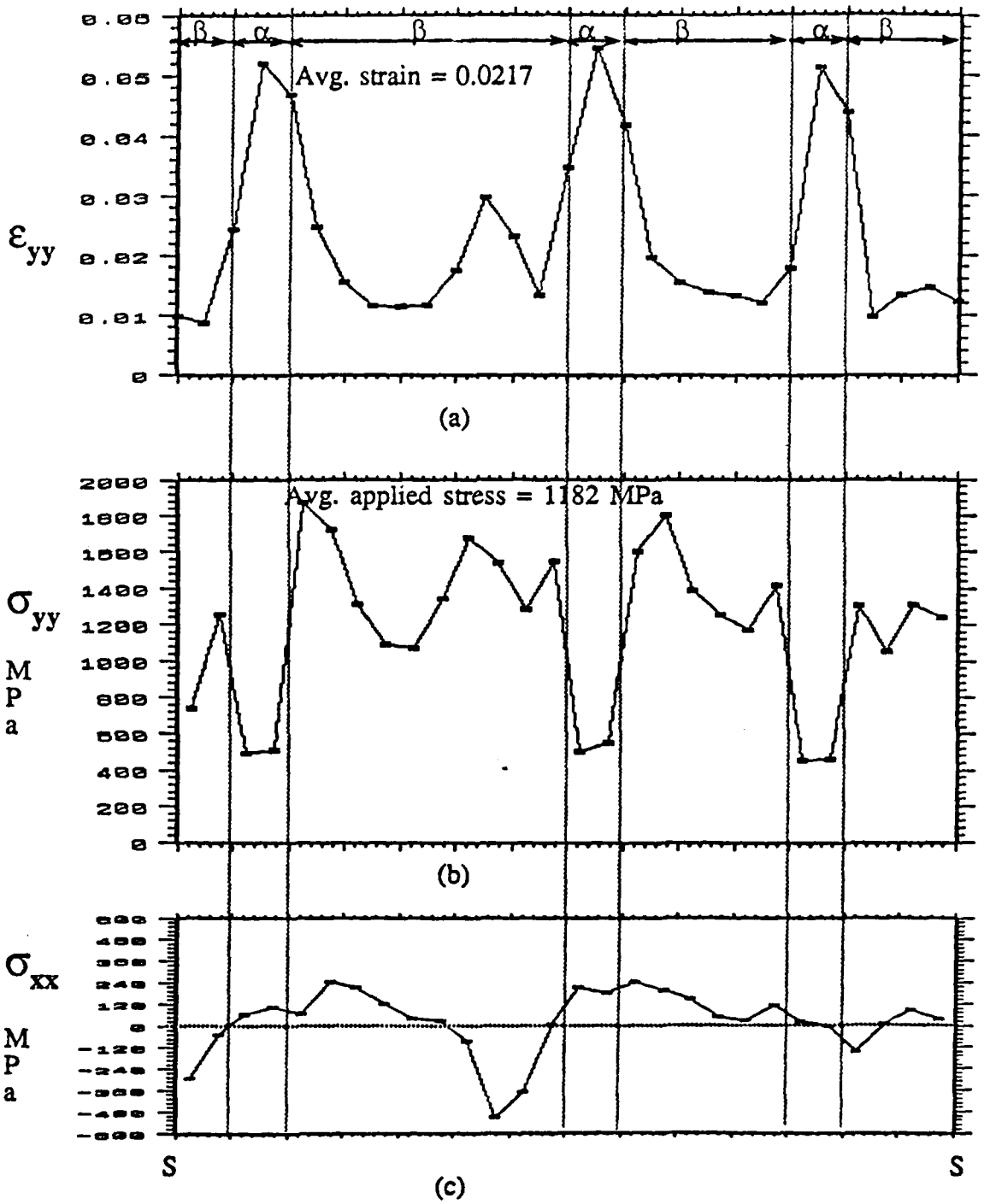

Fig. 47 Stress and strain distributions along section S-S of Fig. 6 with a β/α strength ratio of 5 for a 20 vol. % α–80 vol. % β material:
(a) Longitudinal strain distribution,
(b) Longitudinal stress distribution, and
(c) Transverse stress distribution.

strength ratio made a significant increase in the strength of the two phase material which is also reflected in the local stress-strain distributions, see Figures 45 to 47. As the strength ratio is increased from 3 to 5 for comparable total strains the stress-strain distributions are similar in nature but the magnitudes are different. For similar total strains in the α–β material the strain ratios are slightly decreasing when the strength ratio is increased from 3 to 5, as seen in Fig. 41. This means that the stress partitioning should be higher i.e. most of the stress should be taken up by the stronger β phase if the β phase is expected to deform to a strain close to that of the α phase. Comparisons of Figs. 45, 46 and 47 shows this trend i.e. the longitudinal stress difference between the α and β phases is getting larger as the strength ratio is increased. Along with the longitudinal stresses, the transverse stress gradients are also increasing with increased strength ratio. Therefore for a given volume and total strain of the phases the magnitude of the hydrostatic tensile stresses will increase with increase in strength ratio. Therefore, it is reasonable to suggest that the total strain at which voids can form in the two phase material with harder phase as the matrix will be decreasing with increased strength ratio of the component phase.

5. CONCLUSIONS

1. It was found that β Titanium alloys exhibit sharp flow stress drops followed by steady state behavior. The extent of flow stress drop depends on strain rate, prior heat treatments, prestrain, amount and nature of alloying elements and temperature. The flow stress drops were attributed to the multiplication of mobile dislocations whereas the subsequent steady state behavior was attributed to the dynamic recovery leading to the formation of subgrains.

2 The alpha- beta Titanium alloy also exhibited flow stress drops and for given temperature and strain rate, the magnitude of the drop increased with increase in beta volume percent.

3. At low strain rates, 0.0002 / sec, and at temperatures in the range 650 - 750 C, the flow stresses of alpha - beta alloys with nearly equal volume percents of phases were found to be much smaller than one would expect on the basis of the law of mixture. This was attributed to interphase interface sliding. This work is being continued.

4. It was found that the currently accepted phase diagram for the Ti -V system overestimate the solubility of V in alpha Titanium at temperatures above 700C. A new phase diagram for this system has been suggested.

5. Based on bulk diffusion considerations and considering the growth of alpha and beta phases as a two way diffusion process of solute and solvent, the isothermal particle coarsening behavior was modeled. The particle size predicted at 700 K by this model for the Ti - Mr systems was found to be different from those obtained experimentally. This was attributed to a mixed (Grain Boundary Plus Bulk) diffusion control at 973 K.

6. It was found that the rate controlling mechanisms for the particle coarsening in equiaxed type microstructures of two phase Titanium aloys depend on the diffusivities of alloying elements as well as the temperature. For the Ti- Mn system, it is suggested that the rate controlling mechanism changes from mixed (grain boundary plus bulk) diffusion control at 973 K toward predominantly bulk diffusion control at 1108 K. Similarly , for the Ti - V system, it is suggested that the rate controlling mechanism changes from predominantly grain boundary diffusion control at 973 K towards mixed diffusion control at 1073 K.

7. For the first time, the matrix grain growth in the presence of growing second phse particles in two phase alloys was modeled. These models are based on classical expressions for the driving pressure for grain growth and a modified form of Zener retardation to account for particles which are located at triple junctions. These models resulted in the first order non - linear differential equations which were solved by a computer program based on the Runge - Kutta method. In these models, the particle shape effect as well as the grain boundary curvature contributions to the retardation force have been incorporated. The grain sizes predicted by these models were found to be close to those experimentally obtained.

8.. A two-dimensional FEM method has been employed to determine the stress-strain relationships for various two phase (α-β) materials where the volume of β was varied from 20 to 80 percent. For a given volume percent, the strength ratio of β to α was varied from approximately 2 to 5 where the strength (0.2 % YS) of α was kept constant at 368 MPa.

9. For a given strength ratio, the flow stresses corresponding to 0.2 % and 0.5 % off-set plastic strains of the two-phase materials did not vary linearly with the volume percent of β. For materials with β less than 20 %, it was found that increasing the strength ratio has no significant effect on the flow stresses. This is was attributed to the fact that the softer α phase could deform relatively freely without the harder β phase undergoing plastic deforma-

tion.

10 It was found that transverse stresses develop as a result of the interaction between phases. In general, the transverse stresses were tensile in the softer α phase and the maximum transverse tensile stresses were observed at regions in the α phase sligthly away from the α/β interface for materials with α as the matrix suggesting that these regions are the favorable sites for the initiation of voids. For materials with β as the matrix, transverse tensile stresses were found in the α at the α/β interfaces, and also in the β phase near the α/β interfaces suggesting that all of these regions are favourable sites for void nucleation.

6. REFERENCES

1. R. E. Smallman : Modern Physical Metallurgy, Butterworths Publishing Co., London, 1985.
2. NASTRAN users Manual Level 17.5, Sept. 1983, Document NASA SP - 222 (06), Published by National Aeronautics and Space Administration, Washington DC.
3. Ankem and Margolin : Metall. Trans. A , 1982, Vol. 13 A, p. 595.
4. Ankem and Margolin : Metall. Trans. A , 1982, Vol. 13 A, p. 603.
5. G. Grewal and S. Ankem, Proceedings of the Sixth World Conference on Titanium, Cannes France, Editions de Physique, France, Eds. P. Lacombe, R. Tricot and G. Berenger, 1988, Vol. 1, pp. 265 -268.
6. S. Ankem and J. G. Shyue, M.N. Vijayshankar and R J. Arsenault,Mat. Sci. & Eng., Vol. A 111, 1989, pp. 51 - 61.
7. G. Grewal and S. Ankem : Metall. Trans. A, Vol 20 A, 1989, pp. 334 - 337.
8. G. Grewal and S. Ankem : Metall. Trans. A, Vol. 20 A , 1989, pp. 39 -53.
9. G. Grewal and S. Ankem, Metall. Trans. A, Vol. 21A, 1990, pp. 1645-1654.
10. M. N. Vijayshankar and S. Ankem: Proceedings of the International Conference on Recrystallization in Metallic Materials, Wollongong, Australia, Published by TMS, 1990, pp. 673-679.
11. G. Grewal and S. Ankem: Acta Metall. Mater. Vol. 38, No.9, 1990, pp. 1607-1617.
12. M.N. Vijayshankar and S. Ankem : Accepted for publication in Materials Science and Engineering.
13. R. W. Honeycombe and W. Boas, Aust. J. Sci. Res., 1 (1948) p. 70.
14. L. M. Clarebrough and F. R. Perger, Aust. J. Sci. Res., 5 (1952) p. 114.
15. L. M. Clarebrough, Aust. J. Sci. Res., 3 (1950) p. 72.
16. Y. Tomota, K. Kuroki, T. Mori and I. Tamura : Mat. Sci. Eng., 1976, Vol. 24, p. 85.
17. R. G. Davies: Metall. Trans. A, 1978, Vol. 9A, p. 41.
18. R. G. Davies: ibid., p. 451.
19. R. G. Davies: ibid., p. 671.
20. Peter Ostrom : Metall. Trans., 1980, Vol. 12A, p. 355.
21. S. T. Mileiko: J. Mater. Sci., 1969, Vol. 4, p. 974.

22. G. Garmong and R. B. Thomson: Metall. Trans., A, 1973, Vol. 4, p. 863.
23. F. C. Holden, H. R. Ogden, and R. I. Jaffee : J. of Metals, Feb. 1954, p. 169.
24. H. R. Ogden, F. C. Holden and R. I. Jaffee : J. of Metals, Jan. 1955, p. 105.
25. F. C. Holden, H. R. Ogden, and R. I. Jaffee : J. of Metals, May. 1956, p. 521.
26. F. C. Holden, H. R. Ogden, and R. I. Jaffee : J. of Metals, Oct. 1956, p. 1388.
27. H. Fischmeister, J. O. Hjalmered, B. Karlsson, G. Linder and B. Sundstrom : Proc. Third Int. Conf. Strength of Metals and Alloys, Inst. of Metals and Iron & Steel Inst., Cambridge & London, 1973, vol. 1, p. 621.
28. B. Karlsson and B. O. Sundstrom : Mat. Sci. Eng., 1974, Vol. 16, p. 161.
29. H. Fischmeister and B. Karlsson : Z. Metallkunde, 1977, Vol. 68, p. 311.
30. J. Jinoch and S. Ankem : Mat. Sci. Eng., 1978, Vol.34, p. 203.
31. Ankem and Margolin : Metall. Trans. A, 1982, Vol. 13A, p. 595.
32. Ankem and Margolin : Metall. Trans. A, 1982, Vol. 13A, p. 603
33. Ankem and Margolin : Metall. Trans. A, 1986, Vol. 17A, p. 2209.
34. J. E. Dorn and C. D. Starr : Relations of Properties to Microstructure, American Society for Metals, Metals Park, OH, 1954, p. 71.
35. K. Cho and J. Gurland : Metall. Trans. A, 1987, Vol. 19A, p. 2027.
36. H. Unckel: J. Inst. of Metals, 1937, vol. 61, p. 171.
37. R. W. K. Honeycombe and W. Boas: Aust. J. Sci. Res., 1948, vol. A1, p. 70.
38. B. Karlsson and B. O. Sundstrom: Mat. Sci. & Eng., 1974, vol. 16, p. 161.
39. H. Fischmester and B. Karlsson: Z. Metallk, 1977, vol. 68 (5), p. 311.
40. G. Liden: Mat. Sci. & Engr., 1979, vol. 40, p. 5.
41. J. L. Murray : "Binary Alloy Phase Diagrams", Editor - in- Chief T. B. massalski, ASM Metals Park, Ohio, 1986, Vol.2 , p. 2134.

7. TECHNICAL PRESENTATIONS AND PUBLICATIONS

PRESENTATIONS

1. "The Effect of Temperature on the Grain Growth of Two-Phase Titanium Alloys", G. Grewal and S. Ankem, 1988 TMS Annual Meeting.

2. "High Temperature Tensile Deformation Behavior of Two -Phase Titanium Alloys', M.N. Vijayshankar and S. Ankem, 1988 TMS Annual Meeting.

3. "Particle Growth in Two - Phase Titanium Alloys", G. Grewal and S. Ankem, Sixth World Conference on Titanium, June 6 -9, 1988 Cannes, France.

4. "Particle Coarsening Mechanisms in α–β Titanium Alloys", G. Grewal and S. Ankem, 1988, TMS Fall Meeting.

5. "The Dynamics of Grain Growth in Two - Phase Titanium Alloys", G. Grewal and S. Ankem, 1989 TMS Annual Meeting.

6. "High Temperature Tensile Deformation Behavior of β- Titanium Alloys", M.N. Vijay-Shankar and S. Ankem.

PUBLICATIONS

1. "Particle Growth in Two - Phase Titanium Alloys", G. Grewal and S. Ankem, Proceedings of the Sixth World Conference on Titanium, Cannes, France, Published by Editions de Physique, France, Eds. P. Lacombe, R. Tricot and G. Berenger,1988,Vol.1, pp. 265- 268.

2. "The Effects of Volume Percents of Phases on the High Temperature Deformation Behavior of Two Phase Ti- Mn Alloys", S. Ankem and J. G. Shyue, M.N. Vijayshankar and R..J. Arsenault, *Mat. Sci. & Eng.*, Vol. A111, 1989, pp. 51-61.

3. "Solubility of Vanadium in α and β Titanium", G. Grewal and S. Ankem : *Metall. Trans. A*, Vol. 20 A, 1989, pp. 334-337.

4. "Isothermal Particle Growth in Two - Phase Titanium Alloys", G. Grewal and S. Ankem : *Metall. Trans. A*, Vol. 20 A, 1989, pp.39-53.

5. "Particle Coarsening Behavior of α – β Titanium Alloys", G. Grewal and S. Ankem, *Metall. Trans. A*, Vol. 21A, 1990, pp. 1645-1654.

6. "A Rationalization of Strain Softening and Dynamic Recovery in Beta Titanium Alloys", M. N. Vijayshankar and S. Ankem: Proceedings of the International Conference on Recrystallization in Metallic Materials, Wollongong, Australia, Published by TMS, 1990, pp. 673-679.

7. "Modeling Matrix Grain Growth in the Presence of Growing Second Phase Particles in Two - Phase Alloys", G. Grewal and S. Ankem: *Acta Metall. Mater.* Vol. 38, No.9, 1990, pp. 1607-1617.

8. "High Temperature Tensile Deformation Behavior of Beta Titanium Alloys", M.N. Vijayshankar and S. Ankem: Accepted for Publication in Materials Science and Enginee -ring, 1990.

8. DEGREES AWARDED

Masters:

1. J. G. Shyue, Degree Awarded in August 1987.
2. Srinivas N. Neti, Degree awarded in August 1990. (Partial Support)

Doctoral:

1. G. Grewal, Degree Awarded in May 1990.
2. V. Narayana Rao, Admitted to candidacy, expected to graduate in Dec. 1990.

9. HONORS AND AWARDS

Dr. S. Ankem, the principal investigator, is the receipient of the **"1990 ASM International Materials Science Division Research Award".** This is an annual award given to the scientist whose research contributions are identified in the materials science community as being the great contributions to the field.